Species of the *Diaporthe*/*Phomopsis* Complex (DPC) in European soybean and establishment of quadruplex Real-Time PCR for diagnosis

Dissertation

to obtain the doctoral degree of Agricultural Sciences

(Dr. sc. agr.)

Faculty of Agricultural Sciences

University of Hohenheim

Institute of Phytomedicine

Submitted by

Behnoush Hosseini

From Iran, Esfahan

2022

Date of the oral exam:	12.05.2023
Dean:	Prof. Dr. Ralf Thomas Voegele
1. Examiner:	Prof. Dr. Ralf Thomas Voegele
2. Examiner:	Prof. Dr. Matthias Hahn
3. Examiner:	Prof. Dr. Georg Petschenka

Acknowledgements

It is a very pleasant opportunity to express my sincere gratitude and appreciation to all those people who supported me during my doctoral research program.

I would like to express my deepest gratitude to my supervisor **Prof. Dr. Ralf Thomas Voegele** for his patient guidance and continuous dedicated support during my Ph.D.. I wish to thank him for giving me the opportunity to work in his lab under his supervision, his kind assistance and efforts, for his friendly support in getting scholarships, and also for giving me the opportunity to attend conferences for professional development. His immense knowledge, critical review of the proposals, abstracts, and manuscripts, scientific discussions, and kind guidance encouraged me to move forward and will remain thought-provoking for the rest of my life.

I would like to express my sincere appreciation to **Dr. Tobias Link** for his leadership with constructive criticisms, excellent comments, valuable suggestions and discussions, reviewing the abstracts, manuscripts and reading this thesis, and support to ensure that my research was carried out efficiently. Moreover, his scientific knowledge and motivation towards molecular science inspired me to make progress in molecular methods. I am also grateful to Tobias for believing in my abilities, making me believe in my own abilities, and encouraging me to supervise Humboldt Reloaded, laboratory project, BSc, and now also MSc students.

I am grateful to **Dr. Abbas El-Hasan** for helpful discussions, his collaboration on the identification of fungi as mycologist expert, and in biological control, and for reviewing my first paper.

I am thankful to **all my colleagues** at the Institute of Phytomedicine for their constant support. My sincere thanks to **Heike Popovitsch**, not only for her technical assistance in the lab but also for her motherly kind manner, which enabled me to adapt to a new culture and country. I would like to thank **Barbara Kaufmann** for her instructions in making accurate and beautiful microscopic pictures, **Sibylle Berger**, **Bianka Maiwald**, and **Manfred Konert** for technical assistance. I wish to thank **Janina Seitz**, **Anna Hummrich**, **Seema Pawar**, **Martin Rieker**, and **Christian Trautmann** for creating an always good working atmosphere, for tips and willingness to help and for many chats and celebrations that brightened up everyday laboratory work and helped improving my German language skills, especially **Grace Ngatia** and **Daniela Hirschburger**, who always were the first to help me with problems.

I thank the students who worked with me on the project for their BSc theses. **Maren Himmel** worked with me on absolute quantification. The results of **Marcel Röbig** on biological control, **Kathrin Schwörer** on growth of *Diaporthe* spp. in the plant, and **Verena Jauß** on expression of PR genes in soybean will be important for continuing my research.

I gratefully acknowledge the **Faculty of Agricultural Science** and the **Food Security Center of the University of Hohenheim** for doctoral fellowships via the **State Graduate Fund** and **German Academic Exchange Service (DAAD)**, respectively. I am grateful to "**Bundesanstalt für Landwirtschaft und Ernährung (BLE)**" for financial support within the project "SoySound" (2815EPS082).

I would like to thank **Taifun-Tofu GmbH**, the **Landwirtschaftsbetrieb Zschoche**, and the **Landwirtschaftliches Technologiezentrum (LTZ) Augustenberg** for providing infected and healthy soybean seed lots.

Finally, I wish to express my gratitude to **my family** for their unconditional support, encouragement and love throughout my studies. My deepest appreciation to my parents who raised me and supported me in all my academic pursuits. No matter near or far, they have always stood behind me and stuck with me through thick and thin. To them, I am eternally grateful for their love, support, and sacrifices. Thank you to my sister, her husband, and their lovely daughters, for always being there for me and being generous with their love and encouragement despite the long distance between us.

B.Scs. completed within the project presented in this thesis:

Marcel Röbig, 2019

In vitro Versuch zur Wirksamkeit verschiedener Mikroorganismen gegen *Diaporthe* spp.

Kathrin Schwörer, 2020

Dokumentation des Infektionsverlaufes von *Diaporthe* spp. an Soja (*Glycine max* L. (Merr.)) nach künstlicher Inokulation mit verschiedenen Methoden

Maren Himmel, 2020

Beurteilung von Methoden zur DNA-Präparation aus Sojasamen und Grundlagen für die Quantifizierung von *Diaporthe* spp.

Verena Jauß, 2021

Establishment of a method to measure the expression of PR genes in soybean

Publications

Hosseini, B., El-Hasan, A., Link, T., and Voegele, R. T. (2020). Analysis of the species spectrum of the *Diaporthe*/*Phomopsis* complex in European soybean seeds. Mycological Progress **19**: 455–469. DOI: 10.1007/s11557-020-01570-y

Hosseini, B., Voegele, R. T., and Link, T. I. (2021). Establishment of a quadruplex real-time PCR assay to distinguish the fungal pathogens *Diaporthe longicolla*, *D. caulivora*, *D. eres*, and *D. novem* on soybean. PLoS ONE **16**: e0257225. DOI: 10.1371/journal.pone.0257225

Akintayo, S. O., Hosseini, B., Vahidinasab, M., Messmer, M., Pfannstiel, J., Bertsche, U., Hubel, P., Henkel, M., Hausmann, R., Voegele, R. T., and Lilge, L. (2022). Biocontrol activity, including surfactin induction and proteomic response of lipopeptide producing *Bacillus velezensis* strains to fungal plant pathogens, *Diaporthe* spp.. Submitted in Environmental Microbiliolgy and Environmental Microbiology Reports.

Table of contents

Figures

Tables

Abbreviations

AFLP	amplified fragment length polymorphism
APDA	acidified potato dextrose agar
BCAs	biological control agents
BLAST	Basic Local Alignment Search Tool
bp	base pair
ca.	circa
CAL	calmoduline
CBS	Central Bureau of Fungal Cultures (Centraalbureau voor Schimmelcultures)
CJA	carrot juice agar
CMC	carboxymethylcellulose
Cq	quantification cycle (synonymous with Ct)
Ct	cycle threshold (synonymous with Cq)
cv.	cultivar
Cy5	cyanine 5
DC	*Diaporthe caulivora*
ddH_2O	double-distilled water
DE	*Diaporthe eres*
DL	*Diaporthe longicolla*
DN	*Diaporthe novem*
DNA	desoxyribonucleic acid
dNTPs	deoxynucleoside triphosphates
DPC	*Diaporthe*/*Phomopsis* Complex
DSD	*Diaporthe* seed decay
DSMZ	Deutsche Sammlung von Mikroorganismen und Zellkulturen
dsDNA	double stranded DNA
dt	decitonnes
E	efficiency
EC	European Commission
EDTA	ethylenediaminetetraacetic acid
EtOH	ethanol
EU	European Union
FAM	6-carboxyfluorescein
FW/F	forward primer
GM	genetically modified
h	hour
ha	hectare
HEX	Hexachlorofluorescein
HIS	histone-3
HPTLC	high-performance thin-layer chromatography
ITS	internal transcribed spacer
IZS	Irmgard Zingen-Sell
LOD	limit of detection

LSU	large ribosomal subunit
LTZ Augustenberg	Landwirtschaftliches Technologiezentrum Augustenberg
LWB	Landwirtschaftsbetrieb
MEGA	Molecular Evolutionary Genetics Analysis
min	minutes
NCBI	National Center for Biotechnology Information
N-fixing	nitrogen-fixing
no.	number
NTC	non template control
P	TaqMan Probe
PCR	polymerase chain reaction
PCWDEs	plant cell wall-degrading enzymes
PDA	potato dextrose agar
PSD	*Phomopsis* seed decay
R	ratio / quotient
R^2	coefficient of correlation for the standard curve
RAPD	random amplified polymorphic DNA
rcf	relative centrifugal force
Real-time qPCR	real-time quantitative PCR
RFLP	restriction fragment length polymorphism
RFU	relative fluorescence unit
RNAseq	ribonucleic acid sequencing
ROX	Rhodamin X
rpm	revolutions per minute
RT	room temperature
RV/R	reverse primer
s	seconds
SDS	sodium dodecyl sulfate
spp.	species pluralis
TAE	TRIS-acetate-EDTA
Taq	*Thermus aquaticus*
TEF1	translation elongation factor 1-α
TRIS	tris(hydroxymethyl)aminomethane
TUB	beta-tubulin
UK	United Kingdom
UKN2	gene with unknown function 2
USA	United States of America
USDA-FAS	United States Department of Agriculture Foreign Agricultural Service
UV	ultraviolet
WA	water agar
w/v	weight/volume

Summary

Diaporthe seed decay is among the most disruptive soybean diseases around the world, which cause significant yield losses and affect soybean quality. Different *Diaporthe* species cause this disease, while *Diaporthe longicolla* is considered the main causal agent. The species of this fungal complex (genus *Diaporthe* is also called the *Diaporthe*/*Phomopsis* Complex / DPC) have to be accurately identified for epidemiological studies of the disease and for optimal control measures.

To identify the major causal agents of seed decay in Europe, DPC-damaged soybean seeds of various cultivars, that were collected from different fields in Germany, France, and Austria were tested by seed plating. 32 *Diaporthe* isolates could be obtained. The isolates were morphologically identified by the colors and shape of the colony, conidia dimensions, and by whether pycnidia with α- and/or β-conidia or perithecia with ascospores are formed. To corroborate morphological identification, sequences of the internal transcribed spacer (ITS), translation elongation factor 1-α (*TEF1*), and beta-tubulin (*TUB*) sequences were obtained. From the results of both morphological and molecular analyses it became clear that all isolates belong to one of the four species *D. longicolla, D. caulivora, D. eres*, and *D. novem*. The pathogenicity of all strains on soybean was tested. Molecular phylogenies were calculated and based on the above results updated species descriptions were created. This study identified these four species as the main *Diaporthe* pathogens for soybean in central Europe.

A sensitive and accurate method for quick detection of these pathogens was developed based on multiplex real-time PCR. Specific TaqMan primer-probe sets for the four species were designed based on *TEF1* sequences. The primer-probe sets were tested for specificity and efficiency using PCR products and genomic DNA from the four *Diaporthe* species and several other soybean pathogens. These primer-probe sets reliably distinguish the different species and they can be used to detect them in the same reaction by quadruplex real-time PCR. DNA from different soybean plant materials including healthy and infected seeds or seed coats, stems, and leaves was used to test the quadruplex real-time PCR assay.

Application of the assay was extended to quantify the pathogens. Standard curves for the four species were created from serial dilutions of genomic DNA diluted with DNA from soybean tissue. An additional standard curve was created from serial dilutions of soybean DNA diluted with ddH_2O. To gain the ratio of fungal DNA per plant DNA (ng/ng), DNA samples from soybean tissues can now be examined in the new assay and a parallel SYBR® Green-based real-time PCR. The assay was first applied to six soybean seed lots with putative *Diaporthe*

contamination. In all seed lots seeds contaminated with *Diaporthe* species and even some seeds infected with more than one *Diaporthe* species were found, while other seeds were free of the pathogens. The load of fungal biomass varies strongly between individual seeds.

Zusammenfassung

Diaporthe seed decay (*Diaporthe* Samenverfall) ist eine der zerstörerischsten Sojabohnenkrankheiten, die weltweit die Qualität und Quantität der Samen beeinträchtigen. Die Krankheit wird hauptsächlich von *Diaporthe longicolla* zusammen mit anderen *Diaporthe*-Arten verursacht. Die genaue Identifizierung der Arten dieses Pilzkomplexes (die Gattung *Diaporthe* wird auch als *Diaporthe*/*Phomopsis* Komplex / DPK bezeichnet) ist notwendig, um die Epidemiologie der Krankheit zu verstehen und eine optimale Bekämpfung zu ermöglichen.

Um die Hauptverursacher des Samenverfalls in Europa zu identifizieren, wurden DPK-geschädigte Sojabohnensamen verschiedener Sorten, die von verschiedenen Feldern in Deutschland, Frankreich und Österreich stammen, durch „Seed Plating“ untersucht. 32 *Diaporthe*-Isolate konnten erhalten werden. Die Isolate wurden anhand von Farben und Wuchsformen der Kolonien, Abmessungen der Konidien, Existenz von α- und β-Konidien und Bildung von Perithezien identifiziert. Um die morphologische Identifizierung zu bestätigen, wurden Sequenzen des internen transkribierten Spacers (ITS), des Translationselongationsfaktors (*TEF1*) und des Beta-Tubulin (*TUB*) gewonnen. Durch Kombination der Ergebnisse der morphologischen und molekularen Analysen konnten die Isolate den vier Arten *D. longicolla*, *D. caulivora*, *D. eres*, und *D. novem* zugeordnet werden. Die Pathogenität aller Stämme auf Sojapflanzen wurde getestet. Molekulare Phylogenien wurden berechnet und basierend auf den obigen Ergebnissen wurden aktualisierte Artbeschreibungen erstellt. Als Ergebnis dieser Studie können diese vier Arten als die Hauptarten von *Diaporthe* an Sojabohnen in Mitteleuropa angesehen werden.

Eine schnelle, sensitive und exakte Methode zum Nachweis dieser Pathogene basierend auf multiplex real-time PCR wurde entwickelt. Auf der Grundlage von *TEF1*-Sequenzen wurden vier artspezifische TaqMan Primer-Sonden Sets entwickelt. Die Spezifität und Effizienz der Primer-Sonden Sets wurden mit PCR-Produkten und genomischer DNA der vier *Diaporthe*-Arten und einiger anderer Sojabohnen-Pathogene getestet. Diese Primer-Sonden Sets ermöglichen eine zuverlässige Unterscheidung der unterschiedlichen Arten und sie können verwendet werden, um die Arten mit der quadruplex real-time PCR parallel nachzuweisen. Darüber hinaus wurde der quadruplex real-time PCR Assay an verschiedenen Pflanzenmaterialien getestet, darunter gesunde und infizierte Sojasamen oder Samenschalen, Sojastängel und Blätter.

Ebenfalls wurden die Voraussetzungen zur Nutzung der quadruplex real-time PCR für die Quantifizierung der Erreger geschaffen. Aus seriellen Verdünnungen genomischer DNA der *Diaporthe*-Arten, die mit DNA verdünnt wurden, die aus Sojabohnengewebe präpariert wurde, wurden Standardkurven erhalten. Eine zusätzliche Standardkurve wurde aus seriellen Verdünnungen von mit ddH_2O verdünnter Sojabohnen-DNA erstellt. Um die Menge an Pilz-DNA pro Pflanzen-DNA (ng/ng) zu quantifizieren, können nun DNA-Proben aus Sojabohnengewebe in dem neuen Assay und einer parallelen SYBR® Green-basierten real-time PCR untersucht werden. Der Assay wurde mit DNA-Proben aus sechs Sojabohnen-Samenchargen mit mutmaßlicher *Diaporthe*-Kontamination getestet. In allen Samenpartien waren Samen infiziert mit *Diaporthe* spp. und es wurden sogar einige Samen gefunden, die mit mehr als einer *Diaporthe*-Art infiziert waren, während andere Samen frei von den Pathogenen waren. Die Menge an Pilzbiomasse scheint zwischen einzelnen Samen sehr unterschiedlich zu sein.

1 Introduction

1.1. Soybean

Soybean (*Glycine max* (L.) Merr.) from the genus *Glycine*, is an annual subtropical plant and a member of one of the largest plant families, Fabaceae (Leguminosae) (Hartman et al. 2015). Soybean is grown as a commercial crop and is among the five most important agricultural crops in the world (Savary et al. 2019). The bulk of the world's soybeans are processed into the two fractions meal and oil.

Soybean seeds contain 18-22% oil and 38-42% protein and are the best sources of unsaturated fatty acids and vital amino acids (Patil et al. 2018). The major part of soybean oil (95%) is employed as vegetable oil and the rest (5%) utilized for products such as cosmetics and hygiene items (Liu, 2008). 98% of soybean protein is made into soybean meal for animal feed and 2% is processed to make soy flours, and soy food products such as tofu, soybean milk, soy hamburger and many others for human consumption (Goldsmith, 2008).

Soybean is originally from China where it was domesticated over 3,000 years ago and nowadays in addition to China it is grown in other Asian countries, the Americas, Africa, and Europe (Hartman et al. 2015). Soybean is produced in large scale predominantly in the Americas with roughly 37% (144,000 million tons) of the world's supply produced in Brazil, 31% (119,884 million tons) in the USA, and 13% (52,000 million tons) in Argentina, but only 0.7% (2,800 million tons) in the European Union (EU) in 2021-2022 (USDA-FAS, 2022). The EU countries import 95% of their demand for soybean especially from the Americas (European commission, 2019). However, soybean production in the EU is increasing. This is due to a search for vegetarian protein sources as part of a strategy to reduce the dependence on imports. Also, there is a preference for not genetically modified (non-GM) products. In addition there are agronomical and ecological reasons for more soybean production in Europe. European agriculture needs more diversification and would benefit from an additional N-fixing legume that also has high economic value. This would help introduce new rotations and reduce pests, diseases, and weeds in the main crops that dominate so far (Coleman et al. 2021). As a result, the production in Europe not only for soybean but also for other important grain legumes such as feed peas, field beans, and sweet lupins has been increasing over the past few years (www.donausoja.org) (Figure 1.1). The acreage of soybean has doubled from 2011 to 2018 and it is still possible to massively increase soybean production. In 2018 4.3 million ha in Europe were planted with soybean what yielded

10 million tons of soybeans. Soybean cultivation up to 6 million ha seems realistic by 2025, which would be an increase of 40 % from 2018 (www.donausoja.org). The expected harvest (15 million tons) would cover 35 - 40 % of consumption in the EU, which currently amounts to around 40 million tons of soy (beans equivalent).

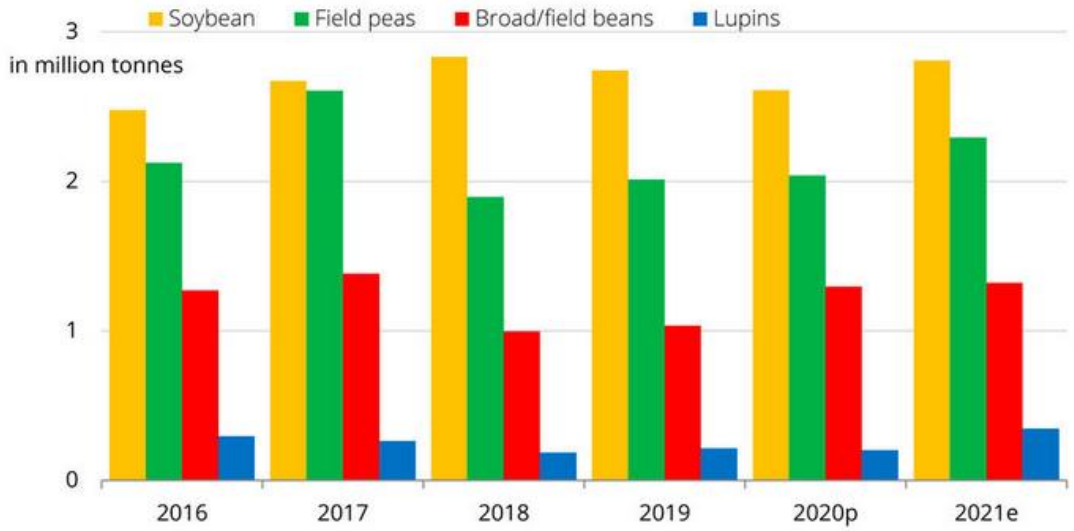

Figure 1.1: Harvest amount of the main legumes in the EU.
Legume production has grown considerably in the EU up to 2021. Soybean is considered the primary legume crop, and accounts for around 43 % of grain legume production. Due to larger soybean acreage and also rising yields approximately 2.8 million tons could be harvested in 2021, which was 8 % more than 2020. (e = estimate, p = preliminary; source: European Commission)

By a large margin Italy is the biggest soy producer among the EU countries. The acreage there accounts for almost a third of the entire area in the EU. Second is Romania with 173,000 ha. Until 2017 that was France. Other countries in the EU all make up for portions below 10 % of the total (IDH and IUCN NL, 2019).

1.2. Cultivation of soybean in Germany

Since 2000 soybean is cultivated in Germany and the area under cultivation and yield have expanded significantly between 2015 and 2021 or 2022 respectively as can be seen in Table 1.1 and Figure 1.2. Due to a constant increase in soybean acreage from the south of Germany to northern states, production of soybean has risen more than tenfold since 2012. The soybean area for 2021 was 34,300 ha, which was up 1.4 % year-on-year. According to the German Federal Statistical Office, around 104,000 tons of soybeans were harvested in Germany in 2021, the largest amount so far. Bavaria and Baden-Württemberg in the south of Germany are the foremost states with 80 % of the soybean acreage (www.destatis.de).

Table 1.1: Development of soybean area under cultivation in Germany from 2007 to 2022 (https://www.sojafoerderring.de/links-mehr/statistik/)

(Flächen in ha)	2007	2008	2009	2010	2011	2012	2013	2014	2015	2016	2017	2018	2022
Bayern	411 (84)	339	953 *(197)*	2423	3002	2682	3773	4279	7248	6629	8.400	12.465	**30.400**
Baden-Württ.	279	260	382	734	1031	1410	2178	2836	5899	5866	6.565	7.246	**8.700**
Brandenburg	0	2	85	62	165	236	330	1233	1132	693	400	600	**2.200**
Hessen			8 öko				90	160	436	392	500	700	**1.700**
Mecklenb.-Vorp.								179	365	242	200	200	**700**
Niedersachsen								300	380	351	500	700	**1.300**
Nordrhein-Westf.					10	45	75	140	142	197	225		**800**
Rheinland-Pfalz (GA)	17	22	22		48	96	145	140	250	*200?*	*250*	*374*	**k.A.**
Saarland								10	5	20	25	21	**100**
Sachsen			9	64	101	108	121	143	386	*200?*	*400*	*500*	**1.500**
Sachsen-Anhalt		67	61	114	199		356	555	1014	887	1.000	900	**2.700**
Thüringen	6	1	21	44	148	145	349	203	343	300?	300	300	**800**
Deutschland	900 ?	800 ?	1.500 ?	3.500 ?	4.500	5.000	7.500	10.000	17.600	15.770	19.100	24.100	**51.400**

In 2021 yields were relatively high, especially compared to the low yields of the drought year 2020. In Brandenburg they rose by 65 %; Baden-Wuerttemberg, Lower Saxony and Hesse also reported increases of 37 - 48 % (Figure 1.2).

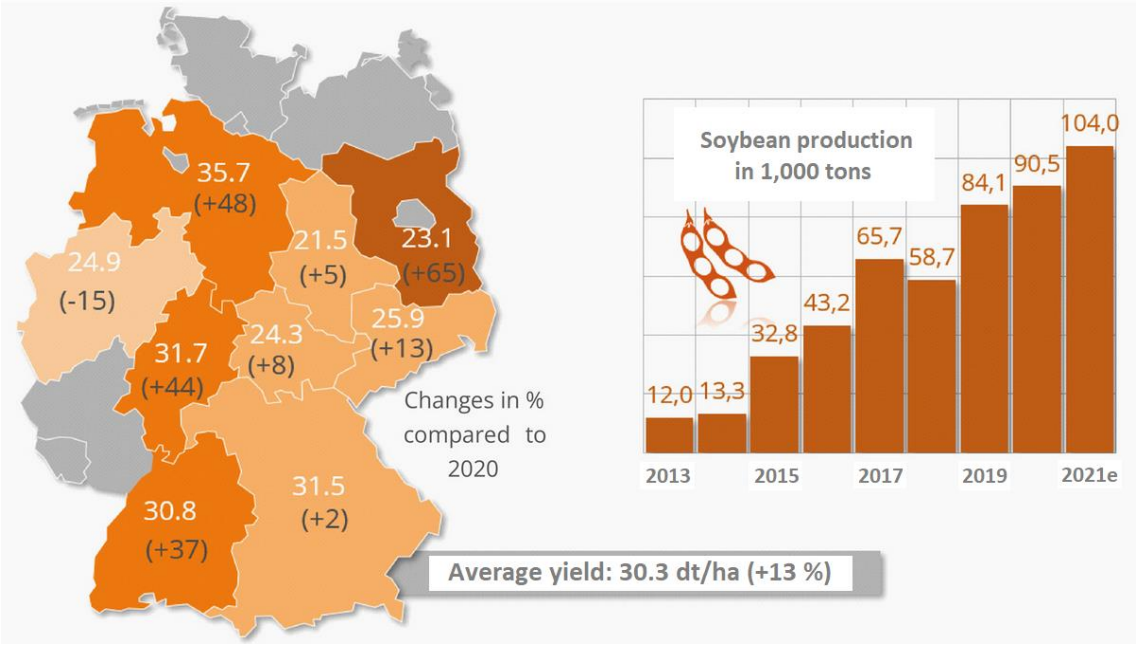

Figure 1.2: Soybean yields in Germany in 2021.
Map on the left shows decitonnes per hectare (dt/ha), graph on the right shows total soybean production in Germany. (e = estimate; source: Federal Statistical Office)

1.3. Soybean plant growth stages

The stages of a soybean plant can be assigned clearly according to the numbering system presented below. Moreover, this system can be utilized to describe disease incidence at a definite stage of soybean growth. For disease assessment, first a sample of soybean plants (individual leaves or plants, group of plants, or all plants in a pot) are selected randomly. The severity of infection for each unit in the sample is calculated and averaged. Then the vegetative stage is determined by using Table 1.2.

Vegetative (V) and reproductive (R) growth stages are considered separately (Table 1.2). The two primary stages are called VE (emergence) and VC (cotyledon), and the next V stages are numbered based on how many trifoliate leaves have grown. By definition the reproductive stages begin when the first flower appears and from there the plant develops through pod formation, seed development, and plant maturation.

Table 1.2: Soybean plant growth stages (Hartman et al. 2015)

Stage	**Vegetative**
VE	Emergence: cotyledons above soil surface.
VC	Cotyledon: unifoliolate leaves unrolled sufficiently so leaf edges are not touching.
V1	First node: fully developed leaves at unifoliate node.
V2	Second node: fully developed trifoliate leaf at first node above unifoliate node.
V3	Third node: three nodes on main stem with fully developed leaves, beginning with unifoliate node.
VN	N: number of nodes on main stem with fully developed leaves, beginning with unifoliate nodes.
Stage	**Reproductive**
R1	One flower at any node.
R2	Flower at node immediately below uppermost node with completely unrolled leaf.
R3	Pod 0.5 cm long at one of four uppermost nodes with completely unrolled leaf.
R4	Pod 2.0 cm long at one of four uppermost nodes with completely unrolled leaf.
R5	Beans beginning to develop (can be felt when pod is squeezed) at one of four uppermost nodes with completely unrolled leaf.
R6	Pod contains full-sized green beans at one of four uppermost nodes with completely unrolled leaf.
R7	Pods yellowing; 50 % leaves are yellow (physiological maturity).
R8	95 % of pods are brown (harvest maturity).

1.4. Challenges and threats to production

There are several important abiotic and biotic threats to soybean production that can reduce yield and/or seed quality (Hartman et al. 2011). Abiotic factors are nutrient availability, salinity, photoperiod, and weather. The abiotic problems can be ameliorated by careful crop management except for drought, flooding, and frost. A new challenge is climate change, which has major impact on agriculture that needs to react to new weather patterns with changes in temperatures and rainfall (Nelson et al. 2009). Increased levels of CO_2 (Cure and Acock, 1986; Mendelsohn et al. 1994), and specifically elevated temperatures in central

Europe will actually profit soybean production. These changes also may influence some soybean pathogens and alter their importance (Eastburn et al. 2010).

Pathogens, pests, and weeds as biotic threats cause considerable damages to soybeans. The Compendium of Soybean Diseases and Pests (Hartman et al. 2015) lists more than 300 diseases, 35 of which are highly important. In the first edition of this book (Sinclair and Shurtleff, 1975) only 50 diseases were mentioned. Intensive production and cultivation of soybean around the world can be reasons for the increased number of diseases and their spread. Continuous growth of soybean or short two year rotations are conducive for some pathogens that can increase to high densities. This was not the case with former less intensive ways of cultivation, so that only now these pathogens are causing problems. The populations of soybean pests like aphids, beetles, mites, and stinkbugs are increasing as well (O'Neal and Johnson, 2010). The severity of damages are determined by the pathogen and its inoculums and which parts of the plant are affected. On the other hand, weather, susceptibility or resistance of the host plant and whether the plants are growing under optimal conditions or not also play a role together with the plant growth stage (Hartman and Hill, 2010). To reduce losses, several measures are needed. These can be cultural and seed treatment techniques, efficient diagnostics, pesticide and fungicide use, and choice of resistant cultivars (Hartman and Hill, 2010).

In soybean, fungi can cause reduction of seed germination or seedling emergence, diseases of roots and damping-off. In addition, there are foliage and pod diseases that greatly impact seed quality and quantity (Vidić et al. 2013; Hartman et al. 2015). This makes fungi the most important pathogens in soybean. The most frequent soybean fungal pathogens are listed below (Table 1.3) (Hartman et al. 2015). Often, more than one fungal pathogen attack the plants at the same time and it is challenging to distinguish them by the symptoms.

Some of the fungal pathogens introduced in Table 1.3 are not reported from soybean plants in Europe up to now, for example *Phakopsora pachyrhizi* (Asian soybean rust) and *Fusarium virguliforme* (Sudden death syndrome). Recently *Peronospora manshurica* (downy mildew), *Macrophomina phaseolina* (Charcoal rot), *Sclerotinia sclerotiorum* (white mold), and the *Diaporthe* spp. (seed decay, stem canker, and pod and stem blight) have been determined to be the most aggressive pathogens in soybean fields in Europe (Krsmanovic et al. 2020; Wirtz et al. 2021). Since overall in Germany - especially in recent years - the *Diaporthe*/*Phomopsis* Complex (DPC) causes more losses than any other fungal disease of the soybean (Bachteler and Miersch, 2018; Wirtz et al. 2021; www.sojafoerderring.de), this research was focused on studying *Diaporthe* species.

Table 1.3: Fungal pathogens causing soybean diseases

Common name	Causal organisms
Anthracnose	*Colletotrichum truncatum*
Brown spot	*Septoria glycines*
Charcoal rot	*Macrophomina phaseolina*
Pod and stem blight	*Diaporthe sojae*, *Diaporthe* spp.
Phomopsis seed decay[1]	*Diaporthe longicolla*, *Diaporthe sojae*, *Diaporthe* spp.
Stem canker	*Diaporthe caulivora*[2], *Diaporthe aspalathi*[3], *Diaporthe* spp.
Downy mildew	*Peronospora manshurica*
Frogeye leaf spot	*Cercospora sojina*
Fusarium root rot	*Fusarium* spp.
Phytophthora root and stem rot	*Phytophthora sojae*
Purple seed stain/*Cercospora* leaf blight	*Cercospora kikuchii*
Sudden death syndrome	*Fusarium virguliforme*
Rhizoctonia aerial blight	*Rhizoctonia solani*
Asian soybean rust	*Phakopsora pachyrhizi*
Sclerotinia stem rot (white mold)	*Sclerotinia sclerotiorum*
Brown stem rot	*Phialophora gregata*

[1] Petrovic et al. (2021) proposed that *Phomopsis* seed decay be called *Diaporthe* seed decay (DSD).
[2] Santos et al. (2011) shortened the name of *Diaporthe phaseolorum* var. *caulivora* to *D. caulivora* and at the same time also proposed that it should be considered as a separate species.
[3] The previous name of *Diaporthe aspalathi* was *D. phaseolorum* var. *meridionalis* (Santos et al. 2011).

1.5. *Diaporthe*/*Phomopsis* Complex

The genus *Diaporthe* Nitschke (1870) and its asexual states *Phomopsis* (Sacc.) Bubák belongs to the Ascomycota, class Dothideomycota, order Diaporthales, family Diaporthaceae. The genus, also known as *Diaporthe*/*Phomopsis* Complex (DPC), includes several hundreds of species.

In order to avoid competition and confusion in the use of two names, which are used according to the sexual or asexual morph, according to the Rossman recommendation, the older generic name *Diaporthe* has priority over *Phomopsis* for this species complex (Rossman et al. 2015). So, new species of the genus should no longer be named *Phomopsis*, even if no sexual structures can be observed (Chepkirui and Stadler, 2017).

Diaporthe species are widely distributed around the world and they can be non-pathogenic endophytes (biotrophic fungi) in many plants or grow as saprobes (saprotrophic fungi). On the other hand, they are pathogens of many important crops and can even grow as parasites on humans and animals (van Warmelo et al. 1970; Udayanga et al. 2011; Gomes et al. 2013). Pathogenic *Diaporthe* species can grow in plant tissue without causing clearly visible symptoms for a long time. But later they do kill the host tissue and so they should be categorized as hemibiotrophs (Udayanga et al. 2011).

Phytopathogenic species of *Diaporthe* have been seriously studied, particularly those associated with economically important crops such as soybean, sunflower, grapes, citrus, and several diseases associated with fruit and ornamental trees (Udayanga et al. 2012).

Multiple species in the genus *Diaporthe* cause stem canker, pod and stem blight, and seed decay on soybean (Table 1.3), which lead to considerable yield losses, both quantitatively and qualitatively (Backman et al. 1985; Sinclair, 1993; Petrovic et al. 2021). These soybean diseases are introduced below.

1.5.1. *Diaporthe* seed decay

Diaporthe seed decay (DSD) decreases seed quality and occurs in the majority of soybean producing countries, which results in severe yield losses (Sinclair, 1993). The primary causal agent of seed decay is *D. longicolla* along with *D. sojae* and other species of *Diaporthe*. Seeds that are infected with a large amount of the fungus are cracked or split, shriveled, and usually fungal mycelium can be seen on their surface (Figure 1.3 B, C) (Hepperly and Sinclair, 1978). However, sometimes the infected seeds are symptomless and they look healthy (Kulik, 1984).

Figure 1.3: *Diaporthe* seed decay symptoms.
A) Heavily infected soybean field (Image: Crop protection network, soybean disease management, CPN-1007). **B**) Soybeans infected by *Diaporthe* spp. (Image by Daren Mueller, Iowa State University, Bugwood.org.). **C**) Disease symptoms on infected soybeans may be visible or nonvisible (Own image).

Germination of severely infected seeds may be decreased due to seed rot or seedling blight (Sinclair, 1993; Begum et al. 2008). The fungi penetrate into the seeds and colonize the seed coat, cotyledons, and finally the radicle and plumule. Consequently the composition of fatty acids is altered and the protein content of seeds is reduced (Hepperly and Sinclair, 1978; Wrather et al. 2003). *D. longicolla* is principally categorized into seed borne pathogens, but it can also be isolated from stems and pods (Mengistu et al. 2009).

1.5.2. Stem canker

Stem canker has been separated into Northern stem canker and Southern stem canker due to its initial descriptions. *D. caulivora* and *D. aspalathi* are known as the causal agents of

Northern and Southern stem canker, respectively. Northern stem canker was reported for the first time in Iowa in the late 1940s. Until the 1950s the disease spread into the northern Midwestern states of the USA and Canada. The first report of Southern stem canker was in the south of the USA (Mississippi) in 1973. Until 1984 it was detected in all southern states (Backman et al. 1985). Southern stem canker has slight differences in symptomology to Northern stem canker. Southern isolates of stem canker were more aggressive than northern isolates and they are distinguishable in cultural features (Backman et al. 1985).

Cankers in Northern stem canker are dark-brown and sunken, located on the lower nodes of soybean plants, and they become visible right after flowering (R1). Cankers first form on one side of the stem and then may grow over several nodes and at some point around the stem, girdling it, which leads to wilting and death of the plant (Figure 1.4 A). Lesions of Southern stem canker are more delimited and seldom grow around the stem. Both stem canker diseases cause the foliar symptoms chlorosis and necrosis because the fungi produce a phytotoxin and when plants die, leaves remain attached to the stem (Lalitha et al. 1989). The dead soybean plants can be observed in patches in fields (Figure 1.4 B). The affected plants frequently produce fewer and smaller seeds. Stem canker on susceptible cultivars can lead to 50 % yield loss in favorable conditions. Sometimes, a canker is formed on the upper internodes by *Diaporthe* species, killing only the top of the plant (top dieback) (Figure 1.4 C).

Figure 1.4: Stem canker symptoms.
A) Brick red lesions form at the nodes on soybean stems. Later they may expand and girdle the stem and cause premature death of the plants. **B**) Diseased plants can be found in patches within fields. **C**) The cankers on upper nodes lead to top dieback of the plants. (Images by Craig R. Grau, University of Wisconsin–Madison, Crop protection network, soybean disease management, CPN-1006)

Sometimes, however, the stem canker pathogen is growing in the plant but no lesions are formed.

1.5.3. Pod and stem blight

Pod and stem blight is caused by *D. sojae* and the infection often occurs early. The pathogen initially lives in the plant without causing visible symptoms but when the plant is maturing

(R6 to R8) abundant black pycnidia on stems (in linear rows) and pods (in diffused form) appear as a key disease symptom (Mueller et al. 2015) (Figure 1.5).

Figure 1.5: Pod and stem blight symptoms.
On infected soybean stems and pods pycnidia (black dots) are produced. (Image by Craig R. Grau, University of Wisconsin–Madison, Crop protection network, a product of Land Grant Universities)

Due to the growth and accumulation of fungi the upper plant parts may show chlorosis and die. Only if pods become infected, seed decay occurs and has an effect on seed quality.

1.6. *Diaporthe* disease cycle

The species of the genus *Diaporthe* overwinter in harvest residues or in the soil for several years. Weeds as alternative hosts could play a role for survival in the soil as well (Vrandečić et al. 2005, 2010; Thompson et al. 2015). Infected soybean seeds are considered as the most important source of inoculum, as they have the capability to spread *Diaporthe* species to fields that were previously free of these pathogens. Fungal fruiting bodies (pycnidia and perithecia), which are formed on infested residues, ooze spores (conidia and ascospores). Spores are spread by rain splash and wind early in the growing season and infect young plants (Figure 1.6).

Cankers on stems normally do not appear during the vegetative stages of soybean growth but only become visible upon entry of the plants into the reproductive stages. Spores are produced and secondary infections are caused by them. These later infections do not have a significant impact on disease development, however. In case of pod and stem blight, the fungus attacks pods during the R5 and R6 growth stages and if the infection is severe, the seeds are decayed. Once the plants move into the R7 growth stage, pod colonization declines drastically.

Despite the great importance of *Diaporthe* pathogens, many details regarding infection and colonization of soybean are still unclear. Little is known about the penetration mechanism and about virulence factors like phytotoxins or effectors, even information on which tissues are colonized by which species and which symptoms are caused can still be unreliable since molecular diagnosis of the species in different tissues has been little applied so far.

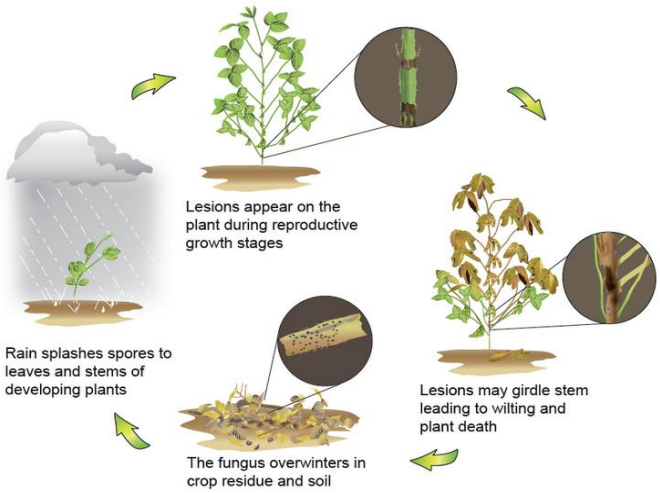

Figure 1.6: Northern stem canker disease cycle.
The disease is most problematic in warm and humid conditions. During the early stages of soybean growth the fungal spores are spread to lower tissues of soybean stems causing stem canker characteristics. Seed decay takes place through pod development (R3-R8) and delayed harvest can lead to more severe seed infection. (https://cropprotectionnetwork.org/encyclopedia/stem-canker-of-soybean)

1.7. *Diaporthe* management

To prevent introduction and spread of *Diaporthe* pathogens in soybean production regions disease management tactics can be applied before and after soybean planting, which are described below.

1.7.1. Before planting

Diaporthe species are seed borne pathogens. Severely decayed seeds may fail to germinate. Infected seeds can also germinate but the seedlings show damping-off and they cannot continue to grow and become mature plants (Sinclair, 1993). Therefore, the first thing to do for management of DSD, is seed health testing. Conventional seed testing methods include seed examination by visual inspection, selective culture media, seedling grow-out assay, and serological assays. All of these have restrictions like inefficiency and low sensitivity (Brill et al. 1994; Li, 2011; Kumar et al. 2020). Alternatively, molecular methods can be put to use. They can be more sensitive, specific, easy to implement, and fast. Molecular methods have made good progress to detect *Diaporthe* spp. in seeds (Zhang et al. 1997, 1998, 1999; Santos et al. 2011). However, real-time PCR and multiplex PCR assays have not been developed into routine seed-testing methods in laboratories.

Fungicides can be effectively used for seed treatment when more than 15 % of seeds are infected (Hobbs et al. 1985) even though by current recommendations seed samples like this should not be used. Seed germination, and consequently seedling emergence and yield can be

enhanced by applying fungicide (Xue et al. 2007). The same study also showed that treatment of seeds with *Bradyrhizobium japonicum* and the biocontrol agent *Clonostachys rosea* in addition to the fungicide, can have an additional effect (Xue et al. 2007).

The most economical, effective, and environmentally friendly method to manage DSD is selecting resistant soybean varieties (Jackson et al. 2005; Li, 2011). Soybean cultivars exist that have different levels of DSD resistance in different locations depending on weather conditions (Li and Chen, 2013; Li et al. 2017 a). DSD-resistance genes have also been detected and there is promise in breeding plans for DSD-resistant soybean cultivars (Jackson et al. 2005, 2009).

Warm and wet conditions are favorable for *Diaporthe* reproduction. Therefore, the possibility of *Diaporthe* infection is reduced by planting soybean cultivars that mature outside the most humid period in the year (Reicks, 2017).

Considering the importance of crop debris as harbor for *Diaporthe* pathogens in winter, conventional tillage can be beneficial to accelerate the rate of residue decomposition and reduction of disease (Tyler et al. 1983; Reicks, 2017). It is necessary to remove crop residues and soils from agricultural machines before using them in another field to prevent the transfer of inoculum (Backman et al. 1985; Roth et al. 2020).

Crop rotation can reduce the *Diaporthe* inoculum. Rotations with corn or other cereal crops that are non-hosts are effective against *Diaporthe* stem canker (Li et al. 2015 a).

1.7.2. During the growing season

The chance of seed decay would be higher when potassium is lacking. For that reason, the soil must be fertilized regularly to keep sufficient quantity of potassium (Reicks, 2017).

Proper irrigation and management of other diseases are also important. Drought stress and infestations with nematodes and soybean mosaic virus were found to enhance soybean susceptibility to *Diaporthe* pathogens (Backman et al. 1985; Koning et al. 2001, 2003).

Spraying foliar fungicides during early vegetative stages of soybean plants which show mild to moderate disease symptoms might be efficient to reduce disease severity (Backman et al. 1985).

Well-timed harvesting to prevent exposition of plants to favored conditions, will reduce the risk of seed decay and preserve seed quality (Roth et al. 2020).

1.8. Identification of species of *Diaporthe*

Species recognition in *Diaporthe* has long been based on host association, morphology, culture appearance, and pathogenic characteristics (van der Aa et al. 1990; van Niekerk et al.

2005). As shown by early ITS sequencing in the genus (Rehner and Uecker, 1994), some *Diaporthe* spp. are not limited to just one host. Therefore, in these days the host has little importance to classification of these fungal pathogens.

1.8.1. Morphological identification

The first to reassess the genus *Diaporthe* on a morphological basis was Wehmeyer (1933). Plating surface sterilized soybean seeds on the surface of acidified potato dextrose agar (APDA) plates and evaluation of fungal growth is still a common method to identify *Diaporthe* spp. (Walcott, 2003).

Black and thin perithecia containing asci (singular: ascus) on fungal cultures or plant tissues indicate the *Diaporthe* sexual state (teleomorph phase) (Figure 1.7 A).

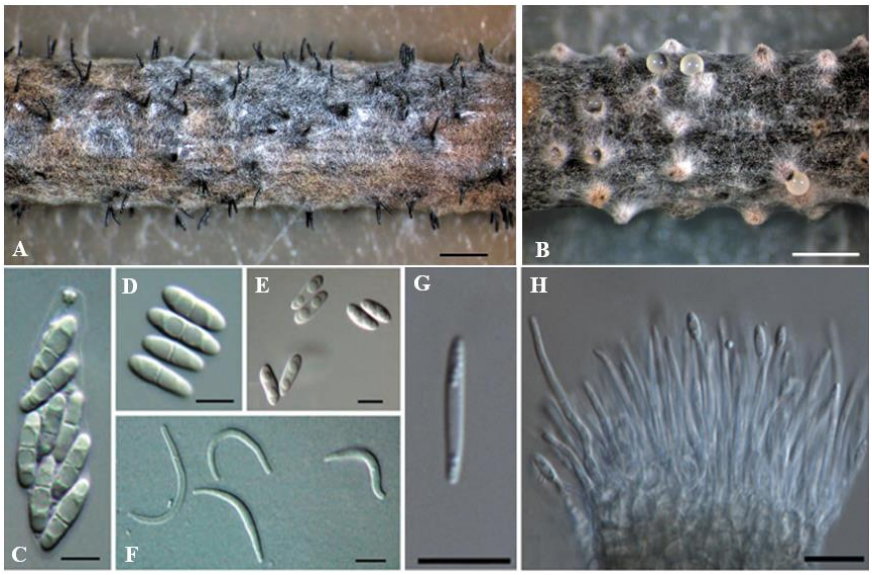

Figure 1.7: Sexual and asexual form of *Diaporthe* species.
A) *D. caulivora* perithecia on *Foeniculum vulgare* stem in culture (CBS H-20461). **B**) *D. longicolla* pycnidia on *F. vulgare* stem in culture (CBS H-20460). **C**) *D. phaseolorum* ascus with 8 ascospores and **D**) Ascospores (PSu1). **E**) *D. phaseolorum* α-conidia on *F. vulgare* stem in culture (PS03) and **F**) β-conidia (PS03). **G**) *D. endocitricola* (ZHKUCC 20-0012, Holotype) Gamma conidia. **H**) *D. endocitricola* (ZHKUCC 20-0012, Holotype) conidiogenous cells and conidiophores. Scale bars (**A**, **B**) 1 mm, (**C**, **D**, **E**, **F**) 5 µm, (**G**, **H**) 10 µm. (Images **A**, **B**, **C**, **D**, **E**, and **F** Santos et al. (2011), images **G** and **H** Dong et al. (2021))

Asci are unitunicate, ellipsoid, widest at the centre and rounded towards the apices, with a conspicuous refractive apical ring and they usually contain eight ascospores (Figure 1.7 C). Ascospores are biseriate to uniseriate in the ascus, fusoid, ellipsoid to cylindrical, straight, inequilateral or curved, septate, and hyaline (Figure 1.7 C, D) (Udayanga et al. 2011). For asexual reproduction (anamorph phase) black to dark brown pycnidia (singular: pycnidium) or pycnidial conidiomata (singular: conidioma) are formed (Figure 1.7 B). Conidiophores are subcylindrical to cylindrical, hyaline, smooth, 1–3-celled, simple or often branched and can release two kinds of conidia, which are hyaline and non-septate and known as α- and

β-conidia (Figure 1.7 H) (Rehner and Uecker, 1994). Some species may produce a third type of conidia which is called gamma (Rosskopf et al. 2000) (Figure 1.7 G). α-conidia are unicellular, aseptate, hyaline, fusiform and usually biguttulate. However, sometimes α-conidia have no guttules and sometimes they have more than two (Figure 1.7 E). β-conidia are aseptate and hyaline as well, but they are filiform, straight or more often hamate and eguttulate (Figure 1.7 F) (Sutton, 1980). Gamma conidia are hyaline, multiguttulate, fusiform to subcylindrical with an acute or rounded apex, while the base is sometimes truncate (Figure 1.7 G) (Rodeva et al. 2009).

Because of overlaps in conidial size and similar conidia and colors and shapes of cultures it is not reliable to delimit species of *Diaporthe* based on morphology alone (Santos et al. 2011; Udayanga et al. 2011; Gomes et al. 2013). Some characteristics like color and shape of mycelium, growth rate, and types of conidia, can even be different on different culture media and depending on the length and conditions of incubation (Brayford, 1990).

Some species can also be distinguished based on different aggressiveness (quantitative variation of pathogenicity or virulence (Pariaud et al. 2009)). Apart from species identification knowledge about aggressiveness of different species is also important for resistance breeding (Keeling, 1988; Kontz et al. 2016; Ghimire et al. 2019). Aggressiveness on soybean has been recorded for *D. caulivora*, *D. aspalathi*, *D. longicolla*, *D. pseudolongicolla*, *D. eres*, *D. kongii*, *D. sojae*, *D. ueckerae*, *D. unshiuensis*, *D. bacilloides*, *D. flavescens*, and *D. insulistroma* isolates (Li et al. 2010; Petrovic et al. 2015, 2018, 2021; Mena et al. 2020).

1.8.2. Molecular identification

Fungi, like other species, can be classified based on sequence data. Molecular phylogenies have been created for several important pathogenic genera (Shenoy et al. 2007; Cai et al. 2011).

The polymerase chain reaction (PCR) that was developed in the 1980s and its applications have also been broadly used for plant pathogen detection (Lau and Botella, 2017; Hariharan and Prasannath, 2021).

In PCR the DNA sequence that is defined by two primers is amplified *in vitro*. This involves a series of temperature changes, first high temperature (94–98 °C) to separate the DNA strands (denaturation), then lower temperature (50–65 °C) for primer binding and then 72 °C for amplification by the *Taq* polymerase, a heat insensitive enzyme. The PCR reaction generally needs a DNA that includes the sequence of interest (the template), deoxynucleoside

triphosphates (dNTPs), the *Taq* polymerase or one of many alternative polymerases, the already mentioned primers that are oligonucleotides with a sequence that is complementary to the target, and finally a buffer that makes everything work. The temperature sequence described above is repeated in cycles. Only the sequence between the primers is amplified because in later cycles the primers bind also to the product from the first cycles, which then becomes dominant. Roughly, the amount of PCR product doubles with every cycle (Figure 1.8).

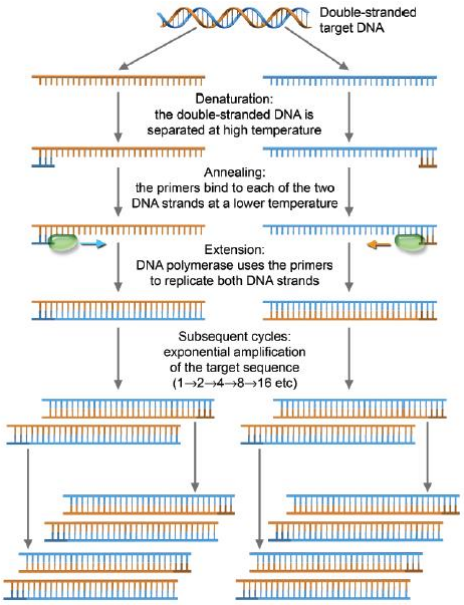

Figure 1.8: Representation of the PCR reaction.
PCR is carried out in three steps: denaturation, annealing, and extension. The new DNA strands are employed as a template for subsequent replication steps which leads to an amplification of the DNA section between the primers. The amount of PCR product is increased nearly two times in each cycle. (https://www.vetfolio.com/learn/article/polymerase-chain-reaction-test-interpretation)

To ensure that the target DNA was amplified, agarose gel electrophoresis is run after performing PCR. Then the PCR products can be sequenced using the same primers which were used for amplification. The obtained sequences are analyzed by comparing with the NCBI GenBank database (https://www.ncbi.nlm.nih.gov/) using BLAST analysis. The species is identified from the species tags attached to the sequences that were found by BLAST.

Genetic diversity in the *Diaporthe* genus was explored successfully by applying PCR assays (Zhang et al. 1997, 1998; Santos et al. 2011). The nuclear ribosomal internal transcribed spacer region (ITS) as a fungal barcode is used commonly for discrimination of *Diaporthe* spp. (van Rensburg et al. 2006; Santos and Phillips, 2009; Schoch et al. 2012). The ITS region has also been employed to develop specific primers to identify *Diaporthe* species. Phom. I and Phom. II primers were designed based on ITS sequences of *D. phaseolorum* and

D. longicolla to detect many *Diaporthe* spp. in soybean plants and seeds by Zhang et al. (1997). The primers DphLe and DphRi were developed to identify *D. phaseolorum* var. *meridionalis* in soybean seeds (Vechiato et al. 2006). Three species-specific TaqMan primer-probe sets PL-3, PL-5, and DPC-3 were designed based on ITS sequences to identify *D. longicolla*, *D. aspalathi*, *D. caulivora*, and *D. sojae* (Zhang et al. 1999).

However, there are species that cannot be reliably resolved with only ITS sequence data (Farr et al. 2002; Santos et al. 2017). Distantly related taxa can be nicely delineated based on ITS sequences. But in comparisons of many species from many hosts ITS fails. Branches in phylogenetic trees should divide into two sub-branches. Nodes like this can be assumed to be resolved. In ITS phylograms of *Diaporthe* with large numbers of taxa nodes with more than two branches can be found. Since the sequences are so similar, there are ITS phylogenies that are probably incorrect (Farr et al. 2002). Therefore, assessing various genes individually or combined is necessary to categorize species of *Diaporthe* correctly. The combination of translation elongation factor 1-α (*TEF1*), beta-tubulin (*TUB*), calmoduline (*CAL*), histone-3 (*HIS*), and large ribosomal subunit (*LSU*) can be used for differentiation of *Diaporthe* species (Udayanga et al. 2015; Petrovic et al. 2016; Chaisiri et al. 2020).

Several PCR-based diagnostic methods have been reported for the identification of *Diaporthe* spp.. Random amplified polymorphic DNA (RAPD), PCR-restriction fragment length polymorphism (RFLP), and amplified fragment length polymorphism (AFLP) methods have been used to distinguish species of *Diaporthe* (Fernández and Hanlin, 1996; Zhang et al. 1997, 1998; Moleleki et al. 2002; Brumer et al. 2018). The differences between the *D. phaseolorum* varities *caulivora*, *meridionalis*, and *sojae* (now defined as different species) were found using RAPD (Fernández and Hanlin, 1996). Zhang et al. (1997) implemented PCR-RFLP to distinguish *D. longicolla*, *D. caulivora*, *D. aspalathi*, and *D. sojae*.

1.9. Real-Time PCR (qPCR) as a tool for the diagnosis of plant pathogens

PCR methods can be improved by real-time monitoring of amplification of a targeted DNA by a fluorescent signal during the PCR. This eliminates the post-PCR processing (running agarose gels), reduces time significantly, and increases the throughput considerably. In addition, qPCR also allows quantification (the q symbolizes this).

The amplification curve of a real-time PCR reaction has three phases (Figure 1.9 A). In the initiation phase, the PCR products are not accumulated enough to emit a fluorescence signal

that is strong enough to be distinguished from the background, caused for example by the template DNA. The background is measured as the baseline, meaning the signal level during the early cycles, typically 3 to 15. As the PCR processes, the additional fluorescence is doubled approximately in every cycle. This phase is named exponential or log phase. The PCR reagents are used gradually by continuing of the reaction and the reaction is slowed and no increase in fluorescence is observed. This last phase defines as the plateau phase.

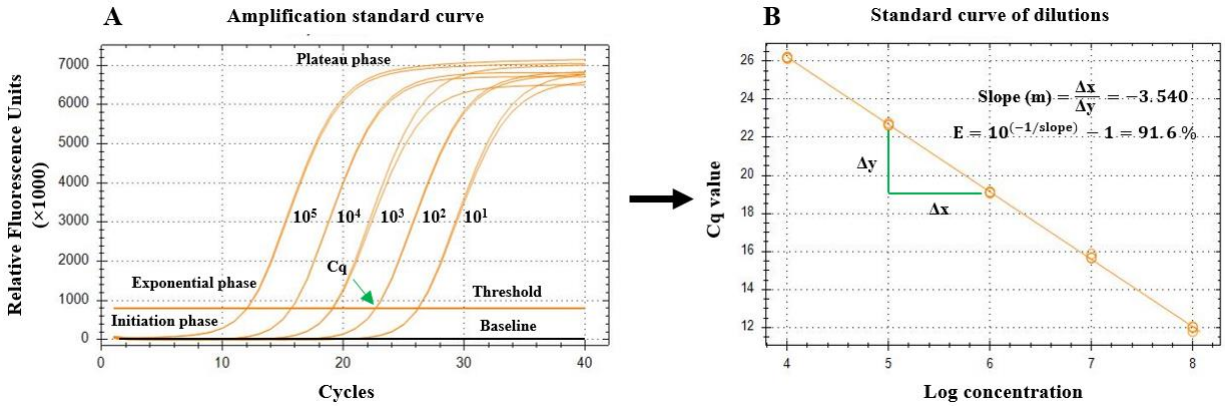

Figure 1.9: Real-Time PCR.
A) Illustration of real-time PCR amplification curves. An optimal real-time (q)PCR plot consists of three phases: initiation, exponential and plateau. **B**) A real-time (q)PCR standard curve for quantification. The x-axis represents copies of the DNA, and the cycle threshold is shown on the y-axis, m = Slope of the regression line, E = the efficiency of PCR reaction (Own images).

The threshold in real-time PCR is the point at which the fluorescence intensity rises clearly above the background. It is normally shown as an even line. This line should intersect the amplification curve close to the start of the exponential phase (Figure 1.9 A). The cycle threshold (Ct) or quantification cycle (Cq) value is the number of cycles it takes the fluorescence intensity to cross the threshold. If there is less target DNA it takes more cycles for the fluorescence intensity to reach the threshold, so higher Cq values represent less target DNA than lower Cq values.

The efficiency (E) in PCR means the fraction of target molecules copied in every cycle. PCR efficiency is determined through standard curves. From standard curves also the limit of detection can be read (Svec et al. 2015). Building a standard curve means to make a series of solutions with known template concentrations (Figure 1.9 B). This is normally a dilution series starting with a concentrated sample with 1:10 dilution steps. Then qPCR is run. The resulting Cqs are used in linear regression against the target concentrations in logarithmic scale. Ideally the slope of the resulting regression line (the standard curve) should be -3.32, which represents 100 % efficiency or doubling of PCR product in each cycle. The efficiency can depend on the length, secondary structure, and GC content of the PCR product. PCR inhibitors and primers and probes also influence efficiency (Svec et al. 2015). Ironically the

apparent efficiency that can be read from the standard curve may be higher than 100 % when PCR inhibitors are present or primer dimers or other artefacts are formed in the reaction.

Real-time PCR can be used quantitatively as well (Hariharan and Prasannath, 2021). For absolute quantification also the standard curve is needed. Since this was constructed with known target concentrations, the target concentrations can also be read from it or rather calculated using the graph formula. For relative quantification Cq values of a target gene are normalized with the Cq values of a reference gene (Livak and Schmittgen, 2001). To quantify pathogens on or in plant material a third option is often used: this is to put the amount of fungal DNA into relation of either total DNA or plant DNA. If the pathogen DNA should be relative to total DNA it is necessary to measure the DNA concentration in all samples that are tested. To gain a value relative to plant DNA qPCR with a gene of the host plant needs to be run in parallel. To calculate the amount of DNA a standard curve for the plant gene is also necessary.

The most frequently used real-time PCR methods are the SYBR® Green dye-based and the TaqMan assays (Figure 1.10).

SYBR® Green is a fluorescent dye which intercalates into the minor groove of dsDNA. In elongation stages of each PCR cycle dsDNA is amplified and emission of SYBR® Green fluorescence is increased (Figure 1.10 A) (Okubara et al. 2005). SYBR® Green as an intercalating dye binds to any dsDNA non-specifically so it can detect different targets, which is an economical advantage. However, this advantage of SYBR® Green is also a disadvantage because it binds to all amplicons equally and the fluorescence signal can correspond to both non-specific and specific products. In the case of formation of non-specific products the identification and quantification would be incorrect (Giulietti et al. 2001).

In the TaqMan method in addition to two primers, another specific oligonucleotide which is known as probe is used. The probe is complementary to a target DNA sequence between the primers (Figure 1.10 B). The probe is labeled at the 5′ terminal nucleotide with a donor fluorophore (as reporter dye) and at the 3′ nucleotide with an acceptor dye (= Quencher).

When the polymerase reaches the probe, the probe is digested by the 5'-exonuclease activity of the *Taq* DNA polymerase. This way, the reporter is cleaved from the quencher and there is no longer energy transfer between the two dyes. After that fluorescence is 200 times stronger. Because fluorescence of SYBR® Green is only 20 fold when intercalated as opposed to free, the greater difference makes the TaqMan assay more sensitive. The TaqMan system is also more specific than SYBR® Green, because the probe can be designed to bind to a specific sequence (Okubara et al. 2005). Furthermore, the possibility of labeling probes with various

fluorescent dyes allows the detection of different target DNAs in a single reaction simultaneously (multiplex Real-Time PCR).

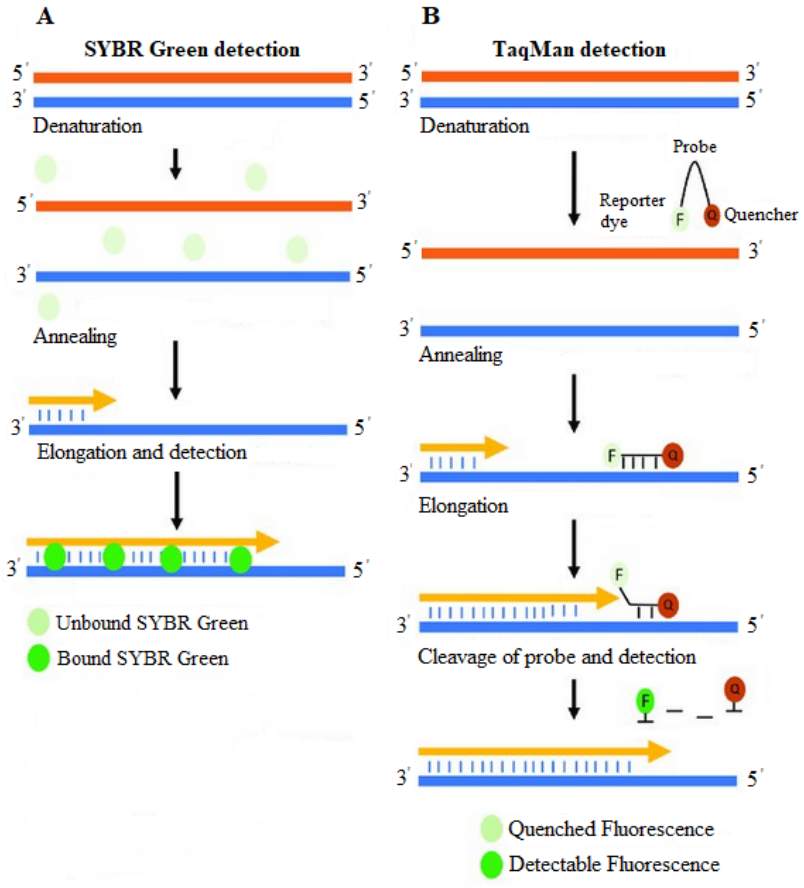

Figure 1.10: Intercalating dye (SYBR® Green) and hydrolysis-based (TaqMan) probe detection. **A**) SYBR® Green detection: SYBR® Green as an intercalating dye binds to dsDNA and in elongation steps of each PCR cycle by production of more amplicons fluorescent signal is increased and detected by the real-time PCR machine. **B**) TaqMan probe detection: TaqMan probes are designed to bind downstream of the primers. When the polymerase reaches the probe its 5' nuclease digests it. Because the fluorophore is no longer close to the quencher moiety fluorescence is emitted (Adams, 2020).

Ongoing interest in the availability of real-time PCR as a quick, sensitive, and quantitative assay for detection and/or quantification of soybean pathogens in plant tissues, soil, and seed samples has resulted in the development of many successful assays (Hartman et al. 2015). For pathogens infecting more than one host real-time PCR detection assays can be used for all hosts. Only the preparation of DNA for the assay may need some modifications. Existing real-time PCR assays based on SYBR® or Eva® Green and TaqMan for detecting fungal pathogens that are relevant in soybean production are listed in Table 1.4.

Table 1.4: Real-time PCR assays for detecting fungal soybean pathogens (Hartman et al. 2015)

Disease(s)	Targeted pathogen	Real-Time PCR Assay type	Reference
Anthracnose	*Colletotrichum* spp.	Eva® Green	Yang et al. 2015
Brown stem rot	*Phialophora gregata*	TaqMan	Malvick and Impullitti, 2007
Purple seed stain/*Cercospora* leaf blight	*Cercospora kikuchii*	TaqMan	Chanda et al. 2014
		SYBR® Green	Upchurch and Ramirez, 2010
Charcoal rot	*Macrophomina phaseolina*	SYBR® Green and TaqMan	Babu et al. 2011
Diaporthe seed decay	*Diaporthe longicolla*	TaqMan	Zhang et al. 1999
Pod and stem blight	*D. sojae*	TaqMan	Zhang et al. 1999
Stem canker	*D. caulivora* and *D. aspalathi*	TaqMan	Zhang et al. 1999
	D. aspalathi	SYBR® Green	Upchurch and Ramirez, 2010
Phytophthora root rot	*Phytophthora sojae*	SYBR® Green	Bienapfl et al. 2011
Asian soybean rust	*Phakopsora pachyrhizi* and *P. meibomiae*	TaqMan	Frederick et al. 2002
	P. pachyrhizi	TaqMan	Barnes et al. 2009
Sclerotinia stem rot	*Sclerotinia sclerotiorum*	TaqMan	Chen et al. 2010
Sudden death syndrome	*Fusarium virguliforme*	TaqMan	Mbofung et al. 2011; Westphal et al. 2014
	F. solani f. sp. *glycines*	TaqMan	Gao et al. 2004; Li et al. 2008

There are also existing qPCR assays to detect *Diaporthe* spp. on soybean. The first real-time PCR assay to detect and quantify *Diaporthe* spp. from soybean seeds was developed by Zhang et al. (1999). Three species-specific TaqMan primer-probe sets PL-3, PL-5, and DPC-3 were designed based on ITS sequences to identify *D. longicolla*, *D. aspalathi*, *D. caulivora*, and *D. sojae*. This assay (PL-3 and DPC-3) was also used by Kontz et al. (2016) to quantify the two stem canker pathogens, *D. caulivora* and *D. longicolla* in plant samples and to assess soybean resistance against these pathogens.

Upchurch and Ramirez (2010) studied the expression of 15 soybean defense-related genes via SYBR® Green real-time PCR assays by using specific primers (DPM) (Miller and Huhndorf, 2005) to detect and quantify *D. aspalathi* in infected soybean tissues. Mena et al. (2020) used DPM primers to quantify the fungal biomass in stems of soybean plants infected with *D. caulivora* by performing SYBR® Green real-time PCR assays.

1.10. Objectives

Because there is demand for regionally grown soybean, cultivation is expanding in Germany. The expansion of soybean cultivation harbors new risks for cultivation. It is to be expected

that soybean diseases and pathogens will increase in Germany in the near future, as has already been observed in other parts of the world. Diseases caused by pathogens from the *Diaporthe*/*Phomopsis* Complex (DPC) are of particular importance. The DPC species cause the most severe damages in soybean cultivation and they appeared also in Germany. *Diaporthe* fungi grow partially endophytic and often become pathogens only at the end of the plant's growth. They are still relatively hard to diagnose and especially in organic farming hard to combat. The DPC species are seed borne pathogens. Therefore, diagnosis is even more important, because spreading of the disease can be avoided through appropriate screenings.

The overall aim of this project was to identify which species of the DPC occur in central Europe, how widespread they are, and how frequently they occur. The findings should then contribute to monitoring of the pathogens and consequently lead to more efficient control. The way to reach this goal was divided into three stages:

First DPC species occurring in central Europe should be identified by testing contaminated soybean seeds using the classical seed plating assay. Identifying the species that could be isolated from these seeds necessitated the use of morphological features and molecular phylogenies. To ensure that the obtained isolates are true soybean pathogens also pathogenicity tests needed to be performed.

To establish the incidence of the species, an assay was needed that is able to specifically diagnose and quantify all relevant *Diaporthe* pathogens. This assay was to be applied for testing on a much grander scale and screening both soybean seeds, plants in the field and the fields (soil and residues) themselves. This necessitated the establishment of a highly efficient method for molecular diagnosis specific for the different species. The method of choice was multiplex real-time (q)PCR using TaqMan probes since this enables the detection of different species in parallel. The specific aim of the second stage was to establish a multiplex qPCR that can detect, distinguish, and quantify all relevant *Diaporthe* species in parallel. This assay should be usable not only for the epidemiological studies planned as stage three of this project but also be applicable for standard testing of seed lots and investigating the aggressiveness of different *Diaporthe* isolates on different soybean cultivars, so it can be used as a tool to prevent epidemic spread and also as a tool in breeding. Optimally the established qPCR based method for diagnosis should be established as a new standard for identification of *Diaporthe* species in Germany. Therefore, different strategies for optimal application of the multiplex qPCR were also investigated.

This thesis describes in detail the isolation and identification of four *Diaporthe* species and the phylogenetic classification of all 32 isolates obtained. Improved species descriptions were

prepared. Also detailed are all steps in establishing a quadruplex real-time (q)PCR assay to detect and quantify these species in soybean plant materials.

The work on stage three is still ongoing. Wide screens of soybean seed are planned as well as sampling of soybean fields all over Germany.

2 Material and Methods

2.1. Chemicals

The chemicals used in this work were obtained from the following manufacturers unless otherwise noted in the text.

AppliChem	AppliChem GmbH, Darmstadt, Germany
Merck	Merck KGaA, Darmstadt, Germany
ROTH	Carl Roth GmbH + Co. KG, Karlsruhe, Germany
Rowa	Becton Dickinson Rowa France, Le Pont-de-Claix, France
SERVA	SERVA Electrophoresis GmbH, Heidelberg, Germany
Th. Geyer	Th. Geyer GmbH + Co. KG, Renningen, Germany

2.2. Kits

The kits used in this work are shown in Table 2.1.

Table 2.1: List of the kits, their application and manufacturers

Term	Application	Manufacturer
DNeasy Plant Mini Kit	DNA extraction	Qiagen, Hilden, Germany
peqGOLD Cycle-Pure Kit	PCR purification	Peqlab GmbH, Erlangen, Germany
peqGOLD Fungal DNA Mini Kit	DNA extraction	Peqlab GmbH, Erlangen, Germany
Qubit DNA BR Assay Kit	DNA quantification	Thermo Fisher Scientific, Waltham, MA, USA
SensiFAST™ Probe No-ROX Kit	Real-Time PCR	Bioline GmbH, London, UK
SensiFAST™ SYBR No-ROX Kit	Real-Time PCR	Bioline GmbH, London, UK

2.3. Plastic consumables

The plastic consumables used in this work are listed below and all except noted otherwise provided by the company Sarstedt (Sarstedt AG + Co. KG, Nümbrecht, Germany).

- Petri dishes (22 mL per 9.0 cm)
- Micro tubes and micro screw tubes (1.5 and 2 mL)
- PCR tubes (200 µL, Multiply®-µStrip Pro 8-strip)
- Falcon tubes (50 mL, 115 × 28 mm)
- Pipette tips (1 mL, 10, 20, and 200 µL) and Biosphere® Filter tips (1 mL, 10, 20, and 200 µL)
- FrameStar® 96-Well Skirted PCR Plates (4titude, Brooks Automation, Chelmsford, MA, USA)

- Sealing tape
- Parafilm (Parafilm M Laboratory Film, Bemis™ PM996, USA)
- Lysing Matrix E tubes, MP Biomedicals GmbH, Eschwege, Germany
- Container for plant tissue culture with lid (175 mL, sterile, Greiner Bio-One GmbH, Germany)

2.4. Technical devices

Technical equipment used in the present study is listed in Table 2.2.

Table 2.2: List of the devices

Technical device	Application	Origin
Cameras:		
AxioCam HRc color microscope camera	Photography	Carl Zeiss AG, Oberkochen, Germany
Camera G15	Photography	Canon, Tokio, Japan
Centrifuges:		
Centrifuge 5417 R	Centrifugation of contents of tubes	Eppendorf AG, Hamburg, Germany
MPS 1000 Mini Plate Spinner Centrifuge	Centrifugation of samples in PCR plates	Labnet International Inc., Edison NJ, USA
Sprout Mini Centrifuge	Centrifugation of contents of tubes briefly	Heathrow Scientifc LCC, Illinois, USA
Counting chambers (Hemocytometers):		
Counting chamber Paul Marienfeld	Determination of the concentration of spores	Paul Marienfeld GmbH + Co KG., Lauda-Königshofen, Germany
Counting chamber Fuchs-Rosenthal	Determination of the concentration of spores	BLAUBRAND®, GmbH + CO KG, Wertheim, Germany
DNA/RNA UV-Clearer	Providing protection against contamination	LTF Labortechnik GmbH + Co. KG, Wasserburg, Germany
FastPrep®-24 homogenizer	Homogenization of biological materials	MP Biomedicals GmbH, Eschwege, Germany
Gel electrophoresis chamber	Gel electrophoresis	Wissenschaftliche Werkstätten, Universität Konstanz, Konstanz, Germany
Gel documentation system (Quantum 1100)	Evaluation of agarose gels	PEQLAB GmbH, Erlangen, Germany
IKAMAG® RET basic magnetic stirrer with heater	Stirring of solutions	IKA®-Werke GmbH + Co. KG, Staufen, Germany
LaminAir HB 2448	Sterile bench	Heraeus Instruments, Hanau, Germany
Microscopes:		
Primo Star	Microscopy	Carl Zeiss AG, Oberkochen, Germany
Axioskop 2	Microscopy	Carl Zeiss AG, Oberkochen, Germany
Inverted microscope (no item name)	Single spore isolation	Carl Zeiss AG, Oberkochen, Germany

PCR-Cyclers:		
Bio-Rad C1000 touch thermal cycler	Amplification/PCR	Bio-Rad Laboratories Inc., Hercules, CA, USA
Eppendorf 5331 Mastercycler gradient thermal cycler	Amplification/PCR	Eppendorf AG, Hamburg, Germany
CFX96™ Real-Time PCR detection system	RT-(q)PCR	Bio-Rad Laboratories Inc., Hercules, CA, USA
Qubit® 2.0 Fluorometer	Quantification of nucleic acids	Thermo Fisher Scientific, Waltham, MA, USA
Rotational vacuum concentrator RVC 2-18	For fast and efficient vacuum concentration	Martin Christ GmbH, Osterode am Harz, Germany
Scales:		
Sartorius analytical balance (resolution up to 0.1 mg)	Weighing micro tubes (1.5 mL)	Göttingen, Germany
KERN KB 3600-2N (resolution up to 3610 g)	Weighting media, agarose, and chemical materials	Kern and Sohn GmbH, Balingen, Germany
Shaking incubator TH25	Shaker–Incubator	Edmund Bühler GmbH, Bodelshausen, Germany
Spectrometer:		
BioPhotometer® plus	Quantification of nucleic acids	Eppendorf AG, Hamburg, Germany
µCuvette® G 1.0	Sample carrier	Eppendorf AG, Hamburg, Germany
Stemi 2000 binocular loupe	Observation of pycnidia and perithecia	Carl Zeiss AG, Oberkochen, Germany
Thermomixer comfort 2 mL	Incubation of reaction mixtures	Eppendorf AG, Hamburg, Germany
Vortex-Genie 2	Mixing of Reaction mixtures	Thermo Fisher Scientific, Waltham, MA, USA

2.5. Software

Software used in this work to analyze the data is shown in Table 2.3.

Table 2.3: List of the software

Software	Application
AxioVision (Release 4.8.3 Special Edition 1, Carl Zeiss AG, Oberkochen, Germany)	Evaluation of pictures
BioEdit (version 7.1.3.0; Hall, 1999)	Biological Sequence Alignment Editor
CFX Manager™ (Bio-Rad Laboratories Inc., Hercules, CA, USA)	Real-Time PCR data acquisition and analysis
Gene Runner (Version 6.5.52x64 Beta, http://www.generunner.net/)	Evaluation of potential secondary structures of primers and probes
GENtle v. 1.9 (http://gentle.magnusmanske.de/) and EditSeq 5.06 and SeqMan 5.06, Lasergene Software Packet (DNASTAR, Madison, WI, USA)	Editing of DNA sequences, assemblies
MEGA-X, version 10.0.5 (https://www.megasoftware.net/, Tamura and Nei 1993; Kumar et al. 2018)	Construction of phylogenetic trees
Microsoft Excel® (Microsoft Corporation, Redmond, WA, USA)	Relative quantification

2.6. Culture media

PDA (Potato Dextrose Agar)

Potato dextrose agar	39 g
Distilled water	1,000 mL

To make APDA (Acidified Potato Dextrose Agar) medium, the pH of PDA medium was adjusted to 4.5 with lactic acid before autoclaving.

CJA (Carrot Juice Agar)

Carrot juice	500 mL
European Agar	15 g
Distilled water	500 mL

Carrot juice was obtained from dm-drogerie markt (Karlsruhe, Germany).

WA (Water Agar)

European Agar	20 g
Distilled water	1,000 mL

PDA, APDA, CJA, and WA culture media were autoclaved at 121 °C and 1.2 bar for 25 min and then cooled to approximately 50 °C with stirring. They were poured into Petri dishes under a sterile bench and allowed to solidify at room temperature (ca. 22 °C) for 24 h before use.

2.7. Buffers

EDTA

EDTA	0.5 M
pH (NaOH)	8.0

The solution was autoclaved and stored at room temperature.

Lysis buffer

Tris	400 mM
EDTA	60 mM
NaCl	150 mM
SDS	1 % (v/v)

The solution was autoclaved and stored at room temperature.

Potassium acetate buffer

Potassium acetate (5 M)	60 mL
Glacial acetic acid	11.5 mL
Distilled water	28.5 mL
pH	4.8

The solution was autoclaved and stored at 4 °C.

TAE (50x)

Tris base	242 g
Glacial acetic acid	57.1 mL
EDTA disodium salt (0.5 M)	100 mL
pH (NaOH)	8.0

For use the buffer was diluted to 1:50 with ddH_2O.

2.8. Solutions

Carboxymethylcellulose (CMC) 1 %

CMC	10 g
Distilled water	1,000 mL

The CMC powder was dissolved in water overnight by constantly stirring, and then the solution was autoclaved and stored at room temperature.

CMC-Polysorbate 20

CMC 1 %	1 L
Polysorbate 20 1 %	1 L

The solution was autoclaved and stored at room temperature.

Octoxinol-9 (Triton X-100) 1 %

Triton	10 mL
Distilled water	990 mL

The solution was autoclaved and stored at room temperature.

Polysorbate 20 (Tween 20) 1 %

Polysorbate	10 mL
Distilled water	990 mL

The solution was autoclaved and stored at room temperature.

Potassium acetate (5 M)

Potassium acetate	490.75 g
Distilled water	Up to 1,000 mL

The solution was stored at room temperature.

Sodium hypochlorite (NaOCl) 1 %

Commercial bleach (12 %)	83 mL
Distilled water	917 mL

The solution was stored at 4 °C.

2.9. Oligonucleotides

The primers used in this work for PCR experiments, sequencing, and real-time PCR assays are listed in Tables 2.4, 2.5, 2.6, and 2.7. The TaqMan primer-probe combinations for real-time PCR experiments were designed as part of this work (under 2.14.8.1.) except for PL-3 and DPC-3, which were designed by Zhang et al. (1999). All oligonucleotides were synthesized by Biomers.net GmbH (Ulm, Germany).

Table 2.4: Oligonucleotides for amplification and sequencing of targets for species identification and phylogenies

Target region	Primer	Sequence (5′→3′)	Tm (°C)	Fragment length (bp)	Reference
ITS	ITS1-F	CTTGGTCATTTAGAGGAAGTAA	54	600	[a]
	ITS4	TCCTCCGCTTATTGATATGC			[b]
TEF1	EF1-728F	CATCGAGAAGTTCGAGAAGG	58	350	[c]
	EF1-986R	TACTTGAAGGAACCCTTACC			
TUB	Bt-2a	GGTAACCAAATCGGTGCTGCTTTC	60	500	[d]
	Bt-2b	ACCCTCAGTGTAGTGACCCTTGGC			

F = Forward primer, R = Reverse primer
[a] Gardes and Bruns (1993), [b] White et al. (1990), [c] Carbone and Kohn (1999), [d] Glass and Donaldson (1995)

Table 2.5: Oligonucleotides for SYBR® Green-based real-time PCR assays

Gene symbol	Primer	Sequence (5′→3′)	Tm (°C)	Fragment length (bp)	Reference
GmUKN2	UKN2F	GCCTCTGGATACCTGCTCAAG	80	79	[a]
	UKN2R	ACCTCCTCCTCAAACTCCTCTG			

F = Forward primer, R = Reverse primer
[a] Hu et al. (2009)

Table 2.6: Oligonucleotides based on ITS sequences of *Diaporthe* isolates for TaqMan real-time PCR assays

Primer-probe set	Primer Probe	Sequence (5′→3′)	Tm (°C)	Reference
PL-3	PL-3 F	CAGAGATTCACTGTAGAAACAAGAGTTT	54	[a]
	PL-3 R	CCGGCCTTTTGTGACAAA	54	
	PL-3 P	FAM-CGGGCTGCTCCCTGTCTCCAG-BMN-Q535	63	
DPC-3	DPC-3 F	TTTATGTTTATTTCTCAGAGTTTCAGTGTAA	54	[a]
	DPC-3 R	GGCGCACCCAGAAACC	54	
	DPC-3 P	Cy5-CGGGCTGCTCCCCGTCTCC-BMN-Q620	68	
DPCE7	DPC-3 R	GGCGCACCCAGAAACC	54	[a]
	DE-7 R	TTATGTTTTGTGCTCAGAGTTTCAGTG	74	[b]
	DPE3-7 P	ROX-CCGRCGGGCTGTCTCAACACC-BMN-Q590	70	[b]
DPCE3	DPC-3 R	GGCGCACCCAGAAACC	54	[a]
	DE-3 R	TTGTGCTCAGAGTTTCAGTG	58	[b]
	DPE3-7 P	ROX-CCGRCGGGCTGTCTCAACACC-BMN-Q590	70	[b]
DPCE(1)	DPC-3 R	GGCGCACCCAGAAACC	54	[a]
	DE-3 R	TTGTGCTCAGAGTTTCAGTG	58	[b]
	DE-7 R	TTATGTTTTGTGCTCAGAGTTTCAGTG	74	[b]
	DPE3-7 P	ROX-CCGRCGGGCTGTCTCAACACC-BMN-Q590	70	[b]

	DPC-3 R	GGCGCACCCAGAAACC	54	[a]
DPCN8	DPN-8 R	CAGAGTTTAGTTGGCCAC	54	[b]
	DPN-8 P	FAM-CCAGGGGGCCTCAGTGAAGAG-BMN-Q530	70	[b]
	DPC-3 R	GGCGCACCCAGAAACC	54	[a]
DPCN11	DPN-11 R	GATTCACCCTAAAAACAGAG	56	[b]
	DPN-11 P	FAM-CTTCCGGGGGCGACCTCCTC-BMN-Q530	70	[b]

F = Forward primer, R = Reverse primer, and P = TaqMan Probe
[a] Zhang et al. (1999), [b] This work
The probes carry FAM, Cy5, or ROX dyes as reporter attached to the 5′-terminal nucleotide and BMN-Q535, BMN-Q620, or BMN-Q590, respectively, as quencher attached to the 3′-terminal nucleotide.
ITS is the target region for all these TaqMan primer-probe sets.
PL-3 and DPC-3 are TaqMan primer-probe sets, which were designed by Zhang et al. (1999) to detect *D. longicolla* and *D. caulivora*, respectively. DPCE7 and DPCE3 are TaqMan primer-probe sets for detection of *D. eres*. DPCN8 and DPCN11 are primer-probe sets for detection of *D. novem*.
The primer-probe set DPCE(1) is a mixture of own reverse primers DE-3 R, DE-7 R; primer DPC-3 R as forward primer; and probe DPE3-7 P.

Table 2.7: Oligonucleotides based on *TEF1* sequences of *Diaporthe* isolates for TaqMan real-time PCR assays

Primer-probe set	Primer Probe	Sequence (5′→3′)	Tm (°C)	Reference
	DPCL-F	TGTCGCACCTTTACCACTG	58	
DPCL	DPCL-R	GAACGATCCAAAAAGCTCTC	58	[a]
	DPCL-P	FAM-GCATCACTTTCATTCCCACTTTCTG-BMN-Q535	72	
	DPCC-F	GCCTGCAAAACCCTGTTAC	58	
DPCC	DPCC-R	CATCATGCTTTAAAAATGGGG	58	[a]
	DPCC-P	Cy5-CTCTTACCACACCTGCCGTCG-BMN-Q620	68	
	DPCE-F	ACTCACTCAATCCTTGTCAC	58	
DPCE	DPCE-R	GAGGGTCAGCATAATATTCG	58	[a]
	DPCE-P	ROX-CCATCAACCCCATCGCCTCTTTC-BMN-Q590	72	
	DPCN-F	AAAACCCTGCTGGCATTAAC	58	
DPCN	DPCN-R	TATTCTTGACAGTTCGTTTCG	58	[a]
	DPCN-P	HEX-TCTACCACTTTCAACCCTATCAATC-BMN-Q535	70	

F = Forward primer, R = Reverse primer, and P = TaqMan Probe
[a] This work
The probes carry FAM, Cy5, ROX, or HEX dyes as reporter attached to the 5′-terminal nucleotide and BMN-Q535, BMN-Q620, or BMN-Q590 as quencher attached to the respective 3′-terminal nucleotide.
TEF1 is the target region for all these TaqMan primer-probe sets.
DPCL, DPCC, DPCE, and DPCN are primer-probe sets for detection of *D. longicolla*, *D. caulivora*, *D. eres*, and *D. novem*, respectively.

2.10. Biological material

2.10.1. Soybean seeds (*G. max*)

Seed lots suspected to contain infected seeds with *Diaporthe* spp. from several locations in Germany, Austria, and France were obtained from Taifun-Tofu GmbH (Freiburg, Germany) and Landwirtschaftsbetrieb (LWB) Zschoche (Südliches Anhalt, Germany) (Table 2.8).

Healthy soybean seeds for controls and for inoculation experiments (apparently healthy; cv. Sultana and Anushka) were received from the Landwirtschaftliches Technologiezentrum (LTZ) Augustenberg (Karlsruhe, Germany).

Table 2.8: Infected soybean seeds were selected from this collection which is listed along with geographic origins

Soybean cultivar	Origin	Region (city/parish)
Anushka 2 [a]	Germany	Südliches Anhalt
Silvia PZO	Austria	Biedermannsdorf
Sigalia	Austria	Bruck / Leitha
Primus	Austria	Buggingen
Sultana	Austria	Deutsch Wagram
Primus [a]	Austria	Dt. Jarndorf
Primus [a]	Austria	Ebergrassing
Sigalia	Austria	Engelhartsstetten
CH 22177	Austria	Haslau
CH 22232	Austria	Haslau
Silvia PZO	Austria	Haslau
Sigalia	Austria	Haslau / Donau
Gallec	Austria	Königstetten
Gallec	Austria	Neuaigen
Amadine	Austria	Oberösterreich
Merlin	Austria	Oberösterreich
Malaga	Austria	Oberösterreich
Primus [a]	Austria	Oberweiden
Korus	Austria	Seyring
Gallec	Austria	Wipfing
Gallec	Austria	Zeiselmauer
Sultana [a]	Germany	Rheinau
Pollux [a]	France	Voiron

[a] Seed samples from these seed lots were screened in order to detect and quantify the amount of *Diaporthe* pathogens via real-time (q)PCR assays (under 2.14.10).

2.10.2. Soybean fungal pathogens

Plates with the soybean pathogens *Sclerotinia sclerotiorum* (Lib.), *Colletotrichum truncatum* (Schwein.), *Cercospora kikuchii* T. Matsumoto &Tomoy., (1925), *Fusarium tricinctum* El-Gholl (1978) and spores of three rust species: *Phakopsora pachyrhizi* (Syd.), *Uromyces fabae* (Bary ex Cooke), and *Uromyces appendiculatus* (Unger) were selected from the University of Hohenheim Phytopathology laboratory collection. For *S. sclerotiorum* two isolates were utilized: *S. sclerotiorum* DSM 1946 (GenBank Accession: MH857810.1; DSMZ, Braunschweig, Germany) and *S. sclerotiorum* IZS (own isolate).

Pure cultures of *Fusarium solani* (Mart.), two isolates of *Alternaria spp.*, and four strains of the *Diaporthe* species *D. longicolla*, *D. eres*, *D. aspalathi*, and *D. foeniculina* (Table 2.9) were obtained from Kristina Petrović (Institute of Field and Vegetable Crops, Novi Sad, Serbia).

The fungi were cultured on plates with acidified potato dextrose agar (APDA) or potato dextrose agar (PDA) for 10 days at 25 ± 2 °C and then they were kept at 10 °C. Agar plugs of

the cultures were transferred to fresh plates regularly to preserve the strains. The rust fungi were propagated on their different host plants.

Table 2.9: *Diaporthe* strains received from Institute of Field and Vegetable Crops in Serbia and their corresponding GenBank accession numbers

Isolate no.	Species	GenBank Accession	
		ITS	*TEF1*
PL-157a / PDS157A	*D. longicolla*	JQ697845	JQ697858
PS-74	*D. eres*	JF430488	JF461474
DC-27(1) / 17-DIA-034	*D. aspalathi*	MK942646	MK941268
PS-22	*D. foeniculina*	JF430495	JF461481

2.10.3. Production of healthy soybean plants

2.10.3.1. Pre-treatment of soybean seed samples

The surface of apparently healthy soybean seeds (cv. Sultana and Anushka) was disinfected by rinsing in 1% NaOCl solution for 30 s. Then the seeds were washed with sterile distilled water and dried on filter paper.

2.10.3.2. Planting soybeans

After surface sterilization, the seeds were incubated in plastic boxes containing wet filter papers (Rotilabo® germ test paper, Carl Roth GmbH + Co. KG, Karlsruhe, Germany) to obtain high humidity at RT. After 7 days, healthy germinated seeds were selected and cultured in pots (2 L) containing a mixture of 50% seedling substrate (Klasmann-Deilmann GmbH, Geeste, Germany) and 50% soil (Gebr. Patzer GmbH, Sinntal-Altengronau, Germany). The pots were kept in the greenhouse at 28 °C under a light/dark cycle of 16/8 h.

2.11. Isolation of *Diaporthe* strains

To isolate *Diaporthe* pathogens from infected seeds (Table 2.8), the method described by Walcott (2003) with some modifications was used.

2.11.1. Plating the seed samples on culture media

21 soybeans were selected randomly from each seed lot (Table 2.8). The surface sterilized seeds were placed on the surface of APDA plates using sterilized forceps (7 seeds per plate).

2.11.2. Incubation

Plates were sealed with Parafilm (Parafilm M Laboratory Film, Bemis™ PM996, USA) and incubated at 24 ± 1 °C under a 12 h light/dark regime. A small agar plug with each putative *Diaporthe* isolate was transferred to a fresh APDA plate. These plates were incubated under the same conditions for 30 - 40 days.

2.11.3. Single spore isolates

For single spore isolates the method published by Choi et al. (1999) was used starting with spore suspensions. Fruiting bodies oozing conidia/ascospores were removed from the surface of a culture of the fungi using sterilized forceps and transferred into sterile water (200 µL) in a 1.5 mL micro tube. The micro tube was then stirred with a vortex to obtain a homogeneous spore suspension. Sixteen squares were marked on the reverse side of a WA plate to help with locating the germinating spores later. Then, 50 µL of the spore suspension were transferred by pipetting onto the surface of the WA plate and spread using a sterile glass rod. The plate was incubated at RT and checked using a microscope within 12 h and then every 24 h to observe germination. When germination of spores was seen, a small piece of agar medium with a single germinated spore was picked up with a sterilized syringe. This was put onto a fresh APDA plate and incubated at 24 ± 1 °C under a 12 h light/dark regime. The cultures were checked after few days; if there was no contamination, a pure culture was obtained.

2.12. Morphological identification of *Diaporthe* species

2.12.1. Colony appearance

Colony appearance of the *Diaporthe* isolates was compared to *Diaporthe* species descriptions in different publications (Nitschke, 1870; Athow and Caldwell, 1954; Kulik, 1984; Hobbs et al. 1985).

2.12.2. Presence of pycnidia and perithecia on APDA cultures

The cultures were also examined with a Stemi 2000 binocular loupe or a Primo Star microscope to check for pycnidia and conidiophores with α- and β-conidia or perithecia with asci and ascospores. For the preparation of microscope slides, lactophenol blue solution (Carl Roth GmbH + Co. KG, Karlsruhe, Germany) was used as staining agent. Pictures were taken with an AxioCam HRC color camera and dimensions of conidia and ascospores were evaluated with AxioVision software.

2.12.3. Evaluation of perithecia and pycnidia production by *Diaporthe* isolates on soybean stems in *in vitro* experiments

To promote the formation of perithecia, stems from four weeks-old healthy soybean plants were cut into 1 cm pieces and they were autoclaved at 121 °C and 1.2 bar for 25 min. The autoclaved stem pieces were placed at the margin of WA plates (five stem pieces per plate). Afterwards, 0.5 × 0.5 cm agar plugs with fungal mycelium of *Diaporthe* isolates were placed in the center of the plates. As control a sterile agar plug was put in the center of WA plates

along with five soybean stem pieces. The plates were incubated at 24 ± 1 °C under a 12 h light/dark regime. The experiment for each of the *Diaporthe* isolates was done in triplicates and production of perithecia and pycnidia was assessed constantly for two months.

2.12.4. Induction of perithecia in *Diaporthe* isolates on Carrot Juice Agar (CJA)

To induce sexual reproduction in *Diaporthe* isolates, the Klittich and Leslie (1988) method was used with some modifications. An agar plug (0.5 × 0.5 cm) taken from a fresh culture of a *Diaporthe* isolate was put into the centre of a CJA plate. The plates were sealed with parafilm and incubated at 25 °C under UV light (256 nm). When mycelium reached the margin of the plates, it was carefully scraped from the surface with a scalpel. One mL 1 % Triton X-100 was spread on the surface using a glass rod. Again the plates were incubated under UV light using the same conditions. Mycelium growing back was again scraped from the plates once it became visible (normally once a week). At the same time the plates were checked for perithecia/pycnidia. Once reproductive structures were observed the treatment was stopped.

2.13. Pathogenicity test

2.13.1. Preparation of spore (conidia/ascospore) suspensions

To produce spores for each *Diaporthe* isolate, the method described under 2.12.4. was used. Once enough pycnidia/perithecia oozing conidia/ascospores were visible on the plates, the plates were used to prepare spore suspensions. CMC-Polysorbate 20 solution (50 mL) was spread on each petri plate with a culture of a *Diaporthe* isolate that was producing an abundance of spores. The mycelium, pycnidia/perithecia, and the spores were carefully detached from the CJA medium using a sterile scalpel. The suspension was filtered through a funnel covered with four layers of sterile gauze (Paul Hartmann AG, Heidenheim, Germany) to remove mycelia and the spore suspension was transferred into an Erlenmeyer flask. One Erlenmeyer flask was also filled with 50 mL CMC-Polysorbate 20 solution as control. The tools used were previously autoclaved and carefully sterilized and flamed after each work step.

2.13.2. Counting spores (conidia/ascospore) with a Hemocytometer

The number of spores in the spore suspensions were counted under the microscope using a Paul Marienfeld Counting chamber (hemocytometer). 20 µL of the spore suspension were placed in each two rectangular grid structures (chambers) ground into the hemocytometer slide in the lower and upper area. The slide was sealed with a cover glass and the spores in the

five quadrants of each chamber were then counted under the microscope. Formula 2.1 was used to calculate the concentration of spore suspensions:

Formula 2.1: Calculation of the number of spores per 1 µL spore suspension

$$\text{spores per } \mu L = \frac{\text{number of spores}}{\text{area } (mm^2) * \text{chamber depth } (mm) * \text{dilution}}$$

- The area of the smallest square was 0.0025 mm^2 and the chamber depth was 0.1 mm.

2.13.3. Inoculation of soybean seeds with spore suspensions

Prior to inoculation, 400 randomly selected Anushka seeds (apparently healthy) were disinfected (under 2.10.3.1.) and then they were incubated in humid chambers under the same condition as described in 2.10.3.2. After 7 days, healthy germinated seeds were selected for inoculation. For each *Diaporthe* isolate, nine germinated seeds were inoculated by soaking in 50 mL spore suspension (4.405×10^4 spores/µL + CMC-Polysorbate 20) in Erlenmeyer flasks for 30 min at RT. Also, nine healthy germinated seeds were transferred into the one Erlenmeyer flask containing just 50 mL CMC-Polysorbate 20 and soaked for 30 min at RT as control treatments.

2.13.4. Planting of the inoculated soybean seeds

The inoculated nine seeds for each *Dipaorthe* isolate were grouped into three groups of three seeds and planted into pots (12 L) with a mixture of 50 % seedling substrate and 50 % soil. A randomized complete block design was used for the pots. Greenhouse conditions were 28 °C and a light/dark cycle of 16/8 h.

2.13.5. Evaluation of stem and pod disease

The plants were first checked for symptoms of stem and pot blight after 3 months and again one, two, and three weeks later. Stem and pod blight symptoms were graded using the self-made disease severity scales shown in Table 2.10 and Table 2.11.

Table 2.10: Stem disease severity scale

	Disease severity scale
0	No symptoms
1	< 25 % of the stem covered with pycnidia
2	26 - 50 % infected area
3	51 - 75 % infected area
4	76 - 100 % fungal structures on almost the whole stem

Table 2.11: Pod blight disease severity scale

	Disease severity scale
0	no changing color
0.5	less than 50 % appearance of brownish color areas on pods
1	> 50 % brownish color areas on pods

2.14. Molecular methods

2.14.1. DNA Extraction

2.14.1.1. DNA extraction from fungal strains

2.14.1.1.1. DNA extraction from fungal strains using the protocol by Liu et al. (2000)

The single spore cultures of the *Diaporthe* strains isolated in this study, *Diaporthe* isolates obtained from Institute of Field and Vegetable Crops in Serbia (Table 2.9), and other important soybean fungal pathogens (2.10.2.) were used for DNA preparation. The isolation of DNA was carried out based on the protocol by Liu et al. (2000). Mycelia were scraped from ten days-old fungal cultures and transferred to 1.5 mL micro tubes containing a few microbeads (Lysing Matrix E tubes) and 500 µL lysis buffer. The tubes were then left at RT for 10 min and during this incubation time the mycelia were homogenized three times by vortexing (30 s). Since this method involves a potassium acetate precipitation, 150 µL potassium acetate buffer was added in the following step. The tubes were vortexed briefly and centrifuged for 1 min at 12,000 rcf. The supernatants were transferred to new 1.5 mL tubes and centrifuged again as described above. Then, the supernatants were transferred carefully to new 1.5 mL tubes and an equal volume of isopropyl alcohol (650 µL) was added. The contents of the tubes were mixed by inversion briefly, centrifuged for 2 min at 10,000 rcf, and the supernatants were discarded. In order to wash the resultant DNA pellets, 300 µL of 70 % ethanol were added and centrifuged for 1 min at 10,000 rpm. The alcoholic supernatants were removed carefully and the DNA pellets were dried for 20 min in a rotary vacuum concentrator. Finally, the DNAs were dissolved in 30 µL of ddH_2O and they were stored at -20 °C.

2.14.1.1.2. DNA extraction from fungal strains using the peqGOLD Fungal DNA Mini Kit

Genomic DNA was prepared from *Diaporthe* isolates (Table 2.12 [a, b]) using the peqGOLD Fungal DNA Mini Kit to test the TaqMan primer-probe combinations.

Mycelia were scraped from ten days-old fungal cultures and transferred to 1.5 mL micro tubes containing a few microbeads (Lysing Matrix E tubes) and 400 µL lysis buffer PL1. Then 15 µL RNase A was pipetted into the micro tubes and they were vortexed for 10 s. The tubes were incubated for 30 min at 65 °C in the heating block (Thermomixer) and they were vortexed 3-4 times for 10 s during incubation. After incubation, 100 µL lysis buffer PL2 was added, mixed by vortexing and the tubes were incubated for 5 min on ice. The lysate was centrifuged for 10 min at 20,000 rcf. The supernatant was pipetted into a Microfilter which was placed in a 2 mL collection tube and centrifuged for 1 min at 10,000 rcf. The flow-through

was transferred into a new 1.5 mL tube and 0.5 volumes (225 µL) of DNA binding buffer was added and mixed well by pipetting. Afterwards, the entire mixture was applied into a PerfectBind DNA column which was placed in a 2 mL collection tube. This was followed by centrifugation for 1 min at 10,000 rcf. The flow-through liquid and collection tube were discarded and the column was placed into a new 2 mL collection tube and 650 µL DNA wash buffer was added. It was centrifuged for 1 min at 10,000 rcf and the flow-through was discarded. Another 650 µL DNA wash buffer was added to the column and then centrifuged again for 1 min at 10,000 rcf. After discarding the flow-through, the empty column and collection tube set was centrifuged for 2 min at 10,000 rcf to dry the column completely. In the last step, the column was placed in a new sterile 1.5 mL tube and to elute DNA, 30 µL ddH_2O was pipetted into the column, incubated for 3 min at RT, and centrifuged for 1 min at 6,000 rcf. The DNA was stored at -20 °C until use.

Table 2.12: *Diaporthe* strains and their corresponding GenBank accession numbers used to test the specificity and sensitivity of the TaqMan primer-probe sets

Isolate no.	Species	GenBank Accession	
		ITS	*TEF1*
DPC_HOH20 [a, d, e]	*D. longicolla*	MK024695	MK099112
DPC_HOH28 [b, c]		MK024703	MK099120
DPC_HOH2 [a, b, c, d, e]	*D. caulivora*	MK024677	MK099094
DPC_HOH3 [a, b]	*D. eres*	MK024678	MK099095
DPC_HOH7 [a, c, d, e]		MK024682	MK099099
DPC_HOH8 [a]	*D. novem*	MK024683	MK099100
DPC_HOH11 [a, c, e]		MK024686	MK099103
DPC_HOH15 [b, d]		MK024690	MK099107

[a] Extracted DNA from mycelium of these *Diaporthe* isolates and also their PCR products was used to test the specificity of the TaqMan primer-probe sets in the real-time PCR assays
[b] Extracted DNA from mycelium of these *Diaporthe* isolates was used to test the specificity of the TaqMan primer-probe sets in the quadruplex real-time PCR assays
[c] Extracted DNA from different amounts of mycelium of these *Diaporthe* isolates was subjected to real-time (q)PCR reactions to construct standard curves for absolute quantification
[d] Spore suspensions of these *Diaporthe* isolates were used in the real-time (q)PCR assays to construct standard curves for absolute quantification
[e] Extracted DNA from mycelium of these *Diaporthe* isolates was used in the real-time (q)PCR assays to construct standard curves for relative quantification

2.14.1.1.3. DNA extraction from fungal strains using the DNeasy Plant Mini Kit

DNA from ten days-old cultures of *Diaporthe* isolates (Table 2.12 [e]) was extracted using the DNeasy Plant Mini Kit to prepare serial dilutions and make standard curves for quantification. Mycelia were scraped from the fungal cultures, transferred to Lysing Matrix E tubes containing 400 µL buffer AP1 and homogenized by vortexing. Then 4 µL RNase A was pipetted into the micro tubes. The tubes were vortexed briefly and incubated for 10 min at 65 °C in the heating block. Each tube was inverted three times during incubation. Then, 130 µL buffer P3 was added, mixed and the tubes were incubated for 5 min on ice. The lysate was centrifuged for 5 min at 20,000 rcf. The supernatant was pipetted into a QIAshredder spin

column which was placed in a 2 mL collection tube and centrifuged for 2 min at 20,000 rcf. The flow-through was transferred into a new 1.5 mL tube carefully without disturbing the pellet. Then, 795 µL buffer AW1, which corresponds to 1.5 times the amount of the lysate, was added to the lysate and mixed by pipetting. In the next step, 650 µL of the mixture were transferred into a DNeasy Mini spin column which was placed in a 2 mL collection tube. This was followed by centrifugation for 1 min at 6,000 rcf. The flow-through was discarded and the remaining amount of the mixture was added to the same DNeasy Mini spin column. It was centrifuged again for 1 min at 6,000 rcf and the flow-through was discarded. The column was placed into a new 2 mL collection tube and 500 µL buffer AW2 was added. It was centrifuged for 1 min at 6,000 rcf and the flow-through was discarded. Another 500 µL buffer AW2 was added to the column and then centrifuged for 2 min at 20,000 rcf. The spin column was removed from the collection tube carefully without coming into contact with the flow-through and it was placed in a new sterile 1.5 mL tube. For elution, 25 µL ddH_2O was pipetted into the column, incubated for 3 min at RT, and centrifuged for 1 min at 6,000 rcf. This step was repeated once more, resulting in a total of 50 µL of solution and it was stored at -20 °C until use.

2.14.1.2. DNA extraction from plant material

Stem samples (each 2 cm) were ground in liquid nitrogen using mortar and pestle for 2 min. Leaf samples (≤ 100 mg) were frozen for 3 min in liquid nitrogen in 2 mL micro screw tubes containing 2 steel spheres (4.50 mm, Niro, Sturm Präzision GmbH, Oberndorf am Neckar). Then the tubes were inserted into the FastPrep®-24 homogenizer. This was run for 20 s at 4 m/s. To avoid heating of the material the tubes were returned to liquid nitrogen for 1 min. Homogenization and cooling was repeated two more times.

For preparation of DNA from seeds, surface-disinfected soybean seeds were soaked in water for 20 min and squeezed to remove their seed coats. Seed coats were placed individually in 2 mL micro screw tubes containing 2 steel spheres, frozen for 3 min in liquid nitrogen, and homogenized using the FastPrep®-24 homogenizer as described above. Uncoated soybean seeds and whole seeds were ground individually in liquid nitrogen by using mortar and pestle for 3 min.

Homogenized plant material (≤ 20 mg) was transferred to 1.5 mL tubes containing 400 µL buffer AP and vortexed. The remainder of the preparation was done using the DNeasy Plant Mini Kit as described in 2.14.1.1.3.

2.14.1.3. DNA extraction from rust pathogens

Spore samples (about 50 mg) of *Phakopsora pachyrhizi* (Syd.), *Uromyces fabae* (Bary ex Cooke), and *U. appendiculatus* (Unger) were ground individually in liquid nitrogen for 2 min using mortar and pestle and isolation of DNA was carried out based on the protocol (Liu et al. 2000) by Heike Popovitsch.

2.14.2. PCR

2.14.2.1. PCR using Phusion DNA polymerase

Three genomic markers, the internal transcribed spacer (ITS) region of the nuclear ribosomal DNA, parts of the translation elongation factor 1-α (*TEF1*) and beta-tubulin (*TUB*) of single spore *Diaporthe* strains isolated in this study, were amplified using the primer pairs ITS1-F/ITS4, EF1-728F/EF1-986R, and Bt-2a/Bt-2b (Table 2.4). PCR reactions were carried out in a Bio-Rad C1000 touch thermal cycler. The amplification was performed in 40 µL reactions and Phusion DNA polymerase (Thermo Fisher Scientific, Waltham, MA, USA) was used for the amplification of target gene fragments for sequencing. The pipetting scheme and the PCR program for PCR are shown in Table 2.13 and Table 2.14.

Table 2.13: Pipetting scheme for a 40 µL PCR reaction with Phusion DNA polymerase

Reagents	Volumes (µL)
5x Phusion HF buffer [a]	8
dNTPs (2 mM) [a]	4
Forward-Primer (5'→3') (10 pmol/µL)	1
Reverse-Primer (3'→5') (10 pmol/µL)	1
Template DNA	1
Phusion DNA polymerase [a] (2 U/µL)	0.4
ddH_2O	24.6
Final volume	40

[a] Thermo Fisher Scientific, Waltham, MA, USA

Table 2.14: PCR program for one PCR reaction with Phusion DNA polymerase

Phase	Temperature (°C)			Time (min:s)		
	ITS	*TEF1*	*TUB*	ITS	*TEF1*	*TUB*
1. Initial denaturation	98	98	98	0:30	0:30	0:30
2. Denaturation	98	98	98	0:10	0:10	0:10
3. Annealing	54	58	60	0:20	0:50	0:15
4. Elongation	72	72	72	0:35	0:35	0:15
5. Repetition from phase 2. – 4. 35 x						
6. Final elongation	72	72	72	10:00	10:00	7:00
7. Final hold	8	8	8	indefinite	indefinite	indefinite

2.14.2.2. PCR using *Taq* polymerase

ITS and *TEF1* regions were amplified using ITS1-F/ITS4 and EF1-728F/EF1-986R primers in individual reactions for *D. longicolla*, *D. caulivora*, *D. eres*, and *D. novem* isolates (Tables 2.4 and 2.12 [a]). PCR reactions were carried out in a Bio-Rad C1000 touch thermal

cycler and the amplification was performed using *Taq* polymerase in 25 µL reactions. The pipetting scheme and the PCR program for PCR are shown in Table 2.15 and Table 2.16.

Table 2.15: Pipetting scheme for a 25 µL PCR reaction with *Taq* polymerase

Reagents	Volumes (µL)
10x *Taq* buffer with $(NH_4)_2SO_4$ [a]	2.5
$MgCl_2$ (25 mM)	2.5
dNTPs (2 mM) [a]	2.5
Forward-Primer (5'→3') (10 pmol/µL)	1.25
Reverse-Primer (3'→5') (10 pmol/µL)	1.25
Template DNA	1
Taq DNA polymerase [a] (1 U/µL)	1
ddH_2O	13
Final volume	25

[a] Thermo Fisher Scientific, Waltham, MA, USA

Table 2.16: PCR program for one PCR reaction with *Taq* polymerase

Phase	Temperature (°C)	Time (min:s)
1. Initial denaturation	95	3:00
2. Denaturation	95	0:30
3. Annealing	58	0:30
4. Elongation	72	0:30
5. Repetition from phase 2. – 4. 35 x		
6. Final elongation	72	5:00
7. Final hold	8	indefinite

2.14.3. Agarose gel electrophoresis

The presence and the size of DNA fragments after amplification via PCR was determined by gel electrophoresis. Depending on the expected size of the fragments (Table 2.4) to be determined, 2 % (w/v) agarose was suspended in TAE (1x), boiled in the microwave with repeated shaking until a homogeneous solution was formed. 6x Loading dye (1 µL, Thermo Fisher Scientific, Waltham, MA, USA) was used to prepare DNA samples (5 µL PCR products) for loading on the agarose gel in order to observe their separation. GeneRuler^{TM} 100 bp^+ DNA ladder (3 µL, Thermo Fisher Scientific, Waltham, MA, USA) was used for sizing and approximation of the DNA bands. The electrophoretic separation of the DNA took place at 100 V for 45 min. To make the DNA bands visible, the agarose gel was stained in 0.0005 % ethidium bromide solution for 10 min and then destained in H_2O for 15 min. The analysis and documentation of the separated DNA fragments was followed with the aid of a Quantum 1100 gel documentation system under UV light.

2.14.4. Purification of PCR products

PCR amplicons were purified using the peqGOLD Cycle-Pure Kit, following the recommendations of the manufacturer. PCR amplicon was transferred to a clean 1.5 mL micro tube and mixed with an equal volume of CP buffer. Then the mixture was applied to a PerfectBind DNA column assembled in a clean 2 mL collection tube and centrifuged at

10,000 rcf for 1 min at RT. The liquid was discarded and the PerfectBind DNA column was washed twice with CG wash buffer (750 µL). After centrifuging at 10,000 rcf for 1 min, the liquid was discarded and the empty column was centrifuged for 2 min at 10,000 rcf in order to dry the column matrix to avoid transfer of salts in buffer. In the last step, the column was placed into a clean 1.5 mL micro tube and 30 µL ddH_2O was pipetted directly onto the column matrix and centrifuged 1 min at 5,000 rcf to elute DNA.

2.14.5. Measurement of DNA concentrations

2.14.5.1. Spectrophotometrical detection by BioPhotometer® plus supplemented with µCuvette® G1.0

The concentration of all dsDNA which were extracted from single spore isolates of *Diaporthe* strains, soybean fungal pathogens (2.14.1.1.1.), plant materials (2.14.1.2.), and rust pathogens (2.14.1.3.) was measured by the BioPhotometer® plus using the µCuvette® G1.0 with an optical path length of 1 mm. First, the cuvette was cleaned by pipetting 2 µL ddH_2O in the middle of the marking on the sample carrier, folding the cuvette together and wiping it with a tissue (**LAB**SOLUTE® laboratory; Th. Geyer GmbH + Co. KG). Then a blank value with 2 µL ddH_2O was generated. The same amount (2 µL) was taken from the DNA sample and pipetted on the sample carrier, inserted into the BioPhotometer® plus. DNA concentration of the samples was determined by measuring the absorption at 260 nm via the BioPhotometer® plus. After each measurement, the cuvette was cleaned with ddH_2O as described above.

2.14.5.2. Fluorometrical detection by Qubit® 2.0 Fluorometer

The concentration of purified PCR products of *Diaporthe* isolates (Table 2.12 [a]) and DNA of *Diaporthe* isolates (Table 2.12 [e]) was detected fluorometrically by using a Qubit® 2.0 Fluorometer in order to obtain a precise measurement. For this purpose, a Qubit™ working solution was prepared by diluting the Qubit™ reagent 1:200 in Qubit™ buffer.

Two assay tubes for the standards (1 and 2) and one tube for each user sample were prepared:
Standard assay tubes = 10 µL Standard from the Qubit® DNA BR Assay Kit (Invitrogen/Molecular probes by life technologies; USA) + 190 µL of Qubit™ working solution
User sample assay tubes = 1 µL of sample + 199 µL of Qubit™ working solution
Thin-wall, clear 0.5 mL Qubit® assay tubes (Thermo Fisher Scientific) were used to prepare 200 µL of working solution for each standard and sample and then all tubes were vortexed briefly and incubated for 2 min at RT. To calibrate the device, the tubes of standard 1 and

standard 2 were initially inserted into the Qubit® Fluorometer, measured and a two-point standard calibration was created. All samples could then be measured one after the other in the device.

2.14.6. DNA sequencing

Purified PCR products of the single spore isolates of *Diaporthe* strains were diluted with ddH_2O according to the formula of Source Bioscience (Berlin) and Microsynth SEQLAB (Göttingen), respectively, and sequenced in both directions.

Source Bioscience: Purified PCR products and primers were prepared in a concentration of 1 ng/µL per 100 bp and 3.2 pmol/µL, respectively. Afterwards, 5 µL from each diluted PCR product were pipetted into 1.5 mL individual micro tubes. Also, 5 µL per reaction from each forward and reverse primer were pipetted into separate 1.5 mL micro tubes. The prepared samples and primers were sent for sequencing.

Microsynth SEQLAB: Purified PCR products were prepared in 18 ng per 100 bp in a volume of 12 µL. The primers were diluted to 10 pmol/µL. Then, the 12 µL purified PCR product solution and 3 µL sequencing primer solution were mixed within one micro tube in a volume of 15 µL and the prepared samples were sent for sequencing.

Forward and reverse sequences were assembled using SeqMan™II and deposited in NCBI's GenBank. Introns and exons in *TUB* and *TEF1* sequences were determined by comparison with previously submitted sequences.

2.14.7. Phylogenetic analysis

The DNA sequences for each *Diaporthe* isolate were aligned using ClustalW as implemented in BioEdit (version 7.1.3.0) (Hall, 1999). Multiple sequence alignments of *Diaporthe* isolates together with sequences of ex-type species were performed for each gene. The concatenated alignment was generated by fusing the *TUB, TEF1,* and ITS alignments in the Windows text editor. Phylogenetic trees were constructed using MEGA-X (Tamura and Nei, 1993; Kumar et al. 2018). Here the maximum composite likelihood method (Tamura et al. 2004) was chosen with default options: a robust test of 100 bootstraps, Tamura-Nei Model, uniform rates, all sites, nearest neighbor interchange, initial tree by neighbor joining, no branch swap filter, and 3 threads.

2.14.8. Real-time PCR

2.14.8.1. Design of TaqMan primer-probe sets

The alignments of the ITS and *TEF1* sequences constructed for the phylogeny analysis (under 2.14.7.), were checked and then sequence alignments of six or four *Diaporthe* isolates,

respectively, representing the full sequence diversity were selected to design the TaqMan primer-probe sets (Table 2.17).

Table 2.17: *Diaporthe* strains and the corresponding GenBank accession numbers for the ITS and *TEF1* sequences used to design the TaqMan primer-probe sets

Isolate no.	Species	GenBank Accession	
		ITS	*TEF1*
DPC_HOH1	*D. longicolla*	MK024676	MK099093
DPC_HOH2	*D. caulivora*	MK024677	MK099094
DPC_HOH3	*D. eres*	MK024678	MK099095
DPC_HOH7		MK024682	MK099099
DPC_HOH8	*D. novem*	MK024683	MK099100
DPC_HOH11		MK024686	MK099103

Melting temperatures (Tm) and potential secondary structures of the selected oligonucleotide sequences were evaluated with Gene Runner (Version 6.5.52x64 Beta). The fluorogenic reporters for TaqMan probes were selected based on the capacity of the CFX96 detection system to resolve overlapping spectra. All oligonucleotide primers and probes were synthesized by Biomers.net GmbH (Ulm, Germany).

2.14.8.2. *In silico* assessment of the specificity of the TaqMan primer-probe sets

Specificity of the selected primers and probes based on *TEF1* sequences (Table 2.7) and the selected primers and probe based on ITS sequences of *D. eres* isolates (Table 2.6) was tested using NCBI's Primer-BLAST (NCBI; https://www.ncbi.nlm.nih.gov/tools/primer-blast/). In "Primer Pair Specificity Checking Parameters" nr was entered as database and as organisms *Diaporthe*, Fungi, *Phytophthora*, *Pythium*, and *Glycine*.

2.14.8.3. Real-time PCR conditions

Real-time PCR was performed using a CFX96 Real-Time PCR system using FrameStar® 96-Well Skirted PCR Plates (4titude, Brooks Automation, Chelmsford, MA, USA). Real-time PCR reactions were prepared using ready to use mixtures, either SensiFAST™ Probe No-ROX mix (2x) or SensiFAST™ SYBR No-ROX mix (2x). All reactions were performed with a final volume of 20 µL. First, the 96-Well plates were pipetted with the master mix and then with the template DNA using Filter tips under the sterile bench (DNA/RNA UV-Clearer). The pipetted plates were sealed with sealing tape (Sarstedt AG + Co KG, Nümbrecht), centrifuged briefly with the Mini plate spinner, placed in the CFX96 Real-Time PCR system, and incubated under the protocol (Table 2.18). The real-time PCR data were analyzed using the CFX Manager™ Software.

Table 2.18: PCR program for real-time PCR assays

Phase	Temperature (°C)	Time (min:s)
1. Initial denaturation	95	3:00
2. Denaturation	95	0:15
3. Annealing/Elongation + Plate read	60	0:45
4. GOTO 2, 39 x		

2.14.8.4. Evaluation of the specificity and efficiency of the TaqMan primer-probe sets

2.14.8.4.1. Singleplex real-time PCR assays

Numbers of copies of DNA of the purified PCR products for each *Diaporthe* isolate (Table 2.12 [a]) were determined by the formula 2.2:

Formula 2.2: Determination of number of copies of DNA

$$\text{DNA copies number} = \frac{\text{Amount of DNA (ng)} * \text{Avogadro's constant}}{\text{Length of DNA template (bp)} * 660\ (\text{g/(mol} * \text{bp)}) * 1 \times 10^9\ (\text{ng/g})}$$

Amount of DNA (ng) = Concentration of PCR products * volume added to the reaction
Avogadro's constant = 6.022×10^{23} molecules/mol
Average mass of 1 bp dsDNA = 660 g/(mol * bp)
Conversion factor for converting ng = 1×10^9 ng/g

Subsequently, serial dilutions of PCR products containing 10^9 to 10^4 copies/µL and also dilution series 1:10, 1:100, and 1:1,000 for the genomic DNA of the *Diaporthe* isolates (Table 2.12 [a]) were prepared and tested in singleplex real-time PCR assays using the designed TaqMan primer-probe sets (Tables 2.6 and 2.7).

The specificity of all TaqMan primer-probe sets, which were designed based on *TEF1* sequences (Table 2.7) and the primer-probe set DPCE(1) [mixture of own reverse primers DE-3 R, DE-7 R; primer DPC-3 R as forward primer; and probe DPE3-7 P] (Table 2.6), which was designed based on ITS sequences of *D. eres* isolates, was tested with genomic DNA from the non-target *Diaporthe* species in singleplex real-time PCR assays. The real-time PCR program and the pipetting scheme for singleplex reactions are shown in Table 2.18 and Table 2.19.

Table 2.19: Pipetting scheme for singleplex real-time PCR assays

Reagents	Volumes (µL)
2x SensiFAST Probe Mix [a]	10
Forward-Primer (5'→3') (10 pmol/µL)	0.8
Reverse-Primer (3'→5') (10 pmol/µL)	0.8
TaqMan-Probe (10 pmol/µL)	0.2
ddH_2O	6.2
Template DNA	2
Final volume	20

[a] Bioline GmbH, London, UK

2.14.8.4.2. Multiplex real-time PCR assays

To assess the quadruplex real-time PCR assay, first all four primer-probe sets DPCL, DPCC, DPCE, and DPCN (Table 2.7) were tested for specificity by adding just one DNA sample. 0.4 ng DNA from target species (Table 2.12 [b]) or different amounts of DNA between 350 ng and 2.5 µg from non-target species (2.10.2.), healthy soybean leaf, and healthy soybean stem, respectively, were added to the mix with all four primer-probe sets. In the second and third steps, two and three different DNA samples of species of *Diaporthe* (Table 2.12 [b]) were tested together, respectively, and in the last step, DNA of all four species was applied. The real-time PCR program and the pipetting scheme for duplex and quadruplex reactions are shown in Table 2.18 and Table 2.20.

Table 2.20: Pipetting scheme for duplex and quadruplex real-time PCR assays

Reagents	Volumes (µL)
2x SensiFAST Probe Mix [a]	10
Forward-Primer [b] (5'→3') (10 pmol/µL)	0.4
Reverse-Primer [b] (3'→5') (10 pmol/µL)	0.4
TaqMan-Probes [c] (10 pmol/µL)	0.1
Template DNA	2
ddH_2O	Variable [d]
Final volume	20

[a] Bioline GmbH, London, UK
[b] From each four forward primer and each five reverse primer 0.4 µL were used in reactions.
[c] From each four probe 0.1 µL were used in reactions.
[d] The amount of water was variable based on the number of primer-probe sets used.

Standards were run in technical triplicates; samples tested for pathogen presence in technical duplicates. No-template controls were included on all plates and for all mixes.

2.14.9. Validation of the quadruplex real-time PCR assay

2.14.9.1. Sampling of plant material

Stem samples were taken from four months-old symptomatic plants artificially inoculated with *D. longicolla* isolates (Table 2.21) in the greenhouse pathogenicity test (2.13.).

Infected seed samples were selected from six seed lots (Table 2.8 [a]) and for each lot, thirty seeds were chosen for DNA extraction.

Leaf and stem samples from four weeks-old healthy soybean plants (2.10.3.) and healthy seeds (cv. Sultana) were used as control.

Table 2.21: Infected stem samples obtained from diseased soybean plants which were inoculated with *D. longicolla* isolates in the greenhouse pathogenicity test

Isolate no.	Species	GenBank Accession	
		ITS	*TEF1*
DPC_HOH17	*D. longicolla*	MK024692	MK099109
DPC_HOH22		MK024697	MK099114
DPC_HOH25		MK024700	MK099117
DPC_HOH26		MK024701	MK099118
DPC_HOH29		MK024704	MK099121

2.14.9.2. Evaluation of the quadruplex real-time PCR assay

To evaluate the ability of the quadruplex real-time PCR assay to detect DNA from *Diaporthe* species, the extracted DNAs from infected stem samples (Table 2.21) and six different seed lots (Table 2.8) under 2.14.1.2. were added individually to the quadruplex reactions including primer-probe sets DPCL, DPCC, DPCE, and DPCN. The extracted DNAs from healthy stem samples and soybean seeds were tested as control as well. The real-time PCR program and the pipetting scheme for quadruplex reactions are shown in Table 2.18 and Table 2.20.

2.14.10. Quantification of the amount of *Diaporthe* DNA in soybean seeds

2.14.10.1. Standard curves for quantification

The DNA of the *Diaporthe* isolates (Table 2.12[e]) was diluted 1:10 to $1:10^6$ with 50 µg/mL DNA from healthy soybean tissue (leaves). To get standard curves for each *Diaporthe* isolate, quadruplex real-time PCR assays with DPCL, DPCC, DPCE, and DPCN, were performed by applying the dilution series using the real-time PCR program and the pipetting scheme for quadruplex reactions (Tables 2.18 and 2.20).

Also, to create a standard curve for plant DNA, DNA of healthy soybean tissue was diluted 1:10 to $1:10^6$ with ddH_2O and the serial dilutions were applied in SYBR® Green-based real-time PCR assays using soybean primers UKN2F and UKN2R (Table 2.5). The SYBR® Green-based real-time PCR reactions were prepared using a ready to use mixture, SensiFAST™ SYBR No-ROX mix (2x). The final volume of all reactions was 20 µL (Table 2.22). No-template controls were included for the assay. Samples were amplified using the two step protocol shown in Table 2.18.

Table 2.22: Pipetting scheme for SYBR® Green-based real-time PCR assays

Reagents	Volumes (µL)
2x SensiFAST™ SYBR No-ROX Mix [a]	10
Forward-Primer (5'→3') (10 pmol/µL)	0.4
Reverse-Primer (3'→5') (10 pmol/µL)	0.4
Template DNA	2
ddH_2O	7.2
Final volume	20

[a] Bioline GmbH, London, UK

2.14.10.1.1. Actual quantification

The amount of fungal DNA (ng) per plant DNA (ng) was quantified for DNAs from six soybean seed lots (Table 2.8). For this, in addition to applying these DNA samples in the quadruplex real-time PCR assays to detect fungal DNA, SYBR® Green-based real-time PCR reactions were carried out in parallel to determine the amount of soybean DNA. The amount of DNA of each *Diaporthe* species and plant for each individual seed was calculated using the

standard curves and the amount of fungal DNA was set in relation to the amount of plant DNA.

2.14.10.2. Absolute quantification of fungal biomass

2.14.10.2.1. Standard curves from *Diaporthe* species mycelia

Mycelia were scraped from ten days-old cultures of *Diaporthe* isolates (Table 2.12[c]) in different amounts in individual micro tubes. The micro tubes (1.5 mL) were weighed first when they were empty and then again after adding the mycelia using a Sartorius analytical balance. The mycelia were homogenized by vortexing using a few microbeads (Lysing Matrix E tubes) in 500 µL lysis buffer. DNA extraction was carried out using the protocol by Liu et al. (2000) as described in 2.14.1.1.1. DNA concentration was determined spectrophotometrically and from each DNA sample, a 1:10 dilution was prepared. Quadruplex real-time PCR assays using primer-probe sets DPCL, DPCC, DPCE(1), and DPCN were carried out with the DNA samples (diluted and undiluted DNA) to assign a Cq value to a certain amount of mycelium. The quadruplex real-time PCR assays were performed using the real-time PCR program and the pipetting scheme shown in Table 2.18 and Table 2.20.

2.14.10.2.2. Standard curves from *Diaporthe* species spores

60 days-old plates of *Diaporthe* isolates (Table 2.12[d]) with an abundance of pycnidia/perithecia (under 2.12.4.) were flooded with 10 mL Polysorbate 20 (0.01 %). Spore suspensions were prepared as described in 2.13.1. and they were transferred into 50 mL falcon tubes. 2 mL of these spore suspensions were transferred to a 2 mL microcentrifuge tube and conidial/ascospores concentrations were determined using a Fuchs-Rosenthal counting chamber as described in 2.13.2. Serial dilutions (10^{-1} to 10^{-7}) of the spore suspensions were prepared in Polysorbate 20 (0.01 %) in 2 mL volume. 1 mL suspension was removed from each of the tubes of the dilution series in order to carry out DNA extraction on the spores based on the protocol by Liu et al. (2000). The suspensions were centrifuged for 5 min at 20,000 rcf. Then 700 µL of the supernatant were removed and discarded. To the pellet and the remaining supernatant, 500 µL lysis buffer and a few microbeads (Lysing Matrix E) were added. This was followed by 10 min incubation. The further steps were carried out as described in 2.14.1.1.1.

Quadruplex real-time PCR assays using primer-probe sets DPCL, DPCC, DPCE(1), and DPCN, were performed with the serial dilutions of spore suspensions and also with the extracted DNAs from each spore suspension for each *Diaporthe* isolate using the real-time PCR program and the pipetting scheme in Table 2.18 and Table 2.20.

2.14.11. Seed soaking

One soybean seed lot (cultivar Anushka 2, Table 2.8) was used to test the seed soaking method. In the first experiment, two times five seeds were soaked in sterile deionized water at a ratio of 5 seeds/5 mL water, with different ratios of healthy and infected seeds (five infected, 4 infected + 1 healthy, 3 infected + 2 healthy, 2 infected + 3 healthy, 1 infected + 4 healthy, and 5 healthy) in separate falcon tubes. The falcon tubes were stored at 4 °C and from each of the soaking solutions, 100 µL aliquots were collected at 0, 1, 2, 3, 4, 5, 6, and 7 h. In the second experiment, three times 100 seeds were soaked randomly in sterile deionized water at a ratio of 100 seeds/100 mL water in separate containers and from each of the soaking solutions, 1 mL aliquots were collected at 0, 1, 2, and 3 h. The aliquots were stored at -20 °C until use. 2 µL of these aliquots were used as template in the quadruplex real-time PCR (Tables 2.18 and 2.20). Two technical replicates were conducted for each aliquot and no-template controls were included as well.

3 Results

In this work, soybean seed lots with putative *Diaporthe* contamination, were obtained from several locations throughout Europe and examined in order to identify the dominant *Diaporthe* species in Europe. For this purpose, DPC species should be isolated using the conventional seed plating method. The species of the single spore isolates was determined based on their morphology. Phylogenies were built from *TUB*, *TEF1*, and ITS sequences and also multi-gene DNA sequence data were generated to get more reliable information to classify the DPC species.

Specific TaqMan primer-probe sets were designed for the detected species based on *TEF1* sequence alignments of *Diaporthe* isolates. The efficiency of the TaqMan primer-probe sets was evaluated by applying genomic DNA and PCR products of the *Diaporthe* isolates. The specificity for each set was tested. The reliability of the resulting quadruplex real-time PCR assay was tested. Standard curves for all four pathogens to enable their quantification were obtained.

3.1. Isolation of *Diaporthe* strains

The first step to elucidate which species of the DPC are relevant in central Europe, was classical isolation of the pathogens from soybean seeds (2.11.). Seeds from Austria, France and southern Germany were used in the isolation study.

32 fungal cultures could be attributed to *Diaporthe* spp. but also other pathogens like *Fusarium* spp. and *Alternaria* spp. were found. Single spore isolates were obtained from the *Diaporthe* cultures and these were identified based on morphological and molecular identification criteria (Table 3.1).

3.2. Morphological identification of *Diaporthe* isolates

The 32 *Diaporthe* isolates were evaluated based on colony appearance and color, formation of anamorph or teleomorph structures, type and dimensions of conidia and ascospores. This put the isolates into the species *D. longicolla*, *D. caulivora*, *D. eres*, and *D. novem*.

The morphological characteristics of the different species as observed by me are described below. Mostly the characteristics conformed with earlier descriptions but nevertheless new/updated species descriptions for the isolates in central Europe were generated. These species descriptions have also been published (Hosseini et al. 2020).

Table 3.1: *Diaporthe* species isolated from European soybean seeds

Species	Isolate no.	Cultivar	Origin	GenBank accessions		
				ITS	*TEF1*	*TUB*
D. longicolla	DPC_HOH1	Sigalia	Austria	MK024676	MK099093	MK161475
	DPC_HOH5	CH 22232	Austria	MK024680	MK099097	MK161479
	DPC_HOH6	Gallec	Austria	MK024681	MK099098	MK161480
	DPC_HOH9	Korus	Austria	MK024684	MK099101	MK161483
	DPC_HOH12	Silvia PZO	Austria	MK024687	MK099104	MK161486
	DPC_HOH13	Gallec	Austria	MK024688	MK099105	MK161487
	DPC_HOH17	Sigalia	Austria	MK024692	MK099109	MK161491
	DPC_HOH18	Primus	Austria	MK024693	MK099110	MK161492
	DPC_HOH19	Primus	Austria	MK024694	MK099111	MK161493
	DPC_HOH20	Silvia PZO	Austria	MK024695	MK099112	MK161494
	DPC_HOH21	Gallec	Austria	MK024696	MK099113	MK161495
	DPC_HOH22	Sultana	Germany	MK024697	MK099114	MK161496
	DPC_HOH23	Sultana	Germany	MK024698	MK099115	MK161497
	DPC_HOH24	Sultana	Germany	MK024699	MK099116	MK161498
	DPC_HOH25	Merlin	Austria	MK024700	MK099117	MK161499
	DPC_HOH26	Gallec	Austria	MK024701	MK099118	MK161500
	DPC_HOH28	Malaga	Austria	MK024703	MK099120	MK161502
	DPC_HOH29	Gallec	Austria	MK024704	MK099121	MK161503
	DPC_HOH30	Silvia PZO	Austria	MK024705	MK099122	MK161504
	DPC_HOH31	Merlin	Austria	MK024706	MK099123	MK161505
	DPC_HOH32	CH 22177	Austria	MK024707	MK099124	MK161506
D. caulivora	DPC_HOH2	Primus	Austria	MK024677	MK099094	MK161476
	DPC_HOH4	Primus	Austria	MK024679	MK099096	MK161478
D. eres	DPC_HOH3	CH 22177	Austria	MK024678	MK099095	MK161477
	DPC_HOH7	Amadine	Austria	MK024682	MK099099	MK161481
	DPC_HOH10	Silvia PZO	Austria	MK024685	MK099102	MK161484
	DPC_HOH14	Primus	Austria	MK024689	MK099106	MK161488
	DPC_HOH27	Sigalia	Austria	MK024702	MK099119	MK161501
D. novem	DPC_HOH8	Sultana	Austria	MK024683	MK099100	MK161482
	DPC_HOH11	Pollux	France	MK024686	MK099103	MK161485
	DPC_HOH15	Pollux	France	MK024690	MK099107	MK161489
	DPC_HOH16	Sigalia	Austria	MK024691	MK099108	MK161490

3.2.1. *Diaporthe longicolla* (Hobbs) J.M. Santos, Vrandečić & A.J.L. Phillips, Persoonia 27: 13 (2011).

Phomopsis longicolla Hobbs, Mycologia 77: 542 (1985).

21 isolates (DPC_HOH1, DPC_HOH5, DPC_HOH6, DPC_HOH9, DPC_HOH12, DPC_HOH13, DPC_HOH17, DPC_HOH18, DPC_HOH19, DPC_HOH20, DPC_HOH21, DPC_HOH22, DPC_HOH23, DPC_HOH24, DPC_HOH25, DPC_HOH26, DPC_HOH28, DPC_HOH29, DPC_HOH30, DPC_HOH31, and DPC_HOH32), which were isolated from seed lots collected from various fields in Austria and Germanys, were allocated to *D. longicolla*. The morphological characteristics of all *D. longicolla* isolates fit the description of Hobbs et al. (1985) with the exception of DPC_HOH18 and DPC_HOH21.

Fluffy and dense aerial mycelium that appeared white with greenish yellow areas grew on the APDA plates for most of the *D. longicolla* isolates (Figure 3.1 A). From the backside, fresh

cultures were white to greenish; yellow and black spots appeared later (Figure 3.1 B). Asexual reproductive structures, pycnidia containing α-conidia, were developed on the surface of the cultures on APDA and on pieces of soybean stems (Figure 3.1 C, D). In contrast to the *D. novem* isolates in this study, this species produced many stromata with long pycnidial beaks. Hyaline and biguttulate α-conidia (5.5 – 7.4 × 2.0 – 2.4 µm) with oval shape were released from the pycnidial ostiole in yellowish or creamy drops (Figure 3.1 C, F). *D. longicolla* produced smaller and wider α-conidia than *D. novem* as well.

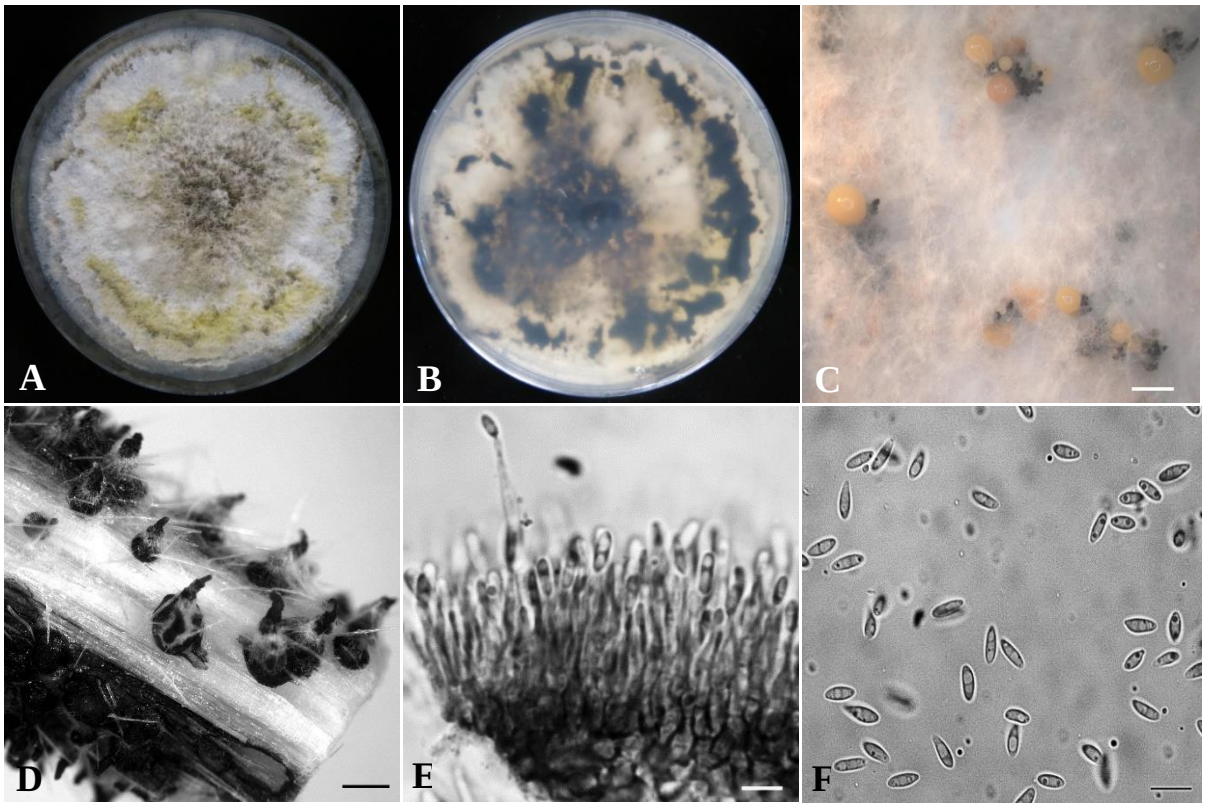

Figure 3.1: Macro- and micrographs of *D. longicolla* (isolate DPC_HOH28).
A) Surface view of the cultures on APDA after one month. **B**) Backside view of the cultures. **C**) Conidiomata sporulating on APDA. **D**) Pycnidia on soybean stem on WA. **E**) Conidiogenous cells and conidiophores. **F**) α-conidia. (**A**, **B**) Diameter of the dishes 9.0 cm. Scale bars **(C**, **D)** 500 µm, (**E**, **F**) 10 µm

3.2.2. *Diaporthe caulivora* (Athow & Caldwell) J.M. Santos, Vrandečić & A.J.L. Phillips, Persoonia 27: 13 (2011).

Basionym: *Diaporthe phaseolorum* var. *caulivora* Athow & Caldwell, Phytopathology 44: 323 (1954).

Isolates DPC_HOH2 and DPC_HOH4, which were isolated from Austrian soybean lots, were grouped as *D. caulivora*. Morphologically, both isolates fit the description of Athow and Caldwell (1954).

Fluffy mycelia of *D. caulivora* isolates on APDA were first white or white-yellow and later yellow-ochre (Figure 3.2 A). From the backside the mycelium appeared light ochre to tan, light yellow, or yellow (Figure 3.2 B). The isolates reproduced sexually. Perithecia were formed after 30 - 40 days (Figure 3.2 C) on APDA plates and after two months on soybean stem pieces on WA (Figure 3.2 D). Formation of perithecia most clearly distinguishes *D. caulivora* from the other species found in central Europe. The perithecia had black and straight necks and developed alone or in groups of two or three (Figure 3.2 C, D). Asci (30.6 – 43.0 × 7.0 – 9.5 µm) with eight ellipsoid ascospores, were enlarged in the middle and had obvious apical rings towards the vertices (Figure 3.2 E). The ascospores (8.3 – 11.0 × 1.7 – 2.9 µm) were translucent, ellipsoidal to fusoid, and septate. They had four guttules, two guttules per cell and the guttules towards the septum were widest (Figure 3.2 F).

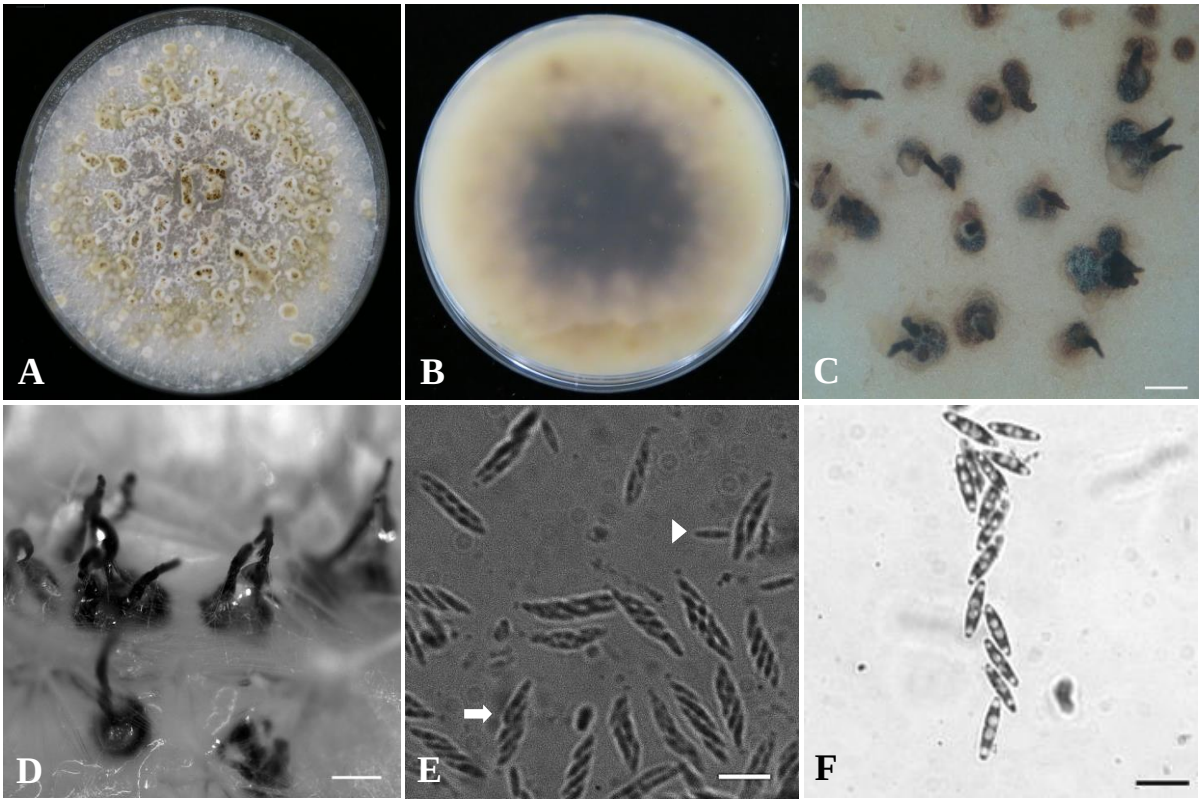

Figure 3.2: Macro- and micrographs of *D. caulivora* (isolate DPC_HOH2).
A) Surface view of the cultures on APDA after one month. **B**) Backside view of the cultures. **C**) Perithecial necks on APDA. **D**) Perithecial necks on soybean stem on WA. **E**) Asci (arrow) and ascospores (arrowhead). **F**) Ascospores. (**A**, **B**) Diameter of the dishes 9.0 cm. Scale bars (**C**, **D**) 500 µm, (**E**) 20 µm, (**F**) 10 µm

3.2.3. *Diaporthe eres* Nitschke, Pyrenomycetes Germanici 2: 245 (1870).

Isolates DPC_HOH3, DPC_HOH7, DPC_HOH10, DPC_HOH14, and DPC_HOH27 fit the description for *D. eres* provided by Nitschke (1870) and they could be isolated from Austrian soybean seed lots.

D. eres isolates grew as white aerial fluffy mycelia with dark pigmentation spots. Also large black stromata were produced (Figure 3.3 A). On the backside of the plates the mycelium appeared grayish (Figure 3.3 B). Reproduction of the isolates was asexual and a bulk with numerous α-conidia and β-conidia protruded from the pycnidia (Figure 3.3 C, D). In the generation of β-conidia *D. eres* differs from *D. longicolla* and *D. novem*. α-conidia were oval and 5.7 – 8.2 × 1.3 – 2.5 µm in size (Figure 3.3 F). β-conidia were unicellular, aseptate, hyaline, filiform, curved at one end, and 22.4 – 31.6 × 1.4 – 1.7 µm big (Figure 3.3 F).

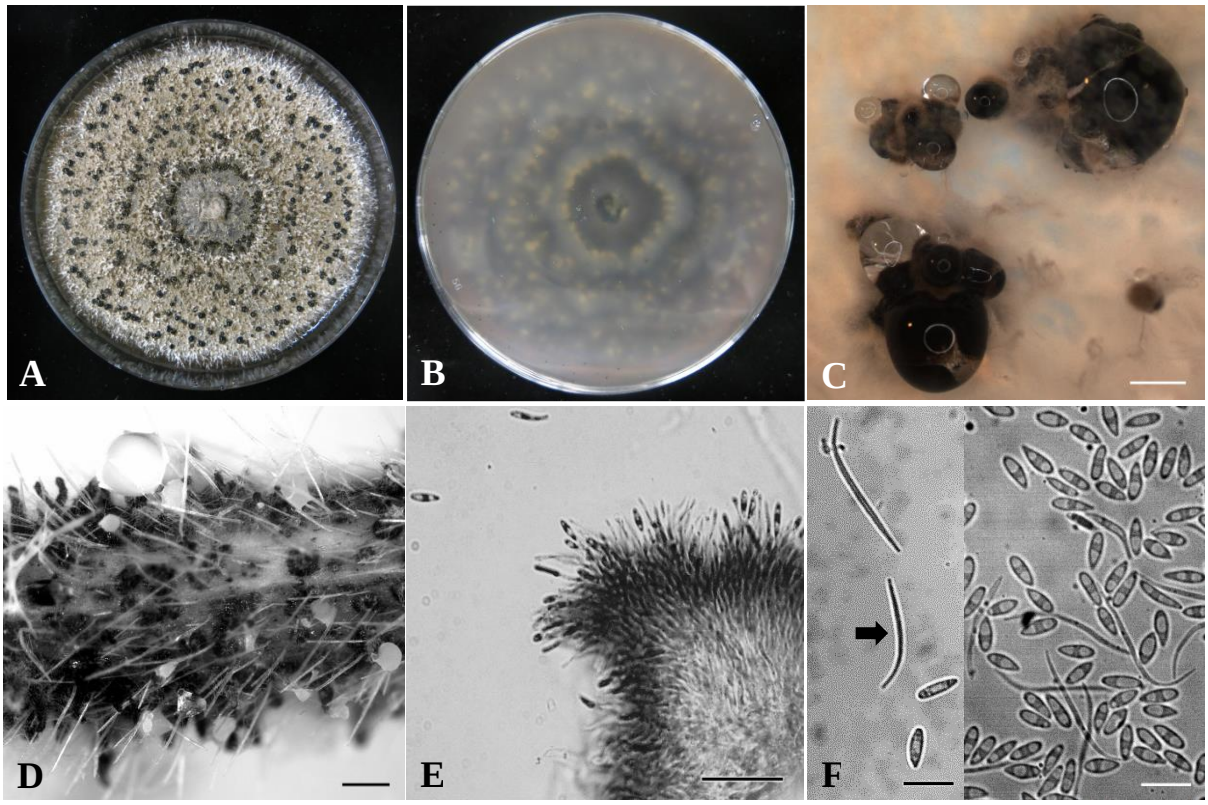

Figure 3.3: Macro- and micrographs of *D. eres* (isolate DPC_HOH3).
A) Surface view of the cultures on APDA after one month. **B**) Backside view of the cultures. **C**) Conidiomata sporulating on APDA. **D**) Pycnidia on soybean stem on WA. **E**) Conidiogenous cells and conidiophores. **F**) α-conidia and β-conidia (arrow). (**A**, **B**) Diameter of the dishes 9.0 cm. Scale bars (**C**) 200 µm, (**D**) 500 µm, (**E**) 20 µm, (**F**) 10 µm

3.2.4. *Diaporthe novem* J.M. Santos, Vrandečić & A.J.L. Phillips, Persoonia 27: 13 (2011).

Anamorph: *Phomopsis* sp. 9 van Rensburg et al. Stud Mycol 55: 65 (2006).

Etymology: Latin for nine, refers to *Phomopsis* sp. 9, the provisional name of the species from 2006 (van Rensburg et al. 2006).

The *D. novem* isolates DPC_HOH8, DPC_HOH11, DPC_HOH15, and DPC_HOH16 came from soybean seeds from France and Austria.

D. novem isolates produced white colonies on APDA, except for the central part that on the surface and back side were between colorless to ochre (Figure 3.4 A, B). The asexual form of this species could be observed. Pycnidia were developed in a huge amount and they exuded abundantly α-conidia as yellow drops (Figure 3.4 D). In comparison to *D. longicolla* and *D. eres*, *D. novem* α-conidia were longer (5.8 – 7.9 × 1.8 – 2.3 µm) and they were hyaline, unicellular, often biguttulate, and ellipsoid (Figure 3.4 F).

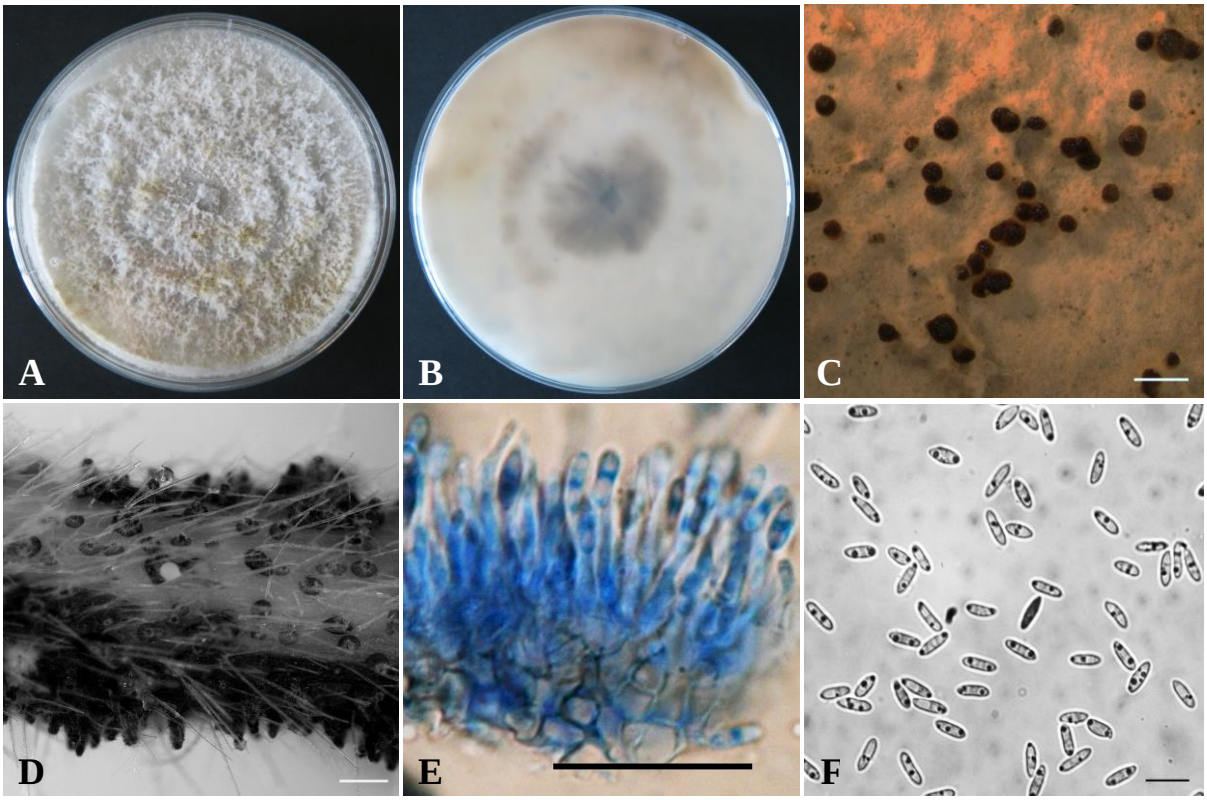

Figure 3.4: Macro- and micrographs of *D. novem* (isolate DPC_HOH16).
A) Surface view of the cultures on APDA after one month. **B**) Backside view of the cultures. **C**) Conidiomata on APDA. **D**) Pycnidia on soybean stem on WA. **E**) Conidiogenous cells and conidiophores stained with lactophenol blue solution. **F**) α-conidia. (**A**, **B**) Diameter of the dishes 9.0 cm. Scale bars (**C**, **D**) 500 µm, (**E**) 20 µm, (**F**) 10 µm

3.3. Molecular identification of *Diaporthe* species

Due to similarity and intra-species variability in the genus *Diaporthe*, morphological features are not adequate for species delimitation (van der Aa et al. 1990; Santos et al. 2011; Udayanga et al. 2011). Therefore, DNA sequence data are needed to classify the *Diaporthe* species precisely.

Indeed, determining the species based on morphological characteristics was problematic for DPC_HOH18 and DPC_HOH21 that differ from the common morphology of *D. longicolla* (3.2.1.). Therefore, molecular tools were applied to confirm the morphological grouping. Even the use of molecular data in addition to morphology only yields unambiguous results

with multi-gene DNA sequence data (Udayanga et al. 2012). Thus, multi-gene DNA sequence data were created as well.

3.3.1. Amplification of ITS, *TEF1*, and *TUB* DNA

Amplification of the molecular markers worked for all 32 *Diaporthe* isolates. The PCR products of ITS, *TEF1*, and *TUB* were about 600, 350, and 500 bp in size, respectively.

3.3.2. Sequence analysis and identification by BLASTN

The three gene regions were sequenced in both directions for all isolates. The isolates were again classified to the four species *D. longicolla*, *D. caulivora*, *D. eres*, and *D. novem* by BLASTN based on the sequences in GenBank (highest score and > 98 % identity). The results matched with the morphological identification. The sequences of the isolates were deposited in GenBank under the accession numbers MK024676 to MK024707 for ITS, MK099093 to MK099124 for *TEF1*, and MK161475 to MK161506 for *TUB* (Table 3.1).

The *TEF1*, ITS, and *TUB* sequences of the 21 *D. longicolla* isolates, were very similar (99–100 %) to the sequences from *D. longicolla* isolates from soybean in Korea and Serbia (Table 3.2). The sequences of the five *D. eres* isolates, were highly homologous to *D. eres* strains from different host and various locations (Table 3.2).

Table 3.2: Highly homologous sequences found when BLASTing the sequences from the new *Diaporthe* isolates from soybean seeds (ex-type strains in bold)

Target region	Species	GenBank accessions
ITS	*D. longicolla*	HQ333500, HQ333502, HQ333504, **HM347700 (CBS 127267)**
	D. eres	KC343074, KC343075, KJ210516, DQ491514, KJ210518, JF430487, JF430493, **MG281083 (CPC 30111)**, **MG281047 (CPC 29825)**, **MG281103 (CPC 30135)**, **MG281099 (CPC 30131)**
	D. caulivora	KC343046, JF418936, JF418934, EU622854, HM625752, **HM347712 (CBS 127268)**
	D. novem	KC343155, KC343157, GQ250225, DQ286285, JQ697841, JQ697843, JF704181, **HM347710 (CBS 127271)**, **HM347708 (CBS 127269)**, **HM347709 (CBS 127270)**
TEF1	*D. longicolla*	AF398896, **HM347685 (CBS 127267)**
	D. eres	KC343801, KJ210553, KJ210540, KJ210541, KJ210551, KJ210549, JF461473, **MG281604 (CPC 30111)**, **MG281568 (CPC 29825)**, **MG281624 (CPC 30135)**, **MG281620 (CPC 30131)**
	D. caulivora	JF461465, **HM347691 (CBS 127268)**
	D. novem	KC343881, HM347697, DQ286259, GQ250363, JQ697854, JQ697856, JF704182, **HM347693 (CBS 127269)**, **HM347695 (CBS 127271)**, **HM347696 (CBS 127270)**
TUB	*D. longicolla*	HQ333510 (strain SSLP-1), HQ333512 (strain SSLP-3)
	D. eres	KJ420823, KJ420810, KJ420785, KJ420822, KJ420800, KJ420783, **MG281256 (CPC 30111)**, **MG281220 (CPC 29825)**, **MG281276 (CPC 30135)**, **MG281272 (CPC 30131)**
	D. caulivora	HQ333513, **KC344013 (CBS 127268)**
	D. novem	**KC344123 (CBS 127269)**, **KC344125 (CBS 127271)**

The sequences of the two *D. caulivora* isolates were very similar to those of *D. caulivora* strains from soybean in Serbia, Croatia, and Korea (Table 3.2). Last, the sequences of the four

D. novem isolates were highly homologous to *D. novem*, *Phomopsis* sp. 9, and *D. pseudolongicolla* isolates from soybean in Croatia and Serbia (Table 3.2).

3.3.3. Phylogenetic analysis

Multiple sequence alignments for the 32 *Diaporthe* isolates including sequences of ex-type strains for each species (Table 3.2) obtained from NCBI were created for *TUB*, *TEF1*, and ITS using ClustalW. A concatenated alignment was generated by fusing the sequences.

All *D. longicolla* sequences were identical (Figures 3.5, 3.6, and 3.7). The *TEF1* and *TUB* sequences of the two *D. caulivora* isolates were identical but in ITS a few bases were different (Figures 3.5, 3.6, and 3.7). The sequences for the *D. eres* isolates showed a few differences in all markers (Figures 3.5, 3.6, and 3.7). The sequences of isolates DPC_HOH10 and DPC_HOH27 are identical as well as those of DPC_HOH3 and DPC_HOH14, while DPC_HOH7 is separate. Sequence-wise, *D. novem* isolates showed the biggest differences (Figures 3.5, 3.6, and 3.7). DPC_HOH15 and DPC_HOH16 are identical but DPC_HOH8 is different from the others in *TUB* (Figure 3.7).

Phylogenetic trees were constructed for all alignments (Figures 3.5, 3.6, and 3.7).

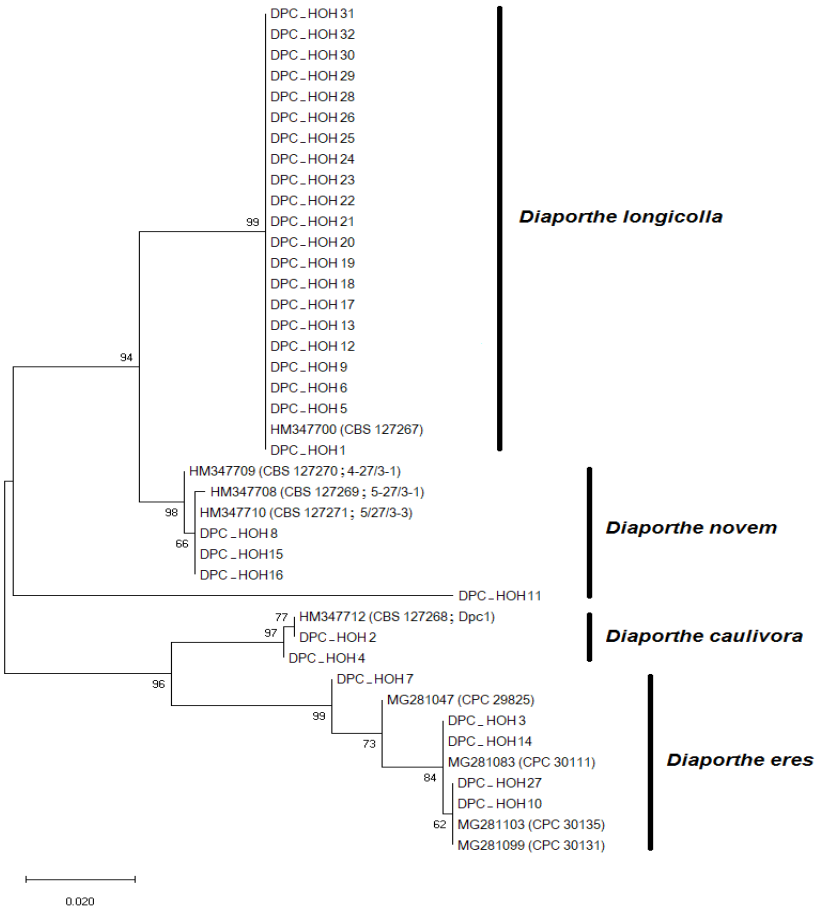

Figure 3.5: Maximum likelihood phylogenetic analysis of the *Diaporthe* species associated with soybean based on ITS. Bootstrap numbers represent percent of 100 replicates. For each species, the ex-type strain sequences were included by their accession numbers followed by strain names and the sequences of the new *Diaporthe* isolates were included by their isolate number. Scale bar: 0.02 substitutions per site. TreeBASE accession: TB2:S24730.

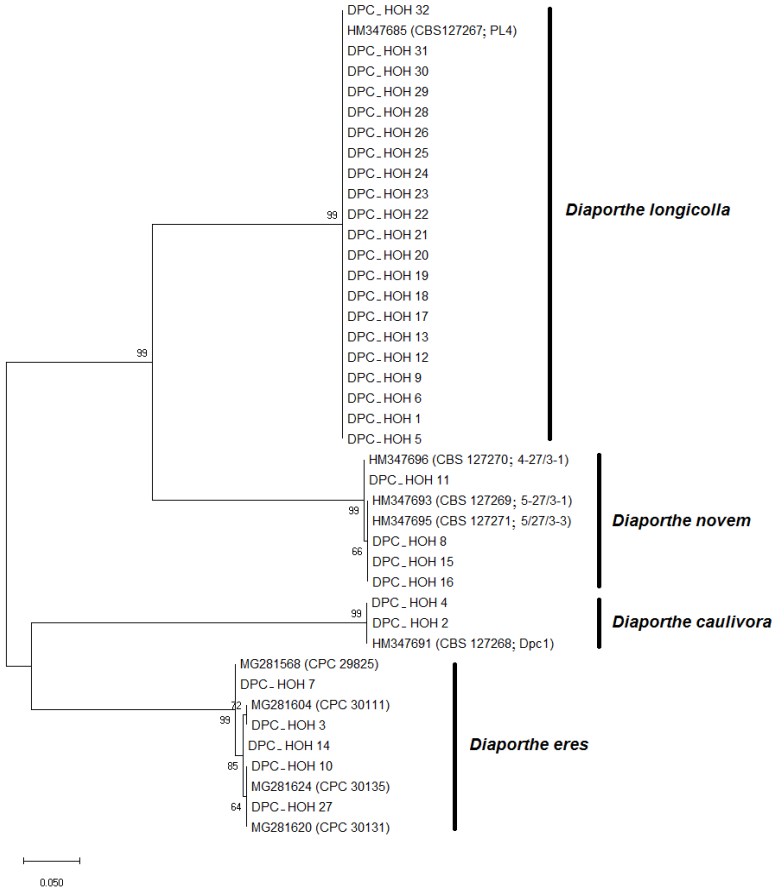

Figure 3.6: Maximum likelihood phylogenetic analysis of the *Diaporthe* species associated with soybean based on *TEF1*. Bootstrap numbers represent percent of 100 replicates. For each species, the ex-type strain sequences were included by their accession numbers followed by strain names and the sequences of the new *Diaporthe* isolates were included by their isolate number. Scale bar: 0.05 substitutions per site. TreeBASE accession: TB2:S24720.

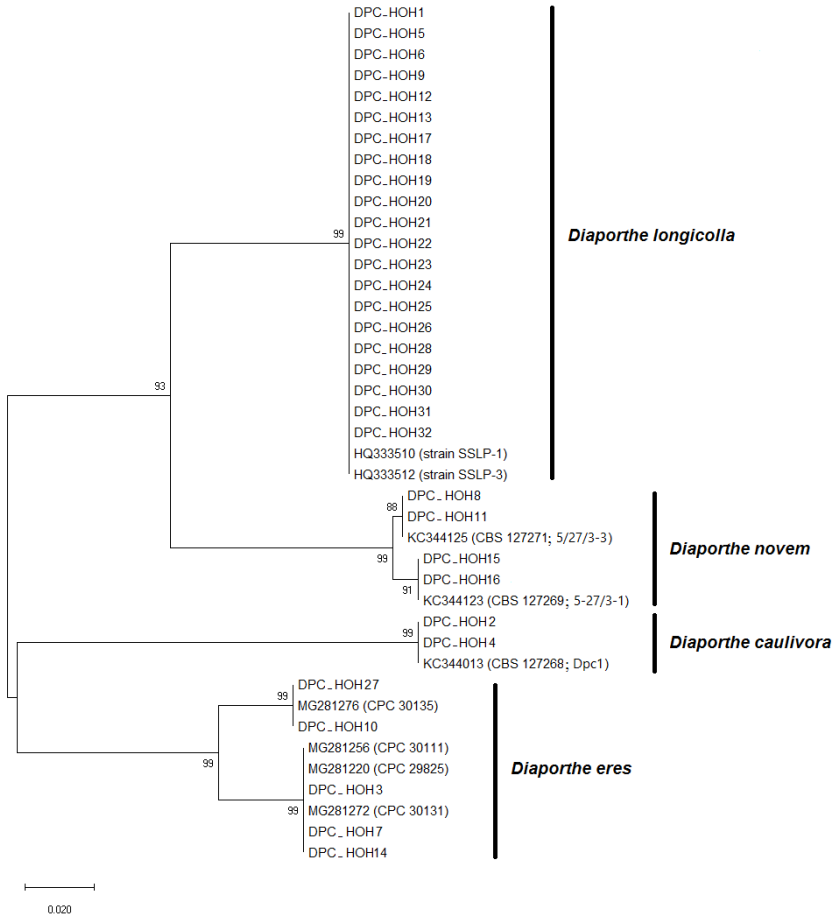

Figure 3.7: Maximum likelihood phylogenetic analysis of the *Diaporthe* species associated with soybean based on *TUB*. Bootstrap numbers represent percent of 100 replicates. For each species, the ex-type strain sequences were included by their accession numbers followed by strain names and the sequences of the new *Diaporthe* isolates were included by their isolate number. Scale bar: 0.02 substitutions per site. TreeBASE accession: TB2:S24724.

Overall, the isolates were grouped the same in the phylogenies for ITS, *TEF1*, and *TUB* (Figures 3.5, 3.6, and 3.7). This is once more corroborated in the combined phylogeny (Figure 3.8).

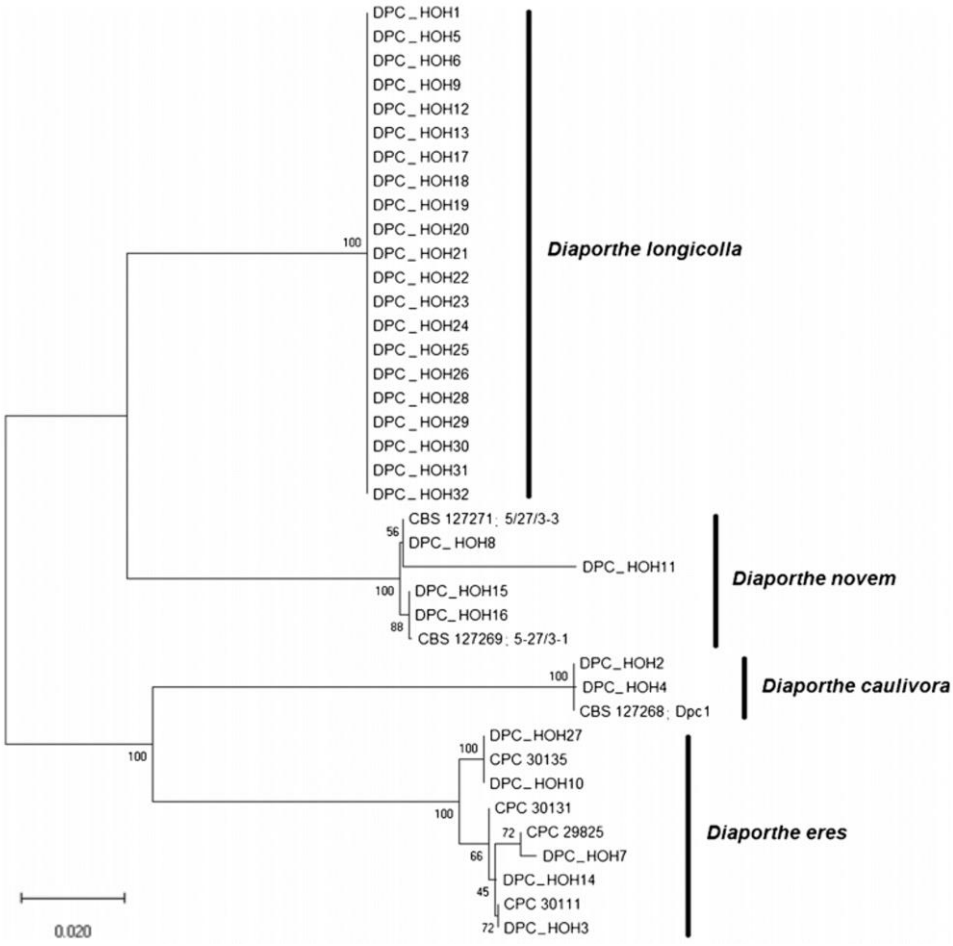

Figure 3.8: Maximum likelihood phylogenetic analysis of the *Diaporthe* species associated with soybean based on the combined three-gene sequence alignment (*TUB*, *TEF1*, and ITS).
Bootstrap numbers represent percent of 100 replicates. For each species, the ex-type strain sequences were included by their strain names. The sequences of the new *Diaporthe* isolates were included by their isolate number. No ex-type strain for which all three sequences were available could be identified for *D. longicolla*. Scale bar: 0.02 substitutions per site. TreeBASE accession: TB2:S24723.

Interestingly, isolate DPC_HOH11 had an ITS sequence that was different from all others (Figure 3.5). In BLASTN against NCBI it was most similar to *Phomopsis* sp. (98 % identity) then *D. pseudolongicolla* (91 % identity) and only then (90 % identity) to *D. novem*. The *TUB* sequence of DPC_HOH11 is identical to DPC_HOH8 and the *TEF* sequence highly similar to all three other *D. novem* isolates. This also brings the *D. novem* isolates together in the combined phylogeny (Figure 3.8). Morphologically DPC_HOH11 clearly also is *D. novem* but the sequence differences still are making it something special.

3.4. Pathogenicity of the *Diaporthe* isolates

To ensure that the DPC_HOHn isolates are pathogens of soybean, soybean seeds were inoculated with spore suspensions (as described in detail in 2.13.).

The pathogenicity of all 32 *Diaporthe* isolates could be proven by performing this experiment (Figure 3.9 A, B).

Figure 3.9: Disease symptoms on soybean plants.
A) Pod and stem blight symptoms on soybean plants caused by *D. longicolla* (isolate DPC_HOH28).
B) Black pycnidia on soybean stems caused by *D. longicolla* (isolate DPC_HOH28).

All *Diaporthe* isolates caused pod blight on inoculated soybean plants when they reached maturity. No considerable differences were noticed between them by evaluating of the discoloration of pods (Figure 3.10).

Checking the formation of black pycnidia on the stems of mature soybean plants revealed some differences between the isolates and the species (Figure 3.11). The highest scores for coverage of the stem with pycnidia were reached by *D. longicolla* isolates, particularly DPC_HOH32, DPC_HOH28, and DPC_HOH26. Among the *D. novem* isolates, just a few pycnidia could be observed on the inoculated plants with DPC_HOH11 and DPC_HOH16. *D. caulivora* and *D. eres* isolates did not show any pycnidia formation.

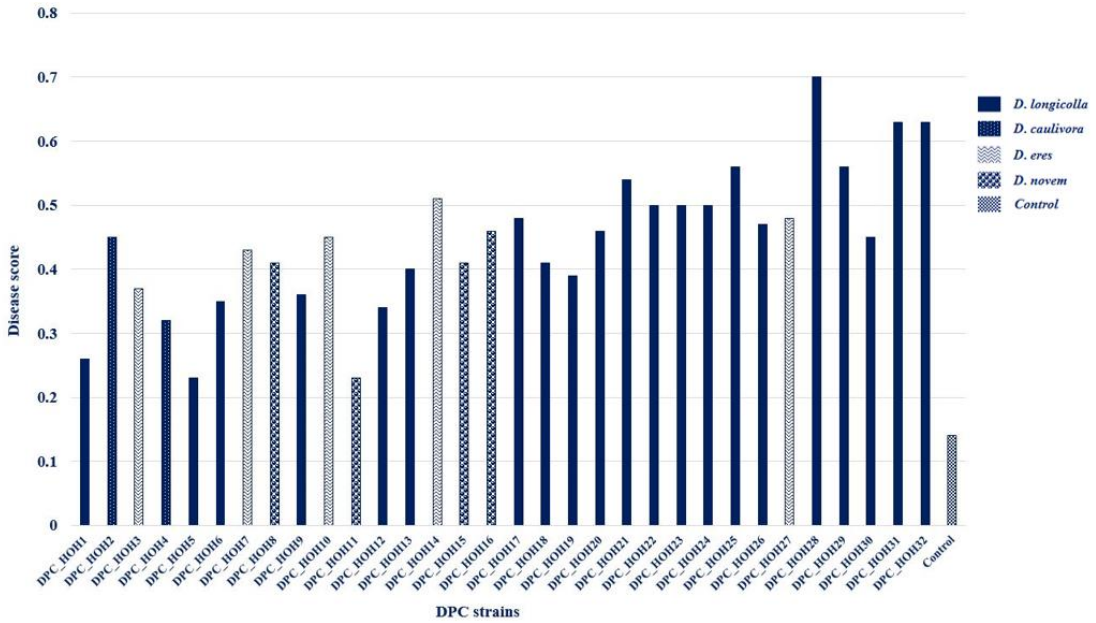

Figure 3.10: Evaluation of pod blight disease on soybean plants which were inoculated by spore suspensions of the 32 *Diaporthe* isolates.
Columns represent the average disease score based on four evaluations of nine plants each (2.13.5.). The species of the different isolates are indicated by the column patterns.

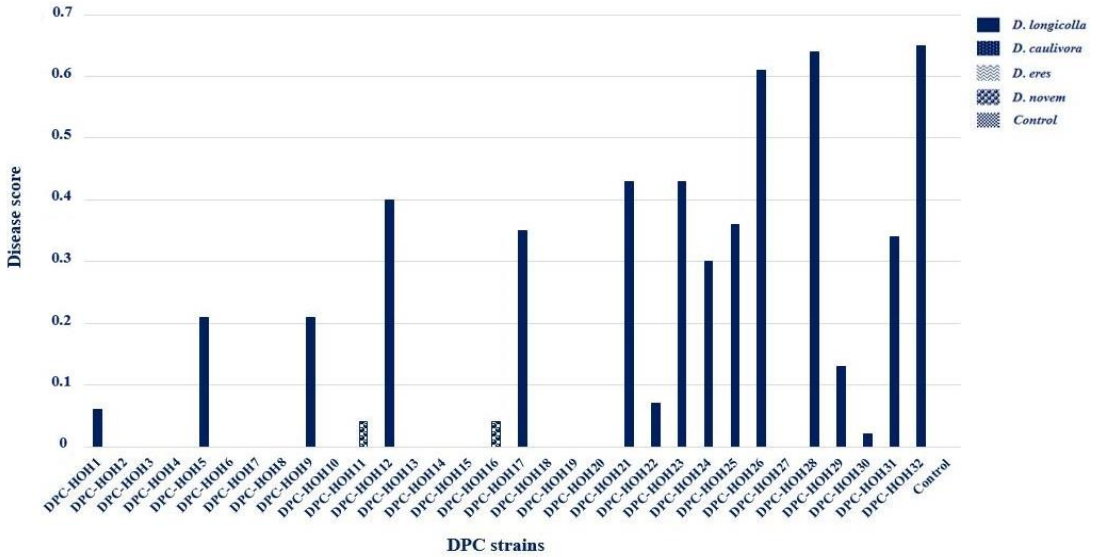

Figure 3.11: Evaluation of accumulation of black pycnidia on soybean stems which were inoculated by spore suspensions of the 32 *Diaporthe* isolates.
Columns represent the average disease score based on four evaluations of nine plants each (2.13.5.). The species of the different isolates are indicated by the column patterns.

3.5. Detection of *Diaporthe* species via real-time PCR

When the *Diaporthe* isolates were adequately characterized and after it was clear from above results that the four species *D. longicolla*, *D. caulivora*, *D. eres*, and *D. novem* are relevant in central Europe, the next stage of this thesis came into focus. This was to establish a method for molecular diagnosis to specifically identify these four species. Consequently,

primer-probe sets were identified, their specificity was assessed and the applicability of the system for seed testing was checked.

3.5.1. Design of TaqMan primer-probe sets

ITS and *TEF1* sequences of the 32 *Diaporthe* isolates along with sequences of ex-type species were aligned but identical sequences were eliminated to recognize which segments of the sequences are conserved and which are variable. Then, the TaqMan primer-probe sets were designed based on these ITS and *TEF1* sequence alignments of *Diaporthe* isolates (Table 2.17, Figure 3.12 A, B).

To detect *D. eres* and *D. novem* specifically, two reverse primers DE-3 R and DE-7 R and one wobble probe DPE3-7 P based on ITS sequences of two *D. eres* isolates DPC_HOH3 and DPC_HOH7; and also two reverse primers DPN-8 R and DPN-11 R and two probes DPN-8 P and DPN-11 P based on ITS sequences of two *D. novem* isolates DPC_HOH8 and DPC_HOH11 were designed *de novo* (Figure 3.12 A). These were combined with primers published by Zhang et al. (1999). Since the reverse primer DPC-3 R designed by Zhang et al. (1999) lies on a sequence stretch that is identical for all four species in this study, it was used as a forward primer for DPCE3, DPCE7, DPCN8, and DPCN11 primer-probe combinations.

After it became clear in duplex assays (see 3.5.2.2. below) that above primer-probe sets cannot be combined in multiplex reactions and efforts to design additional primers and probes in the ITS region showed that there is not enough sequence divergence in ITS to design four primer-probe combinations for multiplex PCR, the species-specific primer-probe sets DPCL, DPCC, DPCE, and DPCN were designed based on *TEF1* sequences. These primers can detect and distinguish *D. longicolla*, *D. caulivora*, *D. eres*, and *D. novem*, respectively, in a quadruplex reaction (Figure 3.12 B, chapter 3.5.3. ff).

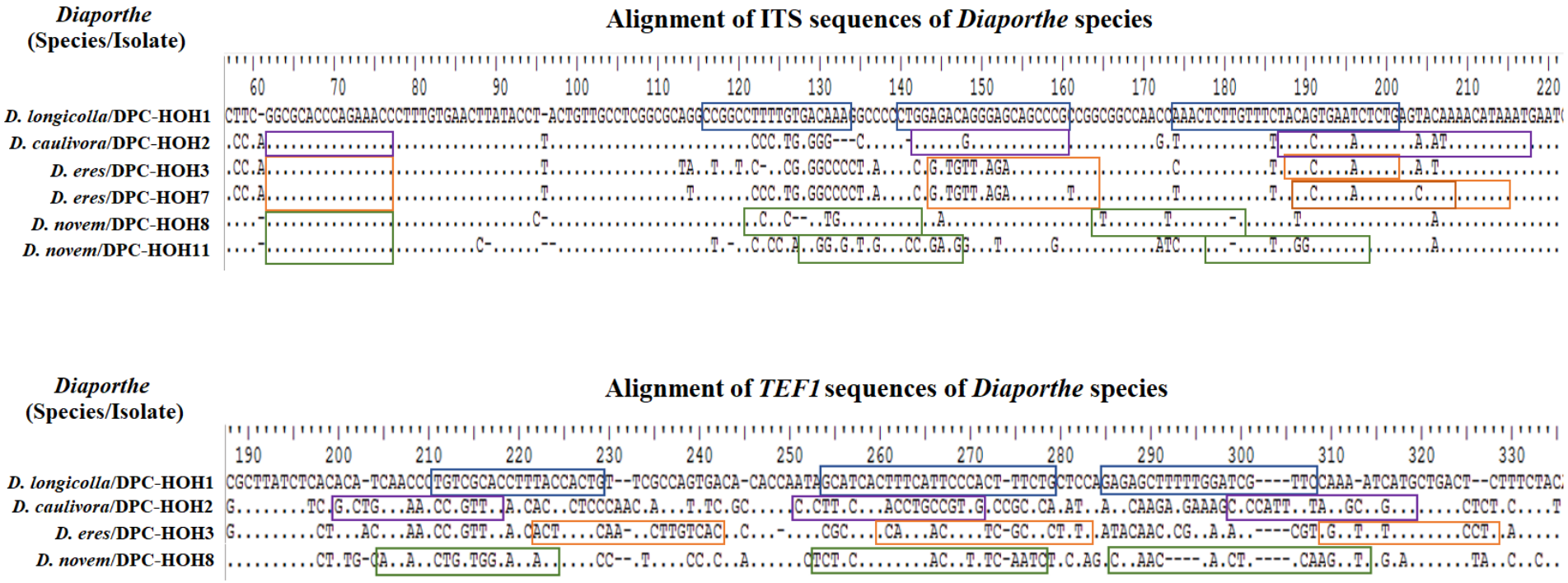

Figure 3.12: Primer and probe specificity based on alignment.
A) Position of TaqMan primer-probe combination PL-3 (blue frames), DPC-3 (purple frames), DPCE3 and DPCE7 (orange frames), DPCN8 and DPCN11 (green frames) in the alignment of ITS sequences of *Diaporthe* species; and **B**) Position of TaqMan primer-probe combinations DPCL (blue frames), DPCC (purple frames), DPCE (orange frames) and DPCN (green frames) in the alignment of *TEF1* sequences of *Diaporthe* species.
Identical nucleotides and gaps are represented by dots and dashes, respectively.
The sequences in the alignment were chosen from all sequences obtained in order to represent all intra specific polymorphisms, identical sequences were removed.

3.5.2. Evaluation of the specificity and efficiency of the TaqMan primer-probe sets PL-3, DPC-3, DPCE3, DPCE7, DPCN8, and DPCN11

The experiments for real-time PCR detection of the four species started with testing primer-probe sets found in the literature and additional primers designed to add to the specificities of the published sets.

From work performed by Zhang et al. (1999) the primer-probe sets, PL-5, PL-3, and DPC-3 based on ITS were available. Here PL-5 gives an amplification with DNA from *D. longicolla*, *D. caulivora*, *D. phaseolorum* var. *sojae*, or *D. phaseolorum* var. *meridionalis*. On the other hand PL-3 is specific for *D. longicolla* and DPC-3 for *D. caulivora*. Therefore, the specificity and efficiency of PL-3 and DPC-3 primer-probe sets were checked for *D. longicolla* and *D. caulivora* isolates in this study. Likewise, the specificity and efficiency of the self-designed primer-probe sets DPCE3, DPCE7, DPCN8, and DPCN11 were assessed for *D. eres* and *D. novem* isolates.

3.5.2.1. Singleplex real-time PCR assays

The efficiency of the primer-probe sets PL-3 and DPC-3 was checked with serial dilutions of ITS PCR products (10^8 to 10^4 copies/µL) and genomic DNA (undiluted, 1:10, 1:100, and 1:1,000) of *D. longicolla* isolate DPC_HOH20 and *D. caulivora* isolate DPC_HOH2, respectively, in singleplex real-time PCR assays (Table 3.3). DPCE3, DPCE7, DPCN8, and DPCN11 were also tested for efficiency in singleplex real-time PCR assays with similar serial dilutions of ITS PCR products and genomic DNA of isolates DPC_HOH3, DPC_HOH7, DPC_HOH8, and DPC_HOH11, respectively (Table 3.3). The efficiencies for the serial dilutions of ITS PCR products and the genomic DNAs were satisfying for all primer-probe sets (Table 3.3).

Table 3.3: TaqMan primer-probe combinations based on ITS sequences for detection and distinguishing *D. longicolla*, *D. caulivora*, *D. eres*, and *D. novem*

Primer-probe set/specificity	Primer Probe	Target isolate	Position [b] (bp)	Fragment length (bp)	Efficiency (%)	
					ITS PCR product	Genomic DNA
PL-3 [a] / *DL*	PL-3 F	DPC_HOH20	174–201	86	87.0	82.2
	PL-3 R		116–133			
	PL-3 P		140–160			
DPC-3 [a] / *DC*	DPC-3 F	DPC_HOH2	186–217	156	89.0	90.8
	DPC-3 R		62–77			
	DPC-3 P		142–160			
DPCE7 / *DE*	DPC-3 R	DPC_HOH3	62–77	147	94.9	-
	DE-7 R		188–208			
	DPE3-7 P		143–163			
DPCE7 / *DE*	DPC-3 R	DPC_HOH7	62–77	154	91.7	-
	DE-7 R		189–215			
	DPE3-7 P		144–164			

DPCE3 / *DE*	DPC-3 R	DPC_HOH3	62–77	140	95.0	-
	DE-3 R		188–201			
	DPE3-7 P		143–163			
DPCE3 / *DE*	DPC-3 R	DPC_HOH7	62–77	147	97.0	-
	DE-3 R		189–208			
	DPE3-7 P		144–164			
DPCE(1) [*] / *DE*	DPC-3 R	DPC_HOH3	62–77	140	98.2	98.6
	DE-7 R		188–208			
	DE-3 R		188–201			
	DPE3-7 P		143–163			
DPCE(1) [*] / *DE*	DPC-3 R	DPC_HOH7	62–77	154	98.3	94.9
	DE-7 R		189–215			
	DE-3 R		189–208			
	DPE3-7 P		144–164			
DPCN8 / *DN*	DPC-3 R	DPC_HOH8	61–76	77	97.4	85.9
	DPN-8 R		164–182			
	DPN-8 P		121–142			
DPCN11 / *DN*	DPC-3 R	DPC_HOH11	61–76	77	97.6	-
	DPN-11 R		177–197			
	DPN-11 P		128–147			

F = Forward primer, R = Reverse primer, and P = TaqMan Probe

[a] TaqMan primer-probe combinations PL-3 and DPC-3, which were designed by Zhang et al. (1999) to detect *D. longicolla* and *D. caulivora* species, respectively. In the sequences of the *Diaporthe* spp. in this study, DPC-3 R is oriented in forward direction, this is why the primer-probe combinations containing it all have an additional reverse primer.

[b] Positions of primers and probes within ITS

[*] The primer-probe set DPCE(1) is a mixture of own reverse primers DE-3 R, DE-7 R; primer DPC-3 R as forward primer; and probe DPE3-7 P.

DL = *D. longicolla*, *DC* = *D. caulivora*, *DE* = *D. eres*, and *DN* = *D. novem*

3.5.2.2. Duplex real-time PCR assays

Duplex real-time PCR assays were performed using Zhang et al. (1999) primer-probe sets PL-3 and DPC-3 and the three newly designed primer-probe sets DPCE(1), DPCN8, and DPCN11 to test their specificity by applying serial dilutions of ITS PCR products (10^8 to 10^4 copies/µL) of the *Diaporthe* isolates. In the duplex assays with the combination of primer-probe sets PL-3/DPC-3, when just PCR products of the *D. longicolla* isolate or just PCR products of the *D. caulivora* isolate were added to the reactions and it was expected to see just one signal from PL-3 P or DPC-3 P, both signals could be observed, which indicates that the specificity that these primer-probe sets have in singleplex reactions is lost in duplex reactions. As reason for this phenomenon it was established that the probes PL-3 P and DPC-3 P bind to the same sequence. This way it became clear that these probes cannot be used together in a duplex reaction (Figure 3.13 A, B). The same was observed for the duplex assays with the combination of primer-probe sets PL-3/DPCE3, when just PCR products of the *D. eres* isolate were applied to the reactions, the signal from probe PL-3 P could be seen (after 36 cycles) along with the signal from probe DPE3-7 P (Figure 3.13 C, D). The results of the duplex assays for the combination of primer-probe sets DPC-3/DPCE3, and

DPC-3/DPCN8, proved the specificity of each of the primer-probe sets, while the primer-probe sets DPC-3, DPCE3, and DPCN8 specifically detected just the DNA of *D. caulivora*, *D. eres*, and *D. novem* isolates, respectively (Figure 3.13 E, F, G, H).

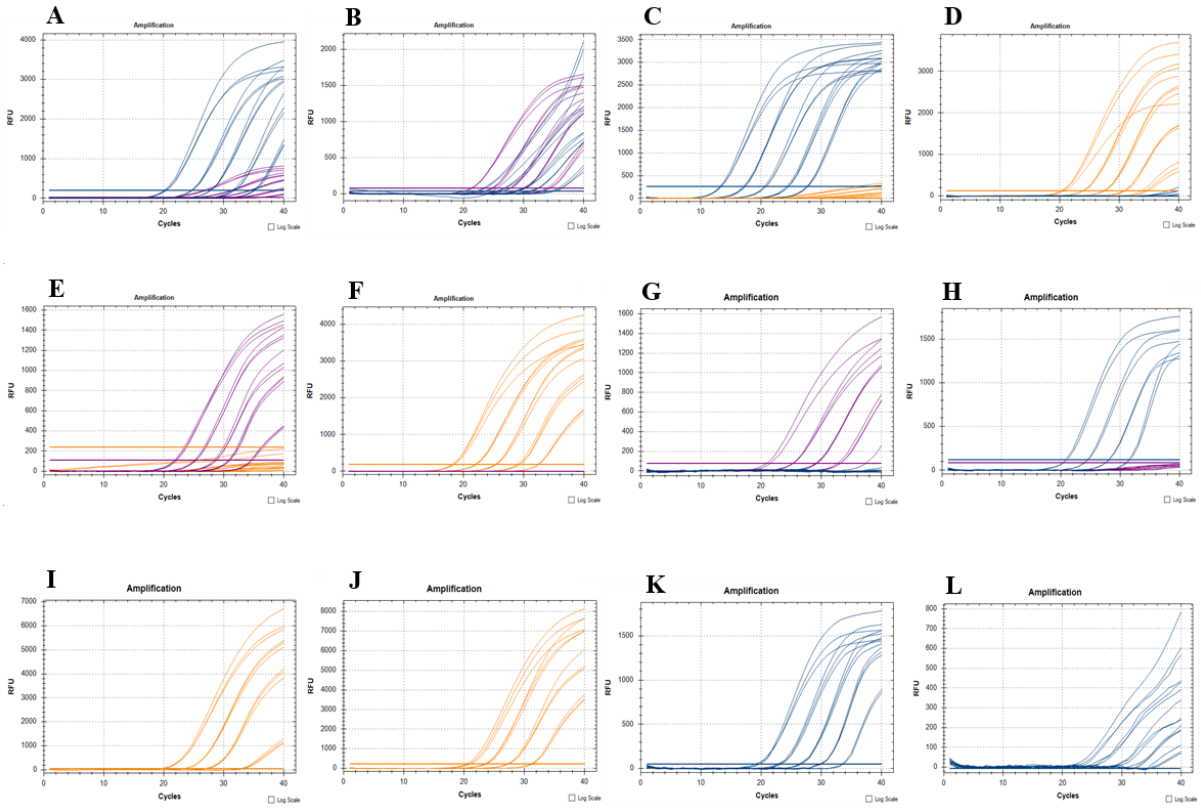

Figure 3.13: Duplex real-time PCR assays using dilution series of ITS PCR products (10^8 to 10^4 copies/µL) of the *Diaporthe* isolates.
A) Dilution series of ITS PCR products of *D. longicolla* isolate DPC_HOH20 in the mix with primer-probe sets PL-3/DPC-3, **B**) Dilution series of ITS PCR products of *D. caulivora* isolate DPC_HOH2 in the mix with primer-probe sets PL-3/DPC-3, **C**) Dilution series of ITS PCR products of *D. longicolla* isolate DPC_HOH20 in the mix with primer-probe sets PL-3/DPCE3, **D**) Dilution series of ITS PCR products of *D. eres* isolate DPC_HOH3 in the mix with primer-probe sets PL-3/DPCE3, **E**) Dilution series of ITS PCR products of *D. caulivora* isolate DPC_HOH2 in the mix with primer-probe sets DPC-3/DPCE3, **F**) Dilution series of ITS PCR products of *D. eres* isolate DPC_HOH3 in the mix with primer-probe sets DPC-3/DPCE3, **G**) Dilution series of ITS PCR products of *D. caulivora* isolate DPC_HOH2 in the mix with primer-probe sets DPC-3/DPCN8, **H**) Dilution series of ITS PCR products of *D. novem* isolate DPC_HOH8 in the mix with primer-probe sets DPC-3/DPCN8, **I**) Dilution series of ITS PCR products of *D. eres* isolate DPC_HOH3 in the mix with primer-probe sets DPCE3/DPCE7, **J**) Dilution series of ITS PCR products of *D. eres* isolate DPC_HOH7 in the mix with primer-probe sets DPCE3/DPCE7, **K**) Dilution series of ITS PCR products of *D. novem* isolate DPC_HOH8 in the mix with primer-probe sets DPCN8/DPCN11, **L**) Dilution series of ITS PCR products of *D. novem* isolate DPC_HOH11 in the mix with primer-probe sets DPCN8/DPCN11.

Interestingly, in the duplex assays for the combination of primer-probe sets DPCE3/DPCE7, both *D. eres* isolates DPC_HOH7 and DPC_HOH3 could be identified (Figure 3.13 I, J) and also applying two reverse primers DE-3 R and DE-7 R along with primer DPC-3 R as forward primer and probe DPE3-7 P in these duplex assays using serial dilutions of ITS PCR products and also genomic DNA of both *D. eres* isolates, revealed that the efficiency increased

compared to when these reverse primers were used alone in primer-probe sets DPCE3 and DPCE7 (Table 3.3). Therefore, in the next real-time PCR assays DE-3 R, DE-7 R, DPC-3 R, and DPE3-7 P was used as primer-probe set DPCE(1) to detect *D. eres*. The combination of primer-probe sets DPCN8/DPCN11 showed that *D. novem* isolate DPC_HOH8 could be identified but for DPC_HOH11 the curves were strange (Figure 3.13 K, L).

Most importantly, the results showed that the primer-probe sets PL-3 and DPC-3 are only specific when used in singleplex reactions. Another reason why the primer-probe sets could not be used together for multiplex reactions was that, the probes of the two primer-probe sets DPCN8 and DPCN11 to detect *D. novem* were designed with the same reporting dye (FAM) as the probe PL-3 P in PL-3 for identification of *D. longicolla*. Therefore, to establish a quadruplex real-time PCR to specifically identify all four *Diaporthe* species simultaneously in one real-time PCR reaction, new primer-probe sets were needed.

3.5.3. New TaqMan primer-probe sets based on *TEF1*

By further assessments of the ITS sequence alignment of *Diaporthe* isolates, it became clear that it is not possible to design sets for more than one species in the ITS region because the sequences are too similar. Due to this, only DPCE(1) primer-probe set designed for *D. eres* located in the ITS region remained in use with the two reverse primers DE-3 R and DE-7 R along with DPC-3 R (one of the primers reported by Zhang et al. 1999), and DPE3-7 P. In this special case the lower divergence between sequences in the ITS region was an advantage, since the primer-probe set can detect both *D. eres* strains DPC_HOH3 and DPC_HOH7 which differ in their ITS sequences.

By alignment of *TEF1* sequences of *Diaporthe* isolates, more sequence regions could be found to design specific primer-probe sets (Figure 3.12 B). First only DPCL, DPCC, and DPCN were used, while DPCE(1) based on ITS was kept. Only later also DPCE was designed based on *TEF1*, especially to improve on the comparability of quantification results of the four species. Because of that, both DPCE(1) and DPCE are considered in several of the following sections.

Primers and probes which were designed based on *TEF1* sequences of *Diaporthe* isolates and primer-probe set DPCE(1) based on ITS sequences of *D. eres* isolates, were checked for specificity using Primer-BLAST. Because the specificity checking only works with primer pairs, not with single oligonucleotides, the test was run three times for all primer-probe sets, combining forward primer with reverse primer (FR), reverse primer and probe (RP), and forward primer and probe (FP). The output species were noted for all three combinations;

only species returned by both FR and RP were considered to be detected by the set. These species are listed below in Table 3.4.

Table 3.4: *In silico* assessing of the specificity of the TaqMan primer-probe sets

Primer-probe set / specificity	Output species [a]
DPCL / *DL*	***Diaporthe longicolla***, *Diaporthe sojae*, *Diaporthe unshiuensis*, *Diaporthe* sp. isolate G.04, *Diaporthe phaseolorum*, *Diaporthe* sp. Strain SAUCC194.63, *Diaporthe tectonendophytica*
DPCC / *DC*	***Diaporthe caulivora***, *Diaporthe phaseolorum* var. *caulivora*
DPCE(1) / *DE*	***Diaporthe eres***, *Phomopsis velata*, *Diaporthe nobilis*, *Diaporthe citrichinensis*, *Diaporthe melonis*, *Phomopsis fukushii*, *Phomopsis mali*, *Diaporthe rosicola*, *Diaporthe amygdali*, *Diaporthe phaseolorum*, *Diaporthe oraccinii*
DPCE / *DE*	***Diaporthe eres***, *Diaporthe vacuae*, *Diaporthe mahothocarpus*, *Diaporthe nobilis*, *Diaporthe fukushii*, *Diaporthe perniciosa*, *Diaporthe lonicerae*, *Diaporthe castaneae-mollisimae*, *Diaporthe bicincta*, *Diaporthe neilliae*, *Diaporthe biguttusis*, *Diaporthe cotoneastri*, *Diaporthe phaseolorum*, *Diaporthe rosicola*, *Diaporthe ellipicola*, *Diaporthe celastrina*, *Diaporthe alnea*, *Diaporthe nitschkei*
DPCN / *DN*	***Diaporthe novem***, *Diaporthe pseudolongicolla*, *Phomopsis* sp. ER 1657, *Phomopsis* sp. ER 1639, *Phomopsis* sp. JMS-2010g, *Phomopsis* sp. JMS-2010e, *Phomopsis* sp. CBS 117165, *Diaporthe* sp. AG-2020c, *Diaporthe gulyae*, *Diaporthe stewartii*, *Diaporthe cucurbitae*, *Diaporthe subordinaria*, *Diaporthe angelicae*, *Phomopsis* sp. DAR73811, *Diaporthe* sp. YPT-2011a

[a] Species names are generally kept as in the Primer-BLAST output, only obvious synonyms were removed. *DL* = *D. longicolla*, *DC* = *D. caulivora*, *DE* = *D. eres*, and *DN* = *D. novem*

These predictions strongly indicate that the primer-probe combinations can discriminate between the four *Diaporthe* species of interest and do not lead to amplification with other soybean pathogens occurring in central Europe.

3.5.4. Evaluation of the specificity and efficiency of the TaqMan primer-probe sets DPCL, DPCC, DPCE, and DPCN

The same testing strategy as described above (3.5.2.) was applied to DPCL, DPCC, DPCE, and DPCN.

3.5.4.1. Singleplex real-time PCR assays

Primer efficiency was tested initially by using serial dilutions of *TEF1* PCR products of the *Diaporthe* isolates to avoid problems with inhibitors. To supplement this, primer efficiency was also examined with serial dilutions of genomic DNA to check conditions that are more similar to the actual screen for *Diaporthe*. Efficiencies for both conditions were satisfying (Table 3.5, Figure 3.14), though surprising differences also occurred. From the results with *TEF1* PCR products it could also be concluded that as few as ten copies or less are detectable.

Table 3.5: TaqMan primer-probe combinations based on *TEF1* sequences for detection and distinguishing *D. longicolla*, *D. caulivora*, *D. eres*, and *D. novem*

Primer-probe set/specificity	Primer Probe	Target isolate	Position [a] (bp)	Fragment length (bp)	Efficiency (%)	
					TEF1 PCR product	Genomic DNA
DPCL / *DL*	DPCL-F	DPC_HOH20	199–217	90	98.2	81.0
	DPCL-R		269–288			
	DPCL-P		239–263			
DPCC / *DC*	DPCC-F	DPC_HOH2	186–204	120	97.7	90.0
	DPCC-R		285–305			
	DPCC-P		237-257			
DPCE / *DE*	DPCE-F	DPC_HOH3	208–227	100	82.4	92.2
	DPCE-R		288–307			
	DPCE-P		244–266			
DPCE / *DE*	DPCE-F	DPC_HOH7	208–227	101		
	DPCE-R		289–308			
	DPCE-P		245–267			
DPCN / *DN*	DPCN-F	DPC_HOH8	192–211	99	94.5	93.0
	DPCN-R		270–290			
	DPCN-P		238–262			
DPCN / *DN*	DPCN-F	DPC_HOH11	193–212	99	95.5	84.2
	DPCN-R		271–291			
	DPCN-P		239–263			

F = Forward primer, R = Reverse primer, and P = TaqMan Probe

[a] Positions of primers and probes within *TEF1*

DL = *D. longicolla*, *DC* = *D. caulivora*, *DE* = *D. eres*, and *DN* = *D. novem*

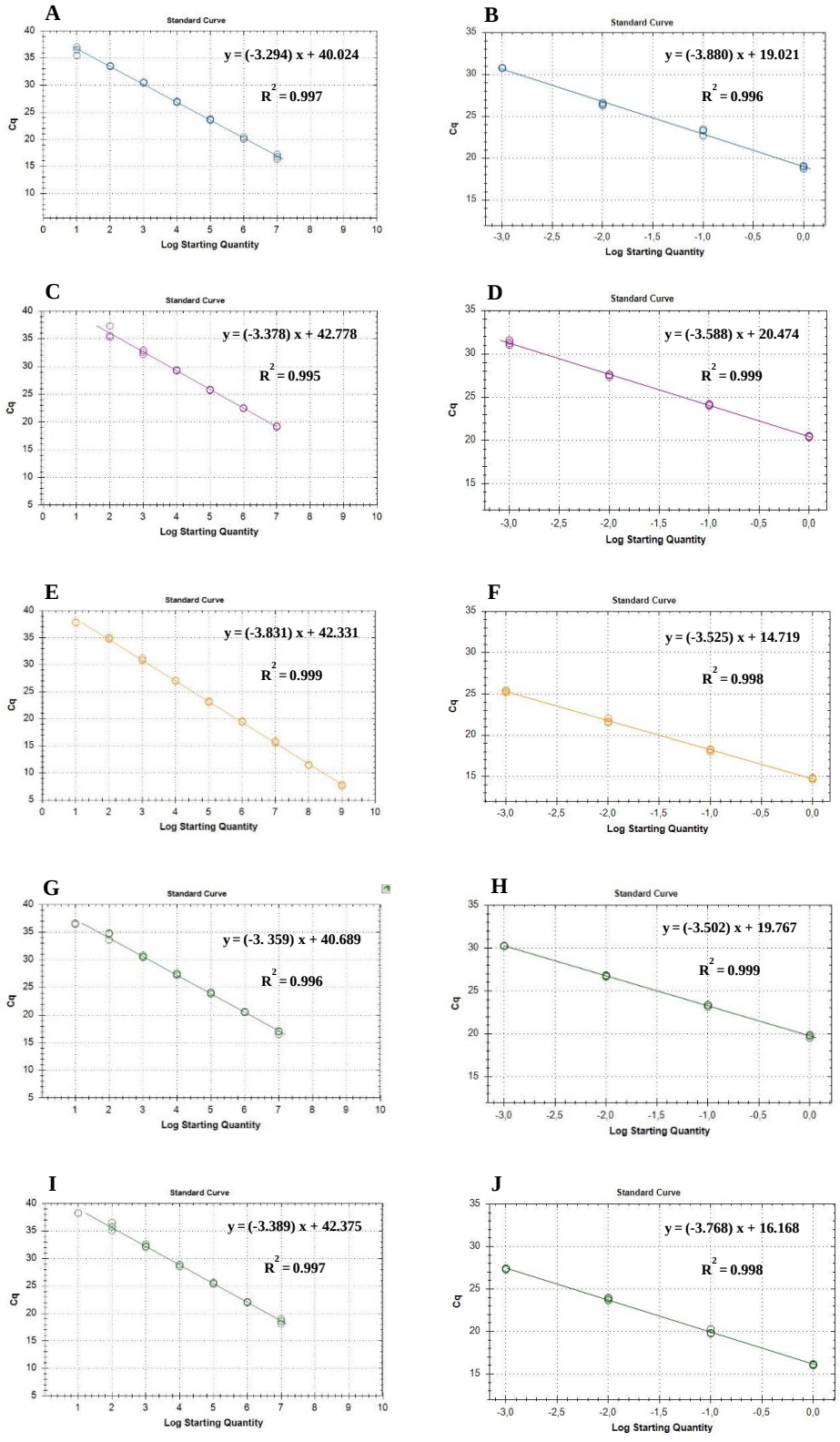

Figure 3.14: Standard curves to determine the efficiency of the primer-probe sets DPCL, DPCC, DPCE, and DPCN in singleplex reactions.

Graphs showing the quantification cycle (Cq) on the y-axis and the quantity of *TEF1* PCR product (10 to 10^7 or 10^9 copies) (**A**, **C**, **E**, **G**, **I**) or genomic DNA (undiluted, 1:10, 1:100, and 1:1,000) on the x-axis (**B**, **D**, **F**, **H**, **J**) for *D. longicolla* isolate DPC_HOH20 (**A** and **B**), *D. caulivora* isolate DPC_HOH2 (**C** and **D**), *D. eres* isolate DPC_HOH7 (**E** and **F**), and *D. novem* isolates DPC_HOH8 (**G** and **H**) and DPC_HOH11 (**I** and **J**).

The primer-probe sets DPCL, DPCC, DPCE(1), DPCE, and DPCN were tested for specificity with DNA from the target species and non-target *Diaporthe* species (Figure 3.15). No signal was observed with non-target species which indicates good specificity.

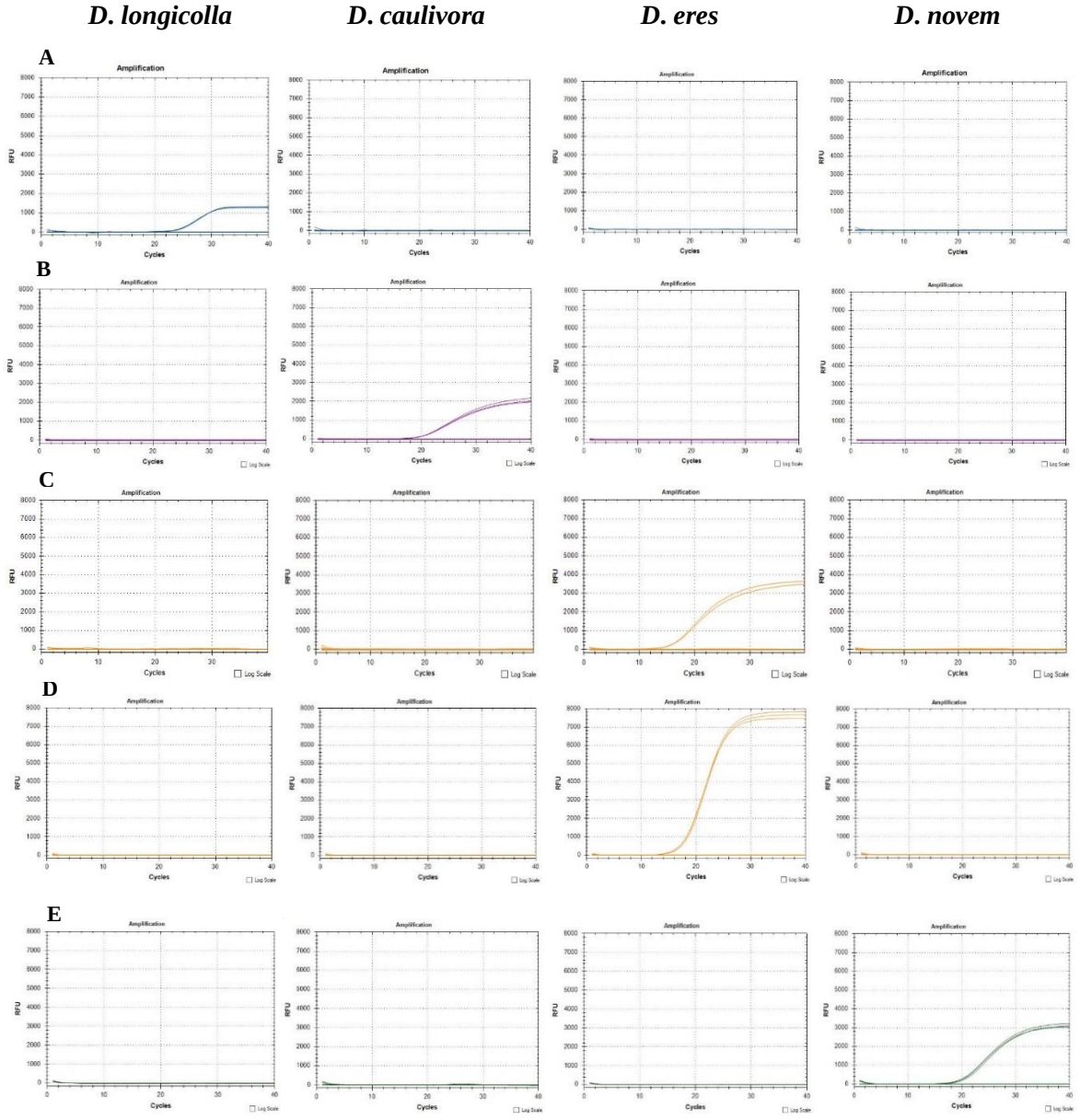

Figure 3.15: Specificity test for each TaqMan primer-probe set with *Diaporthe* species.
Primer-probe sets **A**) DPCL, **B**) DPCC, **C**) DPCE(1), **D**) DPCE, and **E**) DPCN were tested with DNA from *D. longicolla*, *D. caulivora*, *D. eres*, and *D. novem* (from left to right), respectively.

3.5.4.2. Multiplex real-time PCR assays

3.5.4.2.1. Duplex combinations

Tests were performed for all possible combinations of two primer-probe sets based on *TEF1* sequences (Table 2.7) and also for primer-probe set DPCE(1) in combination with DPCL, DPCC, and DPCN primer-probe sets to record the efficiencies of the TaqMan primer-probe sets in duplex reactions. All combinations were tested with parallel concentrations of DNA

from the two species. The observed efficiencies for the duplex reactions were still acceptable (Table 3.6). Also, for undiluted (20 ng) and 1:1,000 diluted genomic DNA from both species in individual reactions Cq values were recorded (Table 3.6).

Table 3.6: Duplex real-time PCR assays

Duplex PCR	Template DNA Species – Target Isolate	Primer-Probe sets	E(%) [a]	Cq 20 ng DNA [b]	Cq 20 pg DNA [c]	Cq 20 ng and 20 pg DNA [d]	Cq 20 pg and 20 ng DNA [e]
				Same concentration of DNA of both species		High conc. of DNA of one species combined with a low conc. of DNA of the other species and vice versa	
Set 1	*D. caulivora* – DPC_HOH2	DPCC	85.7	17.9	30.0	18.2	28.7
	D. eres – DPC_HOH7	DPCE	80.6	18.6	30.2	30.1	18.5
Set 2	*D. caulivora* – DPC_HOH2	DPCC	85.7	17.6	29.3	17.7	28.5
	D. novem – DPC_HOH15	DPCN	97.4	14.2	24.6	24.2	14.4
Set 3	*D. eres* – DPC_HOH7	DPCE	80.6	18.1	30.0	18.2	30.0
	D. novem – DPC_HOH15	DPCN	97.4	13.9	24.7	23.9	14.3
Set 4	*D. longicolla* – DPC_HOH28	DPCL	88.4	17.8	30.4	16.7	28.9
	D. caulivora – DPC_HOH2	DPCC	85.7	17.7	29.5	28.6	17.9
Set 5	*D. longicolla* – DPC_HOH28	DPCL	88.4	17.2	29.5	17.7	28.3
	D. eres – DPC_HOH7	DPCE	80.6	18.2	29.9	29.8	18.2
Set 6	*D. longicolla* – DPC_HOH28	DPCL	88.4	16.0	28.2	17.5	28.8
	D. novem – DPC_HOH15	DPCN	97.4	14.1	24.5	24.2	14.2
Set 7	*D. eres* – DPC_HOH7	DPCE(1)	2636.4	20.2	22	24.9	25.6
	D. caulivora – DPC_HOH2	DPCC	94.4	20.4	28.8	32.0	18.5
Set 8	*D. novem* – DPC_HOH15	DPCN	92.1	19.3	26.5	19.7	25.5
	D. eres – DPC_HOH7	DPCE(1)	89.3	15.9	23.1	22.7	15.5
Set 9	*D. longicolla* – DPC_HOH28	DPCL	96.5	23.1	28.8	23.4	30.4
	D. eres – DPC_HOH7	DPCE(1)	85.6	16.4	23.7	24.1	16.5

Each quantification cycle (Cq) value is the average of technical duplicates.

[a] Efficiencies of primer-probe sets in the duplex reactions. Dilution series of both species were used; the same dilution for both species.

[b] Cq values measured in reactions where undiluted DNA from both of species was used.

[c] Cq values measured in reactions where 1:1,000 diluted DNA from both of species was used.

[d] Cq values measured in reactions where DNA from the first species in the set was undiluted and DNA from the second species of the set was diluted 1:1,000.

[e] Cq values measured in reactions where DNA from the first species in the set was diluted 1:1,000 and DNA from the second species of the set was undiluted.

To establish how detrimental high concentrations of a different template would be to the reaction, extra experiments were carried out where low concentrations of one template were combined with high concentrations of the other. Again, Cq values were documented (Table 3.6). These tests prove the capability of the primer-probe sets to discriminate two species of *Diaporthe* in parallel. Applying two different templates does not have a significant effect on the performance of the assay even if the other, competing template was present in much higher concentration than the target template (Table 3.6). A surprising result was recorded for *D. eres* in combination with *D. caulivora*, when the two primer-probe sets DPCC and DPCE(1) were used in duplex real-time PCR reactions. Here the Cq measured for the undiluted DNA was much higher than expected. This also resulted in a very high calculated

efficiency. It is assumed that the reason for this result was a polymerase inhibitor, but it is not clear where it came from, especially because the same effect did not appear with any of the other combinations. These results for DPCE(1) also contributed to the later decision to replace it by DPCE.

3.5.4.2.2. Quadruplex real-time PCR assays

The first test for the full assay was once more a test for specificity. DNA from the different species was added individually to the reaction mixture with the primer-probe sets DPCL, DPCC, DPCE, and DPCN. In all cases, only a signal from the specific reporting dye was obtained (Figure 3.16 A-D). *D. longicolla* and *D. eres* isolates from another collection were also tested. Here also amplification could be seen. It can be concluded that the primer-probe sets only amplify DNA from their own target species. Two non-target *Diaporthe* spp., eight other soybean pathogens, and three additional rust fungal species tested negative. DNA from healthy soybean leaves or stems also was not amplified (Figure 3.16 E). Overall this shows good specificity of the whole quadruplex assay.

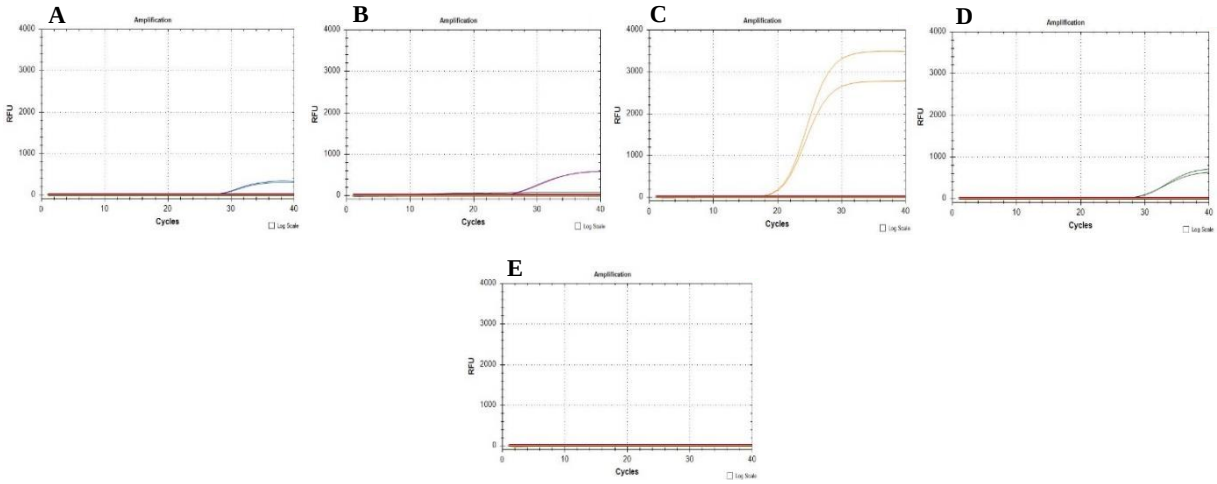

Figure 3.16: Specificity of the quadruplex real-time PCR assay using primer-probe sets DPCL, DPCC, DPCE, and DPCN.
Since the graphs for different isolates of the target species and also of all the non-target species are highly similar, only one representative graph is shown each. 0.4 ng DNA from **A**) *D. longicolla* DPC_HOH28, **B**) *D. caulivora* DPC_HOH2, **C**) *D. eres* DPC_HOH3, and **D**) *D. novem* DPC_HOH15 was added individually to the mix that contained all four primer-probe sets. **E**) Shows the result for the non-target species *D. aspalathi*, *D. foeniculina*, *C. kikuchii*, *F. solani*, *Alternaria* sp., *S. sclerotiorum* DSMZ, or *S. sclerotiorum* IZS, *C. truncatum*, *F. tricinctum*, *P. pachyrhizi*, *U. fabae*, *U. appendiculatus*, healthy soybean leaf, and healthy soybean stem. For these species and also *D. longicolla* isolate PL-157a and *D. eres* isolate PS-74 DNA amounts varied between 350 ng and 2.5 µg.

When DNA samples of two or three different *Diaporthe* species were tested together, the quadruplex assay still had its full specificity and correctly discriminated the present species (Figure 3.17 A-J).

As a final test, DNA from *D. longicolla*, *D. caulivora*, *D. eres*, and *D. novem* was applied to the same PCR reaction. Signals from all four probes can be seen (Figure 3.17 K), which proves that the assay can detect all four *Diaporthe* species in parallel.

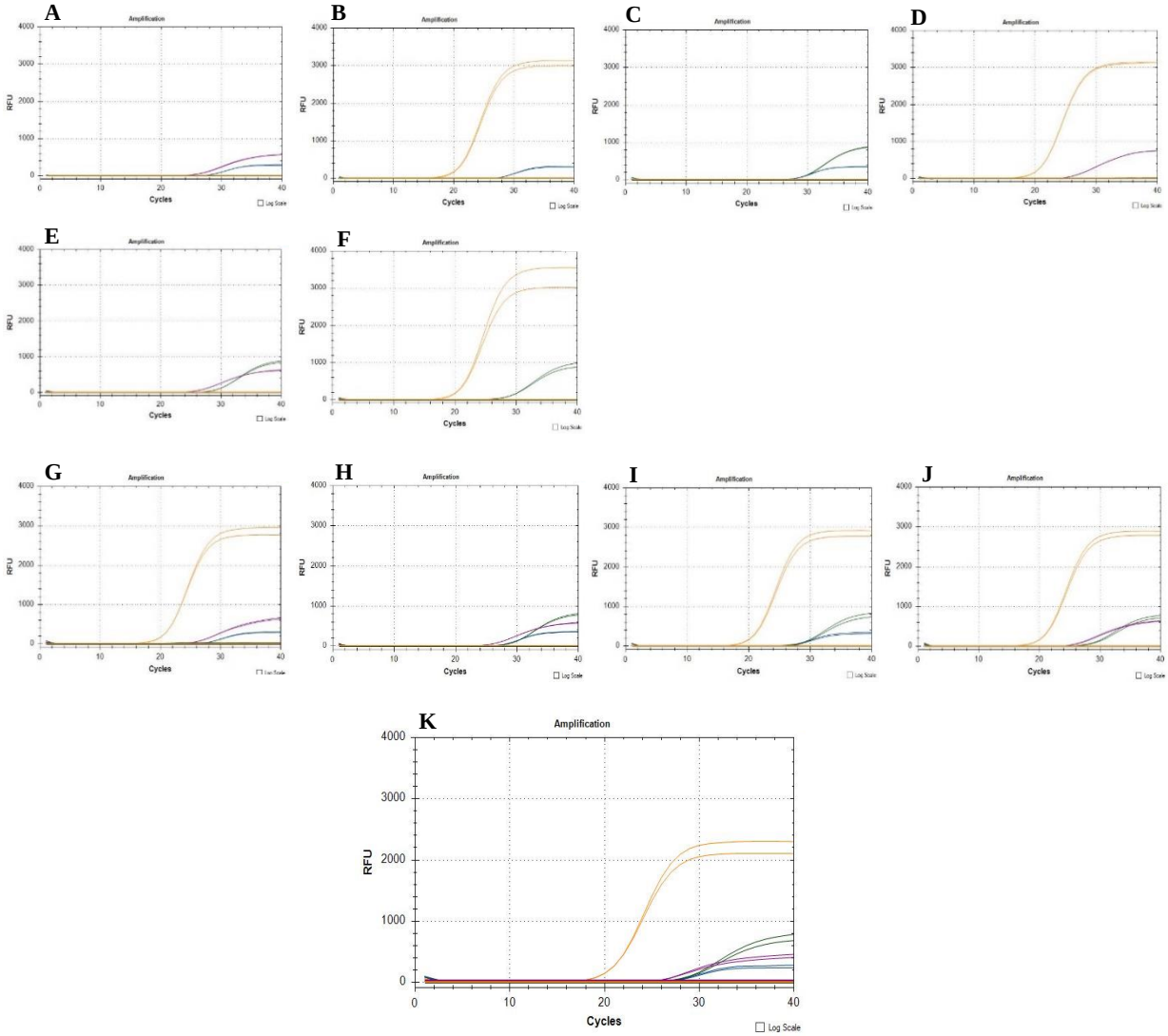

Figure 3.17: Specificity of the quadruplex real-time PCR assay using primer-probe sets DPCL, DPCC, DPCE, and DPCN.
Parallel detection of two (**A-F**), three (**G-J**), or all four (**K**) different *Diaporthe* species in the quadruplex real-time PCR assay using primer-probe sets DPCL, DPCC, DPCE, and DPCN. 0.4 ng DNA from **A**) *D. longicolla* (blue) and *D. caulivora* (purple), **B**) *D. longicolla* and *D. eres* (orange), **C**) *D. longicolla* and *D. novem* (green), **D**) *D. caulivora* and *D. eres*, **E**) *D. caulivora* and *D. novem*, **F**) *D. eres* and *D. novem*, **G**) *D. longicolla*, *D. caulivora*, and *D. eres*, **H**) *D. longicolla*, *D. caulivora*, and *D. novem*, **I**) *D. longicolla*, *D. eres*, and *D. novem*, **J**) *D. caulivora*, *D. novem*, and *D. eres*, and **K**) *D. longicolla*, *D. caulivora*, *D. eres*, and *D. novem* were added to the mix that contained all four primer-probe sets.

The mixture of the four primer-probe sets DPCL, DPCC, DPCE(1), and DPCN was tested the same way as described above for DPCL, DPCC, DPCE, and DPCN. This combination can also detect *D. longicolla*, *D. caulivora*, *D. eres*, and *D. novem* in parallel in one PCR reaction (Appendix 7.1., Figure 7.1).

3.5.5. Validation of the quadruplex real-time PCR assay

The whole assay was designed for detecting *Diaporthe* in infected plant tissues. To show that this is possible, DNAs from artificially infected stem samples (Table 2.21) and soybean seed samples known to be infected with *Diaporthe* (Table 2.8) were tested in quadruplex real-time PCR reactions with the primer-probe sets DPCL, DPCC, DPCE, and DPCN.

3.5.5.1. Infected soybean stems

D. longicolla DNA was detected in all symptomatic samples (Figure 3.18 A, C). For samples from healthy stems the assay gave no signal (Figure 3.18 B, D).

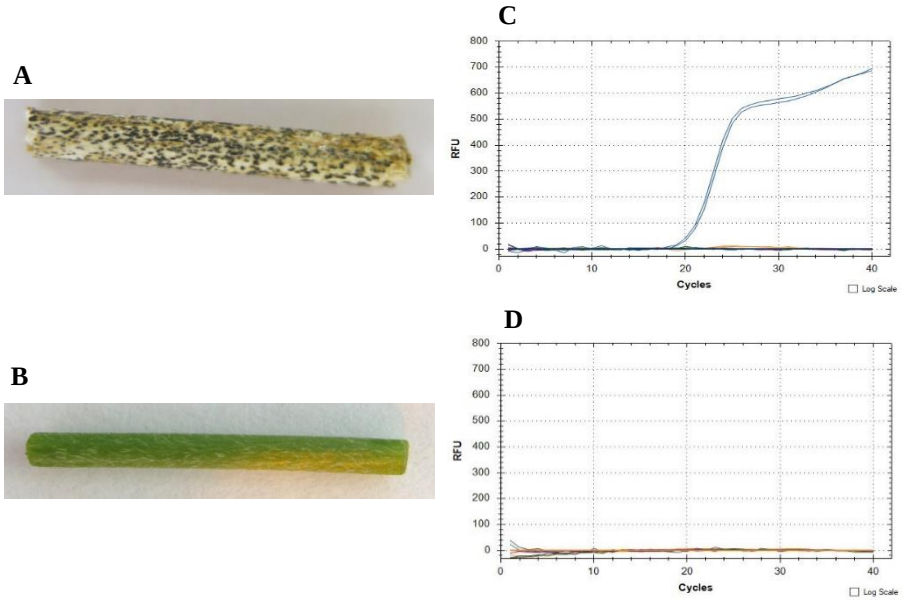

Figure 3.18: Validation of the quadruplex real-time PCR assay.
A) Soybean stem sample inoculated with *D. longicolla* isolate DPC_HOH26, **B**) Healthy soybean stem sample, **C** and **D**) Quadruplex real-time PCR on the stem samples shown in **A** and **B**, respectively.

3.5.5.2. Screening soybean seeds

Since *Diaporthe* spp. are seed borne, screening of seed lots will probably become the most useful application for this real-time PCR assay. Therefore, it was tested for detection of the *Diaporthe* pathogens in DNA from soybean seeds. First, DNA preparation was tested from whole seeds, seed coats, and uncoated seeds (each infected and healthy) in order to compare the quality of extracted DNAs for successful amplifications. *D. eres* and *D. novem* could be detected via the quadruplex real-time PCR assays in all DNAs prepared from infected seeds, while no amplification was seen for healthy seeds (Figure 3.19). Also, these trials confirmed the perception that homogenization of seed coats can be accomplished easier and faster than that of whole seeds and uncoated seeds. In the following experiments, DNA was extracted from seed coats of soybeans which were sampled from six different seed lots. These DNAs

were tested in the quadruplex real-time PCR assay. This resulted in the detection of all four *Diaporthe* species from different samples, respectively (Figure 3.21).

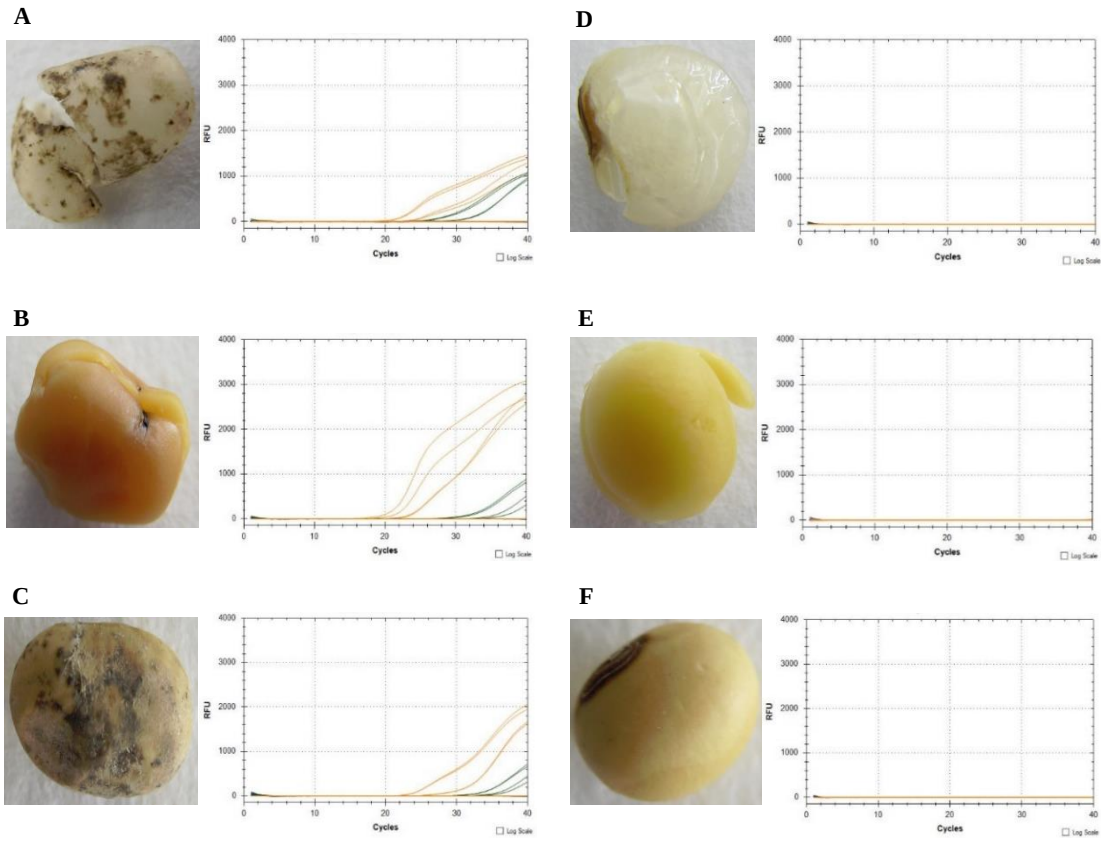

Figure 3.19: Screening soybean seeds via the quadruplex real-time PCR assay.
D. eres and *D. novem* were detected in extracted DNA of **A**) Infected seed coat, **B**) Infected uncoated seed, and **C**) Whole infected seed. No amplification was observed for **D**) Healthy seed coat, **E**) Healthy uncoated seed, and **F**) Whole healthy seed.

3.5.6. Quantification of the amount of *Diaporthe* DNA in soybean seeds

Diaporthe species are seed borne pathogens, which means that they grow in the seeds, but sometimes, especially when the seeds are severely infected, parts of fungal structures, including mycelium or spores, can be observed on the surface of the seeds. Therefore, in principle, there are two possible ways for seed sampling and quantification of the amount of these fungal pathogens: Quantification of fungal (*Diaporthe*) DNA relative to plant (soybean) DNA, and absolute quantification of fungal biomass.

3.5.6.1. Quantification relative to plant DNA

3.5.6.1.1. Standard curves for quantification relative to plant DNA

Since it is common to describe the strength of an infestation of seeds with pathogens in ng fungal DNA per ng plant DNA, DNA dilution series for four representative isolates (Table 3.7) were prepared. The targeted DNA amounts for the dilution series were 20 ng, 2 ng, 200 pg, 20 pg, 2 pg, 0.2 pg, and 0.02 pg DNA per reaction. The actual concentrations were measured precisely using fluorometry and differed slightly. To mimic the actual assay, the

fungal DNA was diluted with soybean DNA. In addition, a dilution series was created with soybean DNA using 20 ng, 2 ng, 200 pg, 20 pg, 2 pg, 0.2 pg, and 0.02 pg DNA per reaction. This DNA was diluted with ddH_2O. With the help of these standard curves (Figure 3.20, Table 3.7) the amount of *Diaporthe* DNA can be calculated from the Cq values.

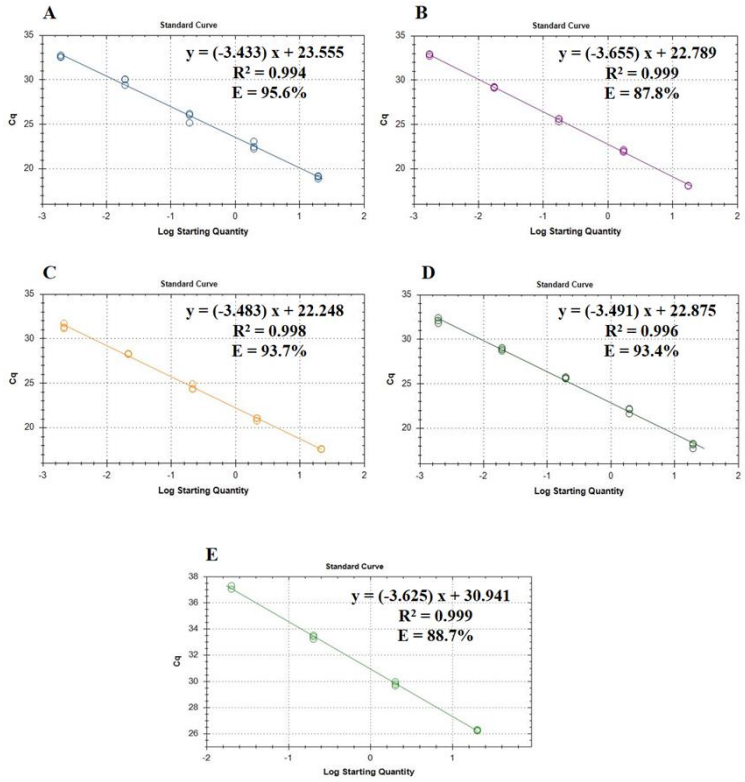

Figure 3.20: Standard curves for quantification of *Diaporthe* spp. using the quadruplex qPCR assay.
A) Graph and data of the standard curve for *D. longicolla*. The highest starting amount was 19.4 ng. The fluorescence threshold was set at 10 RFU. **B**) Graph and data of the standard curve for *D. caulivora*. The highest starting amount was 17.4 ng. The fluorescence threshold was set at 35 RFU. **C**) Graph and data of the standard curve for *D. eres*. The highest starting amount was 21.4 ng. The fluorescence threshold was set at 84 RFU. **D**) Graph and data of the standard curve for *D. novem*. The highest starting amount was 19.4 ng. The fluorescence threshold was set at 42 RFU. **E**) Graph and data of the standard curve for soybean DNA. The fluorescence threshold was set at 1805.70 RFU.

Table 3.7: Functions and additional information derived from standard curves

Species	Isolate [a]	Function [b] [Cq]	LOD [c] [pg]	Cq cutoff [d]
D. longicolla	DPC_HOH20	= 23.6–3.4x	0.2 > X > 0.02	36 > X > 39
D. caulivora	DPC_HOH2	= 22.8–3.6x	0.2 > X > 0.02	35 > X > 38
D. eres	DPC_HOH7	= 22.2–3.5x	0.2 > X > 0.02	33 > X > 36
D. novem	DPC_HOH11	= 22.8–3.5x	2^c > X > 0.02	32 > X > 37
Soybean	-	= 30.9–3.6x	-	-

[a] Isolate from which DNA was prepared for the standard curve experiment.
[b] Function describing the standard curve. x = log10 starting quantity in ng.
[c] Estimate for the limit of detection showing the DNA amount from the standard curve experiment that still gave an amplification and the first amount that did not give amplification. For *D. novem* one of the reactions at 0.2 ng was also negative; this is responsible for the very wide range in this case.
[d] Estimate for the cutoff derived from the LOD: Cq corresponding to the amount still giving amplification and the calculated virtual Cq where no amplification was seen.

Exactly determining the limit of detection (LOD) and a Cq cutoff requires samples with DNA concentrations close to the LOD and several repeats. These experiments have not yet been done. The values presented in Table 3.7 are rough estimates derived from the existing standard curves.

3.5.6.1.2. Actual quantification

The quadruplex real-time PCR assay and a parallel SYBR® Green-based real-time PCR assay for soybean DNA were applied to six different soybean seed lots. The amount of DNA of each *Diaporthe* species and plant for each individual seed was calculated using the standard curves (Table 3.7) and then the amount of fungal DNA (ng) was set in relation to the amount of plant DNA (ng).

A

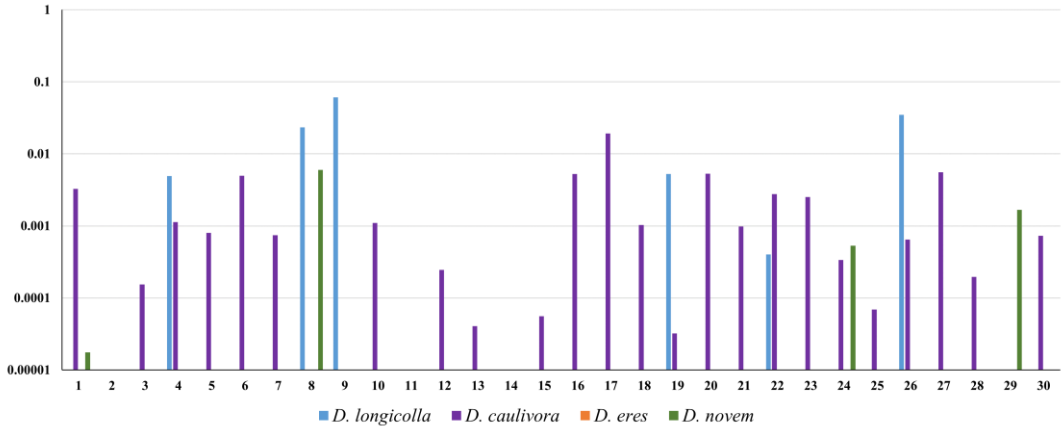

B

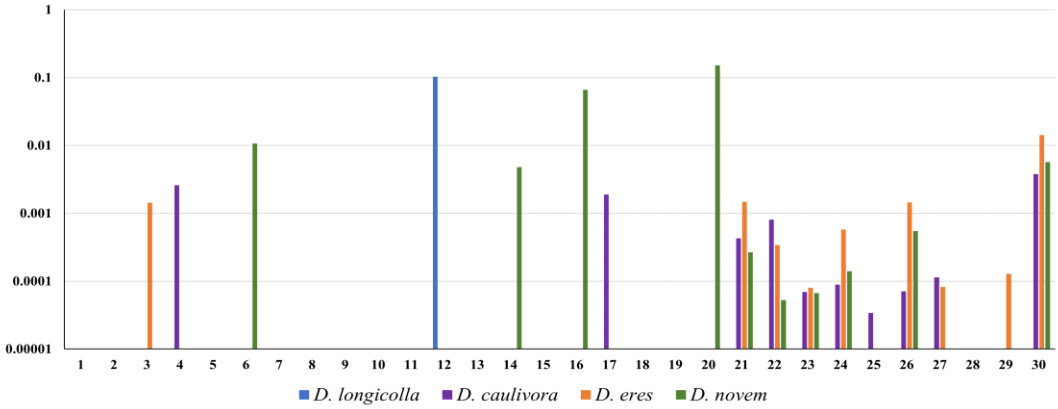

Figure 3.21: Sampling soybean seed lots via the quadruplex real-time PCR assay.
A) Seed lot from a field in Oberweiden, Austria; 27 seeds from 30 seed samples were infected, mostly with *D. caulivora* (purple) and rarely with *D. longicolla* (blue) and *D. novem* (green). **B**) Seed lot from a field in Ebergassing, Austria; 17 seeds from 30 seed samples were infected. Six of the seeds were infected with the three *Diaporthe* spp. *D. caulivora*, *D. novem*, and *D. eres* (orange) and just one of the seeds was infected with *D. longicolla*. Bars represent ng *Diaporthe* DNA/ng soybean DNA; because of the strong variation a logarithmic scale was chosen. The numbers on the x-axis represent the 30 seeds that were individually tested.

All seed lots contained seeds infected with *Diaporthe* spp. and some of the seeds were even infected with more than one *Diaporthe* species, while other seeds were free of the pathogens. Figure 3.21 shows the results from sampling two different seed lots and the results from sampling the other four seed lots are provided in Appendix 7.2., Figure 7.2.

The fungal biomass found in different seeds was highly variable. Here the assay clearly showed its capacity: it allows discriminating infections of seeds with different *Diaporthe* species and it allows the identification of double infections, something that was quite impossible previously.

Establishment of the quadruplex real-time PCR assay for the detection and quatification of the four *Diaporthe* species *D. longicolla*, *D. caulivora*, *D. eres*, and *D. novem*, has also been published (Hosseini et al. 2021).

3.5.6.2. Absolute quantification

Fungal structures (mycelium or spores) that only adhere to the surface of the seeds can be detected with less effort. A defined number of seeds can be simply soaked or washed in water and then this water can be used directly in the real-time PCR assay without the need for DNA extraction (Ramiro et al. 2019). When using this method "seed soaking", the absolute amount of fungal biomass has to be determined. Since the amount of DNA per fungal structures that can be detected in this assay is unknown, providing results in ng fungal DNA per reaction is not very informative. Likewise, absolute quantification is necessary for all samples that do not contain living plant material, for example soil samples or samples of runoff water. Therefore, experiments were performed to create a different set of standard curves for each *Diaporthe* species.

3.5.6.2.1. Standard curves for *Diaporthe* species mycelia

To quantify the mass of *Diaporthe* spp. mycelia, different amounts of mycelia were scraped from cultures of each *Diaporthe* species; these were weighted in individual tubes and homogenized. DNA extraction was performed by using the protocol by Liu et al. (2000), the DNAs were dissolved in 30 µL of ddH_2O and the concentration of DNA for each sample was recorded (Table 3.8). Although it was expected that the DNA concentration increases with increasing mycelial mass, this was not the case for all samples.

Using these samples, quadruplex real-time PCR was performed to obtain standard curves for each fungal species. DNA samples were applied undiluted and diluted 1:10 (Figures 3.22 - 3.25).

Table 3.8: Mass (in mg) and DNA concentration (in µg/mL) of mycelium from *D. longicolla*, *D. caulivora*, *D. eres*, and *D. novem*

Sample	*D. longicolla*		*D. caulivora*		*D. eres*		*D. novem*	
	Mass	**DNA concentration**	**Mass**	**DNA concentration**	**Mass**	**DNA concentration**	**Mass**	**DNA concentration**
1	3	-	7	2	6	20	7	25
2	4	2	11	293	11	30	12	117
3	8	11	18	425	16	53	13	5
4	12	4.3	24	19	19	80	20	293
5	14	24.8	27	46	25	81	22	332
6	15	38	30	59	28	101	25	323
7	20	38	40	44	37	200	31	507
8	22	82.6	43	131	45	112	42	935
9	26	156			53	392	56	1284
10	29	117			61	370		
11	35	93.8						
12	52	110						
13	90	128						
14	131	203						

Figure 3.22 A shows the standard curve for *D. longicolla* applying the undiluted samples, with an efficiency of E = 43.9 % and a correlation of $R^2 = 0.715$. An edited version is shown in Figure 3.22 B. Removed was sample 1 (referring to the order in Table 3.8) from a mycelium mass of 3 mg, because the concentration of DNA could not be measured what indicates a poor yield in the DNA preparation of small amounts of mycelium. Also samples 10 to 14 were deleted because the values did not fit the standard curve. Presumably, this was due to inhibitors, which were a problem with higher mycelium amounts. This curve shows an efficiency of E = 21.4 % but a much improved correlation of $R^2 = 0.965$. Figure 3.22 C shows the standard curve applying the 1:10 diluted samples with an efficiency of E = 51.7 % and a correlation of $R^2 = 0.731$. This standard curve was edited as well by deleting samples 1 and 10 to 14 (Figure 3.22 D). The resulting curve showed E = 26.2 % and $R^2 = 0.923$. Figure 3.22 E shows the standard curve with E = 89.4 % and $R^2 = 0.885$ for the undiluted and diluted samples with ng DNA as starting quantity in the x-axis. Compared to Figure 3.22 A and Figure 3.22 C, the correlation of the curve based on DNA amount is much better and also the efficiency is close to what was observed with the original standard curve (Figure 3.20 A). This indicates that the problems recorded in the other curves are due to inconsistent efficiencies of DNA preparation from different amounts of mycelium rather than any issues with qPCR.

The standard curve for the DNA from *D. caulivora* mycelium has E = 38.6 % and $R^2 = 0.810$ for the undiluted samples (Figure 3.23 A). For the 1:10 diluted samples E = 25.2 % and $R^2 = 0.766$ could be obtained, which were worse than those of the undiluted samples (Figure 3.23 B). Where ng DNA was put instead of g mycelium in the x-axis, the resulting

standard curve using the DNA of the *D. caulivora* mycelium has E = 76.9 % and R^2 = 0.935 (Figure 3.23 C).

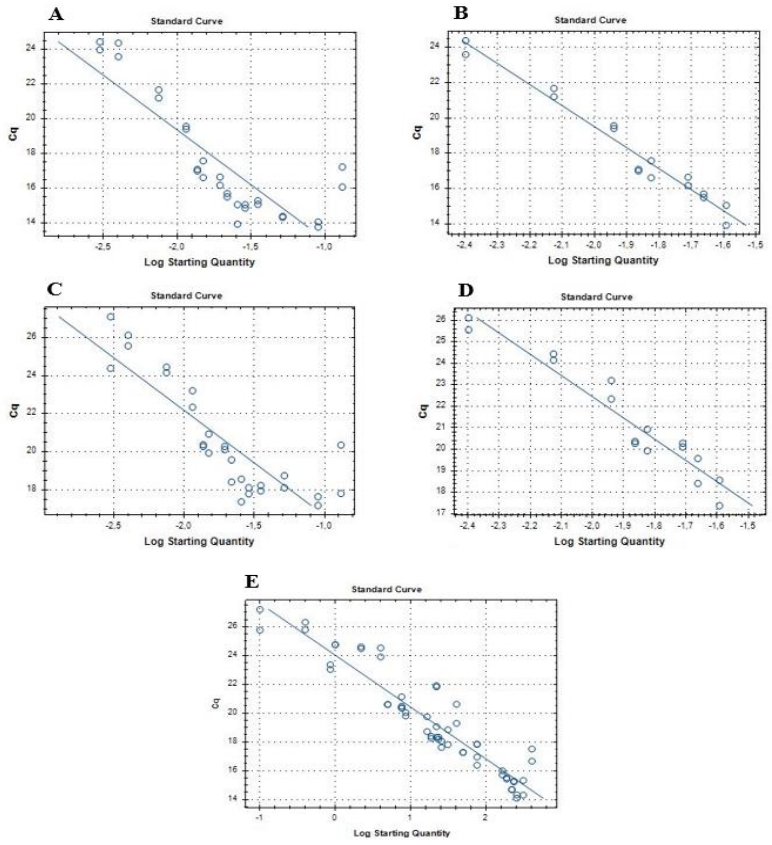

Figure 3.22: Standard curves from extracted DNA of *D. longicolla* (isolate DPC_HOH28) mycelium.
A, **C**) For the undiluted and 1:10 diluted samples, respectively, without editing; **B**, **D**) For the undiluted and 1:10 diluted samples, respectively, after editing; **E**) For the diluted and undiluted samples of DNA from mycelium of the *D. longicolla* isolate DPC_HOH28.
Log Starting Quantity in **A**, **B**, **C**, and **D** corresponds to the amount of mycelium in g.
Log Starting Quantity in **E** corresponds to the amount of fungal DNA from mycelium in ng.
The threshold in **A**, **B**, **C**, and **D** was set to RFU = 20 and in **E** was set to RFU = 29 based on the auto-function of the CFX Manager™ software (Bio-Rad Laboratories Inc.).

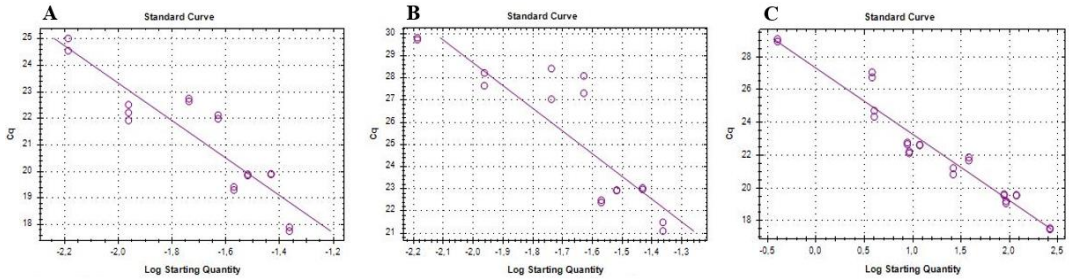

Figure 3.23: Standard curves from extracted DNA of *D. caulivora* (isolate DPC_HOH2) mycelium.
A) For the undiluted samples, **B**) For the 1:10 diluted samples, and **C**) For the diluted and undiluted samples of DNA from mycelium of the *D. caulivora* isolate DPC_HOH2.
Log Starting Quantity in **A** and **B** corresponds to the amount of mycelium in g.
Log Starting Quantity in **C** corresponds to the amount of fungal DNA from mycelium in ng.
The threshold for the data from *D. caulivora* in **A** and **B** was set to RFU = 70 and in **C** was set to RFU = 67 based on the auto-function of the CFX Manager™ software (Bio-Rad Laboratories Inc.).

For most samples of *D. eres* DNA concentrations increased with the mass of mycelium (Table 3.8). A correlation of $R^2 = 0.832$ and an efficiency of E = 61.1 % was determined in qPCR (Figure 3.24 A). In spite of the higher starting quantity, the last samples did not have lower Cq values, which again suggested inhibitors in the samples with large amounts of mycelium (samples 8, 9, and 10). Sample 10 was deleted in editing what resulted in a curve with $R^2 = 0.838$ and E = 68.4 % (Figure 3.24 B). In the graph for the 1:10 diluted samples (Figure 3.24 C) the possible effect of the inhibitors was less visible than with the undiluted samples and an efficiency of E = 66.6 % and $R^2 = 0.870$ were determined.

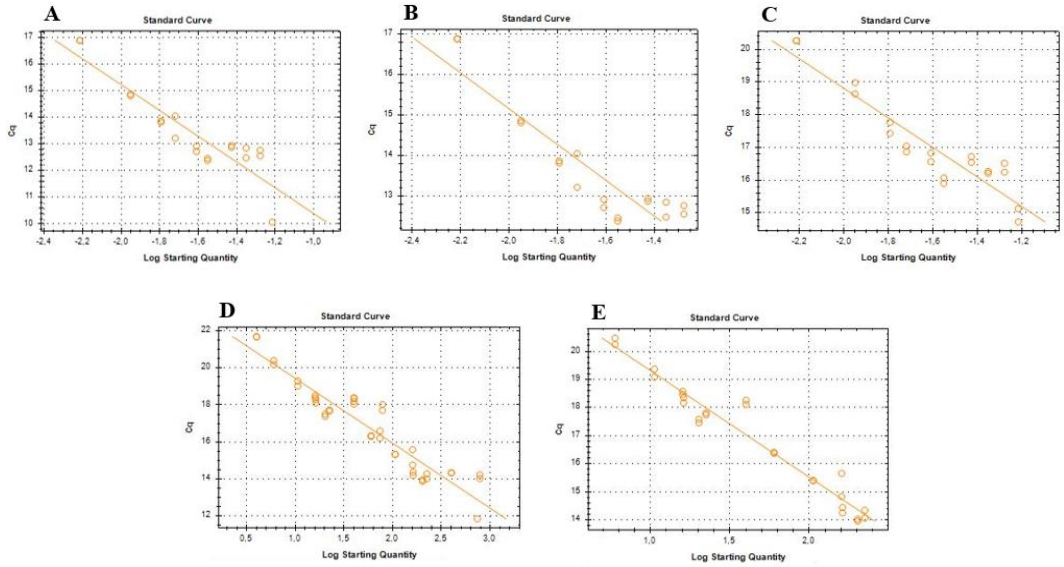

Figure 3.24: Standard curves from extracted DNA of *D. eres* (isolate DPC_HOH7) mycelium.
A) For the undiluted samples, **B**) For the undiluted samples after editing, **C**) For the 1:10 diluted samples, **D**, **E**) For the diluted and undiluted samples of DNA from mycelium of the *D. eres* isolate DPC_HOH7 before and after editing, respectively.
Log Starting Quantity in **A**, **B**, and **C** corresponds to the amount of mycelium in g.
Log Starting Quantity in **D** and **E** corresponds to the amount of fungal DNA from mycelium in ng.
The threshold for the data from *D. eres* in **A**, **B**, and **C** was set to RFU = 250 and in **D** and **E** was set to RFU = 573 based on the auto-function of the CFX Manager™ software (Bio-Rad Laboratories Inc.).

Figure 3.24 D and E shows the unedited and edited standard curves, respectively, for the undiluted and diluted samples with ng DNA in the x-axis. An efficiency of E = 92.7 % and a correlation of $R^2 = 0.889$ resulted from the unedited standard curve, which is near to the efficiency which was observed for the original standard curve (Figure 3.20 C), and an efficiency of E = 83.3 % and a correlation of $R^2 = 0.949$ resulted from the edited standard curve, where Cq values of samples 1, 9, and 10 were deleted.

The DNA concentrations of *D. novem* mycelia were in a relatively constantly increasing order with the exception of sample 3, in which DNA concentration was very low. The standard curve for the undiluted samples had an efficiency of E = 27.2 % and a correlation of $R^2 = 0.557$ (Figure 3.25 A). The standard curve for the 1:10 diluted samples had E = 28.1 % and $R^2 = 0.555$

(Figure 3.25 C). Due to sample 3, which had Cq values in the range of Cq = 25.8 because of a low DNA concentration, the standard curves of the mycelium of *D. novem*, in Figure 3.25 B, D, and F were edited. In addition, sample 9 was also deleted (Figure 3.25 B), since the Cq value appeared to be too high in relation to the log starting quantity. This may have been caused by inhibitors due to a mycelium mass of 56 mg. This is supported by the fact that the 1:10 dilution of sample 9 fits well into the standard curve of the 1:10 diluted samples. After fading out these values, an efficiency of E = 34.3 % and R^2 = 0.954 was observed (Figure 3.25 B). The standard curve of the 1:10 diluted samples looked a little better after editing (removal of sample 3) with E = 40 % and R^2 = 0.980 (Figure 3.25 D).

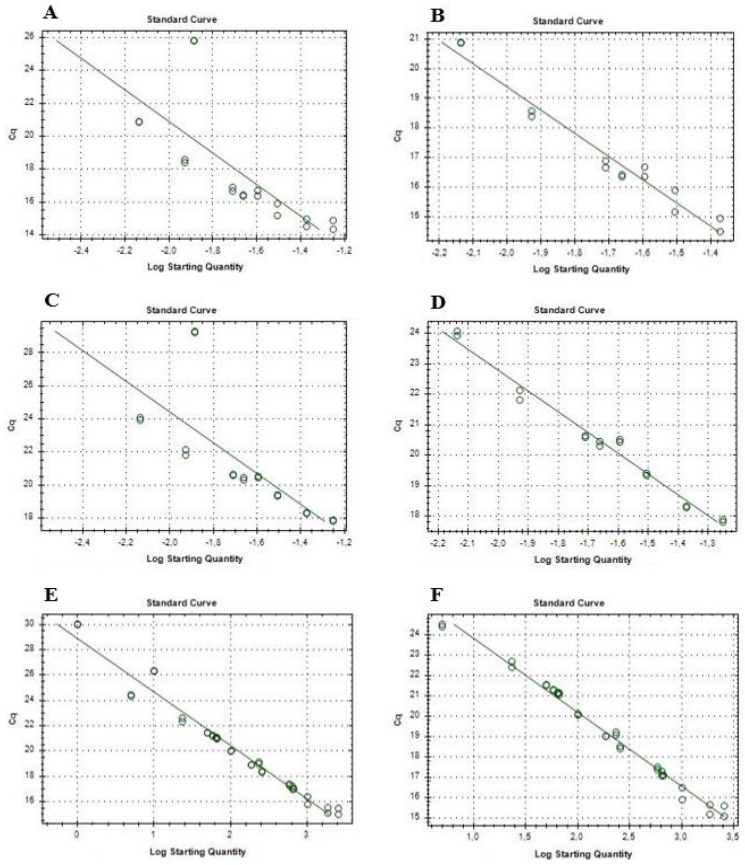

Figure 3.25: Standard curves from extracted DNA of *D. novem* (isolate DPC_HOH11) mycelium. **A**, **C**) For the undiluted and 1:10 diluted samples, respectively, without editing; **B**, **D**) For the undiluted and 1:10 diluted samples, respectively, after editing; **E**, **F**) For the diluted and undiluted samples of DNA from mycelium of the *D. novem* isolate DPC_HOH11 before and after editing, respectively.
Log Starting Quantity in **A**, **B**, **C**, and **D** corresponds to the amount of mycelium in g.
Log Starting Quantity in **E** and **F** corresponds to the amount of fungal DNA from mycelium in ng.
The threshold in **A**, **B**, **C**, and **D** was set to RFU = 100 and in **E** and **F** was set to RFU = 147 based on the auto-function of the CFX Manager™ software (Bio-Rad Laboratories Inc.).

Figure 3.25 E and F shows the unedited and edited standard curves, respectively, for the undiluted and diluted samples, with ng DNA in the x-axis. An efficiency of E = 72.6 % and a

correlation of $R^2 = 0.958$ resulted from the unedited standard curve and an efficiency of $E = 88.4\,\%$ and a correlation of $R^2 = 0.989$ resulted from the edited standard curve.
Again, the curves based on DNA amount were much better than those based on mycelial mass, indicating that the problem with establishing standard curves based on mycelial mass lies with DNA preparation. Since this problem can occur in any experimental setting it can be concluded that this kind of standard curve may not be useful at all.

3.5.6.2.2. Standard curves for *Diaporthe* species spores

During the experiments described in 3.5.6.2.1. it became obvious that different DNA preparation efficiencies for different amounts of fungal material can have a strongly distorting effect on the correlations between fungal mass and Cq values. To avoid this problem, it was tested whether it is possible to directly add fungal structures into the qPCR reactions. Conidia or spores in general are the fungal structures that allow for the best quantification because they can be counted in suspension.
Spore suspensions were prepared from each *Diaporthe* species to quantify these fungi. Seven-concentration serial dilutions were made with defined amounts of spores. Serial dilutions of spore suspension were added individually into the quadruplex real-time PCR assays and in another experiment DNA preparation was carried out on the spore suspensions (3.5.6.2.3.) and the extracted DNAs were added into the quadruplex real-time PCR assays. With this method for absolute quantification, a number of spores can be assigned to the Cq values obtained.

A first standard curve for spore suspensions of *D. longicolla* with three samples (with 8,550; 855; and 85 spores/µL), had an efficiency of $E = 227.8\,\%$ and $R^2 = 0.959$, while for further dilutions the thermal cycler could not detect any fluorescence that exceeded the threshold at $RFU = 30$ (Appendix 7.3., Figure 7.3 A). Since an efficiency of more than 100 % is not realistic, a new serial dilution with 1:2 steps (8,550; 4,275; 2,138; … spores/µL) was made and then the qPCR assay was done by applying these new serial dilutions (Figure 3.26 A). An efficiency of $E = 83.9\,\%$ and $R^2 = 0.959$ was obtained for the standard curve ranging from 17,100 down to 267 spores (seven samples).

The initial standard curve for *D. caulivora* including four samples (with 98; 10; 1; less than one spore/µL) had an efficiency of $E = 140.7\,\%$ and $R^2 = 0.906$ (Appendix 7.3., Figure 7.3 B). A new serial dilution (98, 49, 25, 12, 6, 3, 2, 1 spores/µL) was prepared and the qPCR assay was done again. The standard curve was edited because the samples with most spores had noticeably high Cq values. It was supposed that inhibitors were effective in these samples.

The curve on the remaining samples showed an efficiency of E = 90.2 %, which was rated as good (RFU = 20) (Figure 3.26 B). The correlation was low $R^2 = 0.858$, which was caused by the large differences between two values of one sample. These differences exist with the strong dilutions, which was to be expected. If there is one or less than one spore per 2 µL sample, there is a certain probability as to whether this spore will be picked up during pipetting or not.

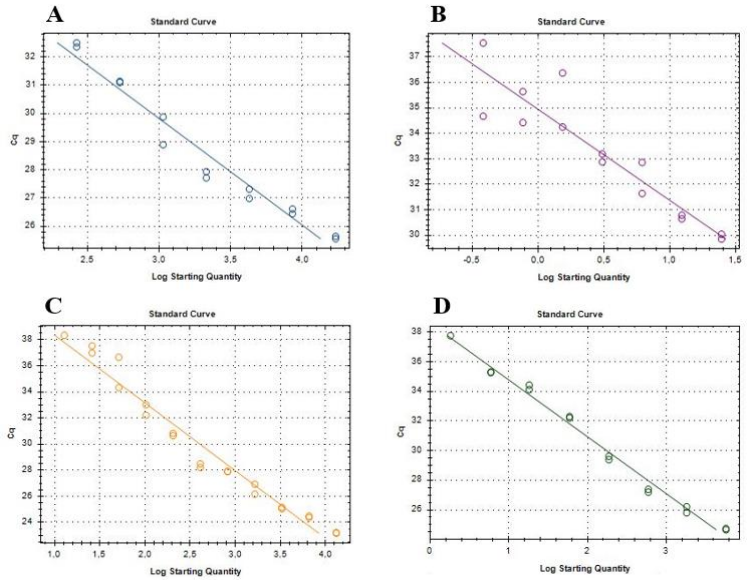

Figure 3.26: Standard curves for *Diaporthe* species spores.
A) *D. longicolla* isolate DPC_HOH20, standard curve for undiluted (17,100 spores in 2 µL) to 1:64 diluted (267 spores in 2 µL) samples. **B**) *D. caulivora* isolate DPC_HOH2, standard curve for 1:4 (49 spores in 2 µL) to 1:256 diluted (less than 1 spore in 2 µL) samples. **C**) *D. eres* isolate DPC_HOH7, standard curve for undiluted (13,174 spores in 2 µL) to 1:1,024 diluted (13 spores in 2 µL) samples. **D**) *D. novem* isolate DPC_HOH15, standard curve for undiluted (5,730 spores in 2 µL) to 2 spores in 2 µL samples. Log Starting Quantity corresponds to the number of spores.

For *D. eres* an initial standard curve with a low efficiency E = 45.1 % and $R^2 = 0.936$ resulted (Appendix 7.3., Figure 7.3 C). The samples were diluted again (8,725; 4,362; 2,181; …; 9 spores/µL). The real-time PCR assay was done with these new serial dilutions (Figure 3.26 C). The efficiency E = 55.9 % and the correlation $R^2 = 0.962$ were increased a little bit for the standard curve.

The initial spore suspensions of *D. novem* gave a standard curve with E = 81.4 % and $R^2 = 0.991$ (threshold at RFU = 30) (Appendix 7.3., Figure 7.3 D). This indicates good efficiency for *D. novem*. Here just additional dilutions of 1:√10 (1:3.16) were added to the series (2,865; 906; 287; 91; 29; 9; 3; 1 spores/µL). Then the efficiency was E = 82.1 % and the correlation $R^2 = 0.988$ (Figure 3.26 D).

Overall these curves now seem quite useful. For *D. caulivora*, *D. eres*, and *D. novem* it was also shown, that even single digit numbers of spores can be detected. For *D. longicolla* a few

more dilutions might have been useful whereas for *D. caulivora* a fully new spore suspension would have been necessary to get to higher numbers.

3.5.6.2.3. Standard curves from extracted DNAs of *Diaporthe* species spores

In addition to applying the spore suspensions of *Diaporthe* species directly into the quadruplex real-time PCR assays to detect spore, DNA extraction was carried out by using the protocol by Liu et al. (2000) for each sample of the dilution series of the four different spore suspensions. The extracted DNAs were dissolved in 30 µL of ddH_2O and the concentration of each sample was measured using spectrometry and recorded (Appendix 7.4., Table 7.1). To create the standard curves, the DNA samples were added in quadruplex real-time PCR assays. Thus the number of spores or the corresponding number of genomes can be assigned to the Cq values obtained during an analysis such as the previous method. The results are explained in Appendix 7.4., Figures 7.4 and 7.5.

Overall it needs to be stated that the curves with DNA prepared from spore suspensions gave little information. It seems obvious that the problem with different DNA extraction efficiencies for different amounts of fungal material was very much the same for spores as for mycelium. Therefore, the only useful standards for absolute quantification are spore dilutions directly applied to qPCR reactions. Fortunately, these can nicely be applied for seed soaking.

3.5.7. Seed soaking

The seed soaking method that can be used to detect fungal material sticking to the seed surface was also tested. Here seeds are just washed with or soaked in water and this water then used directly in real-time PCR reactions. The procedure used (2.14.11.) was based on the description by Ramiro et al. (2019).

By using 2 µL aliquots of the soaking water (after 0-3 h) of five seeds as template in the quadruplex assay, signals for *D. eres* and *D. novem* could be found (Figure 3.27 A-D). Considering the Cq cutoffs (Table 3.7), some of the signals were considered false positives (Table 3.9, gray numbers). The test could show that the seeds were infected with these two *Diaporthe* species (Table 3.9, orange and green numbers).

By using 2 µL aliquots of the soaking water of another sample of five seeds with the same mixes of infected and healthy seeds as above (after 0-7 h), no signals could be observed (Figure 3.27 E).

The use of aliquots of the soaking water (after 0-3 h) of seed samples with 100 seeds sometimes allowed for the real-time PCR detection of *Diaporthe* species but sometimes from the same sample nothing was detected (Figure 3.27 F, G, H). This result seemed random and it

was assumed that when the seeds are soaked, no DNA is released (as assumed by Ramiro et al. (2019)), but fungal structures (spores and mycelium parts) are transferred directly into the real-time PCR reactions. Since it is possible that 2 µL either do contain a spore or do not contain a spore, this would explain the apparent randomness of some of these results.

It was also discovered that with larger amounts of fungal structures, inhibitors can cause a problem for the real-time PCR assay.

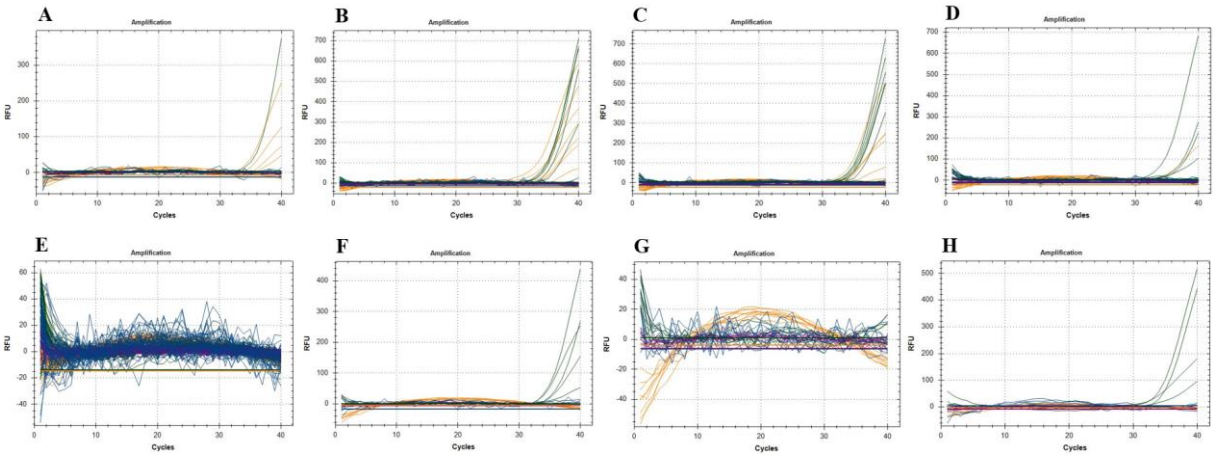

Figure 3.27: Quadruplex real-time PCR results from applying aliquots of soaking water (cv. Anushka 2).
A-E) Seed soaking results for the experiment with five seeds. **A-D**) First sample, **E**) Second sample. **A**) Using aliquots of the soaking water after 0 h, **B**) Using aliquots of the soaking water after 1 h, **C**) Using aliquots of the soaking water after 2 h, **D**) Using aliquots of the soaking water after 3 h. **F**, **G**, **H**) Seed soaking results for the experiment with 100 seeds.

Table 3.9: Seed soaking results for the experiment with five seeds. The table shows all Cq values below the cutoff in color.

Sampling time	*D. eres*						*D. novem*					
	5H*	**1I**	**2I**	**3I**	**4I**	**5I**	**5H**	**1I**	**2I**	**3I**	**4I**	**5I**
0 h	-	-	34.25	35.44	-	34.58	-	-	-	24.07	-	-
	-	-	-	-	-	32.86	-	-	-	-	-	-
1 h	-	-	35.39	26.55	27.38	32.94	-	-	-	34.07	32.77	39.97
	-	-	-	32.26	33.32	30.73	-	-	-	35.14	33.30	33.13
2 h	-	-	-	29.49	32.16	31.38	-	-	27.08	30.30	-	28.84
	-	-	-	31.29	34.57	-	-	-	-	-	-	-
3 h	-	-	-	33.50	33.08	30.85	-	-	31.41	-	33.02	32.07
	-	-	-	28.43	-	-	-	-	-	-	30.21	-

*5H: healthy control, 1I: one infected seed + four healthy, 2I: two infected + three healthy, 3I: three infected + two healthy, 4I: four infected + one healthy, and 5I: five infected seeds.

This approach represents an easy and quick diagnostic method and to overcome the problems that were encountered it must be pursued by using more seeds, resolving the inhibitors problem, and developing suitable absolute quantification methods like dilution series of spore suspensions.

3.6. Experiments covering additional aspects of *Diaporthe* species

The *Diaporthe* spp. (Table 3.1) were examined in some additional experiments. These extra researches went beyond the core aims of this study. Here I shortly present these experiments. They are presented only here; they are not mentioned in other parts of this thesis.

3.6.1. Further characterization of the *Diaporthe* isolates based on mating-types *MAT1-1* and *MAT1-2*

The mating-type (*MAT*) locus has a key role for sexual reproduction in ascomycete fungi (Santos et al. 2010). The *MAT* genes can be useful for mating-type diagnosis in many species in genus *Diaporthe* (Kanematsu et al. 2007; Santos et al. 2010, 2011). The mating-types *MAT1-1* and *MAT1-2* vary in one gene, *MAT1-1-1* and *MAT1-2-1*, respectively. PCR diagnosis of mating-types was done for 30 *Diaporthe* isolates. Primers MAT1-1-1FW (5'-GCA AMI GTK TIK ACT CAC A-3') and MAT1-1-1RV (5'-GTC TMT GAC CAR GAC CAT G-3') for the amplification of part of the α1 box from *MAT1-1-1* gene; and MAT1-2-1FW (5'-GCC CKC CYA AYC CAT TCA TC-3') and MAT1-2-1RV (5'-TTG ACY TCA GAA GAC TTG CGT G-3') for the amplification of part of the HMG domain from *MAT1-2-1* gene were used following the protocol of Santos et al. (2010).

Both mating types were found in different isolates in *D. longicolla*, but never both mating types in the same isolate (Table 3.10). This pattern indicates that *D. longicolla* is heterothallic. This is surprising in a species for which no sexual structures have been observed so far. It is also in contrast to results by Santos et al. (2011), which indicated that both mating-types were present in each of the tested *D. longicolla* isolates. *D. eres* also appears to be heterothallic and *D. novem* as well (Table 3.10). In the *D. caulivora* isolate just *MAT1-2* was found (Table 3.10).

To corroborate the PCR findings, heterothallic isolates (Table 3.10[a]) from the same species with opposite mating-types are being mated for teleomorph induction *in vitro*. Control crosses are included where each isolate is paired with itself. A mating interaction is recorded as negative if no perithecia are formed and successful mating is regarded when perithecia are observed. The method of Brayford (1990) with slight modifications is used to mate the isolates. Isolates grown on PDA and 1/5 PDA (Table 3.10[a]), are inoculated on 2 % WA or synthetic medium (Westergaard and Mitchell, 1974) plates with pieces of healthy autoclaved soybean stems, and incubated for three months under different conditions (at 25 °C in the dark, at 25 °C in the light, at 25 °C in 12:12 h light/dark, at 25 °C under UV light, for three

days in darkness and then at 25 °C in 12:12 h light/dark). Each mating experiment is done in two replications.

Table 3.10: Mating-type diagnosis of the European isolates of *Diaporthe* species

Species	Isolate no.	*MAT1-1-1*	*MAT1-2-1*
D. longicolla	DPC_HOH1	-	+
	DPC_HOH5	+	-
	DPC_HOH6	+	-
	DPC_HOH9	+	-
	DPC_HOH12	-	+
	DPC_HOH13	-	+
	DPC_HOH17[a]	-	+
	DPC_HOH18	+	-
	DPC_HOH19	+	-
	DPC_HOH20	-	+
	DPC_HOH21	-	+
	DPC_HOH22	-	+
	DPC_HOH23	-	+
	DPC_HOH24	-	+
	DPC_HOH25	-	+
	DPC_HOH26	+	-
	DPC_HOH28[a]	+	-
	DPC_HOH29[a]	+	-
	DPC_HOH30	-	+
	DPC_HOH31	-	+
	DPC_HOH32	-	+
D. caulivora	DPC_HOH2[a]	-	+
D. eres	DPC_HOH3[a]	-	+
	DPC_HOH7[a]	-	+
	DPC_HOH10[a]	+	-
	DPC_HOH14	-	+
	DPC_HOH27	+	-
D. novem	DPC_HOH11[a]	-	+
	DPC_HOH15[a]	+	-
	DPC_HOH16[a]	+	-

[a] Heterothallic isolates with opposite mating-types, which are selected for teleomorph induction *in vitro*.

So far, for *D. longicolla*, no fertile perithecia formed under any condition, except for isolates DPC_HOH29 (*MAT1-1*) and DPC_HOH17 (*MAT1-2*) just once, which were incubated at 25 °C in the dark condition and it was not repeatable. This of course is in accordance with earlier experiments but a first description of the sexual phase of this highly important pathogen would be very interesting in mycology.

Perithecia were formed in cultures for *D. caulivora* isolates. Only the mating-type *MAT1-2* was detected in *D. caulivora* isolates but the isolates are self-fertile. Therefore, this species is considered to be homothallic. The same was found for their *D. cauliovra* isolates by Santos et al. (2011).

The *D. novem* and *D. eres* isolates were diagnosed as heterothallic, as in the case of *D. longicolla*. Perithecia did not form in culture. By Santos et al. (2011) for the first time fertile perithecia could be observed by crossing of Croatia's *D. novem* isolates.

The difference between my results for *D. longicolla* and those of Santos et al. (2011) might be explained by either false negatives by me or a false positive by them. However, my results

were highly consistent with many isolates. So, it might be concluded that Santos et al. (2011) either had a true false positive or they did not have a pure isolate.

Most critical was the finding for the *D. caulivora* isolate. This species is self-fertile, so it should have *MAT1-1-1*. Probably the gene sequence is different in this species so that the primers do not amplify. Santos et al. (2011) had the same problem in this case. In order to get more reliable information to further refine the phylogenies, this study still in progress.

3.6.2. Testing of various biological control agents (BCAs) against *Diaporthe* species *in vitro*

The aim of this research was the identification of suitable antagonists, which could be used in future as biological fungicides to control *Diaporthe* diseases.

Two different strains of *Pseudomonas fluorescens* and one strain each of *Bacillus subtilis*, *Trichoderma harzianum*, *T. asperellum*, and *Clonostachys rosea* were tested against *D. longicolla*, *D. caulivora*, *D. eres*, and *D. novem* (Isolates: DPC_HOH20, DPC_HOH2, DPC_HOH7, and DPC_HOH15) by performing dual culture, cellophane diffusion, MTT activity, and bioautography tests. In the course of this work, the two strains *T. harzianum* T-16 and *T. asperellum* T-23 were proven to be effective antagonists against *D. longicolla* and *D. caulivora* using the cellophane diffusion test. Both strains of *P. fluorescens* also showed a recognizable inhibition for *D. longicolla* and *D. caulivora* in the dual culture experiment, but this was not significant. No antagonistic behavior of *C. rosea* against *Diaporthe* spp. could be detected. So far, these experiments only constitute initial screens and additional experiments are required.

Antifungal activities of the four *Bacillus velezensis* strains ES1-02, EFSO2-04 (Akintayo et al. 2022), FZB42 (Krebs et al. 1998), and QST713 (Chen et al. 2007) that are established and characterized lipopeptide (LP) producing strains were tested by dual culture tests *in vitro* against the four *Diaporthe* spp. (Isolates: DPC_HOH20, DPC_HOH2, DPC_HOH7, and DPC_HOH15). Inhibition of the growth of the *Diaporthe* spp. was determined relative to the control experiment in which the fungal pathogens were not antagonized by the *Bacillus* strains. The results showed that all four strains were most potent in inhibiting *D. caulivora* compared with the other tested *Diaporthe* spp.. Fungal mycelia were taken from the region of inhibition and examined microscopically. Morphological abnormalities such as enlargement of the hyphae, swellings, formation of bulbs, or complete disruption of mycelia could be observed, which could be matched with the results of other studies. LP amounts (including surfactin, fengycin, and iturin/bacillomycin) were quantified

in the inhibition zones with an HPTLC system (CAMAG, Muttenz, Switzerland) to determine the impact of *D. longicolla* (DPC_HOH20) interaction with the *Bacillus* strains on LP synthesis. Accumulation of surfactin could be seen in the inhibition zone of ES1-02 and EFSO2-04 strains, which is evidence for induction of surfactin synthesis in the strains by the presence of *D. longicolla*. Increase of bacillomycin L albeit to a lesser degree was induced in strain EFSO2-04. With respect to fengycin, increased synthesis was induced in QST713 and FZB42 on interaction with *D. longicolla*. In continuation of this work, proteome analysis of *B. velezensis* ES1-02 in response to co-cultivation with *D. longicolla* (DPC_HOH20) was performed. 148 protein groups showed significant differential expression in the ES1-02 co-cultured with *D. longicolla* compared with ES1-02 cultured alone under the same conditions. This research is written in detail as a manuscript with the title "Biocontrol activity, including surfactin induction and proteomic response of lipopeptide producing *Bacillus velezensis* strains to fungal plant pathogens, *Diaporthe* spp." and it is submitted to the journal of Environmental Microbiology and Environmental Microbiology Reports.

4 Discussion

Soybean is one of the best and most affordable vegetarian sources for proteins and fat and has been broadly cultivated for several utilizations, especially for animal and human consumption (Hartman et al. 2015).

Demand for soybean in Europe as well as in other countries is growing. However, most soybean used in Europe is imported from the biggest producers and domestic production has only grown slightly and especially in the southeastern and eastern parts of the EU (IDH and IUCN NL, 2019; Coleman et al. 2021; Omari et al. 2022). Europe is making an effort to raise soybean production to diminish its dependency on imports and to produce non-GM soybean for human nutrition and animal fodder. At the same time, more legume production can minimize negative environmental consequences associated with continuous cereal production by diversifying the cropping systems and reducing the need for nitrogen fertilization (IDH and IUCN NL, 2019; Hufnagel et al. 2020).

When more soybean is grown in central Europe, it can be supposed that soybean pathogens that are destructive in other soybean production areas will gain importance there, too.

Diaporthe/*Phomopsis* Complex (DPC) species cause serious soybean diseases leading to significant losses in yield and quality of seeds (Backman et al. 1985). However, no studies have been performed for detection of these species on soybean seeds in central Europe. Therefore, as part of an effort to determine the dominant soybean pathogens in central Europe, the genus *Diaporthe* was analyzed in this thesis.

Starting with the incubation of DPC-damaged soybeans on APDA, 32 *Diaporthe* strains were isolated. The strains were assessed based on their morphology and molecular phylogenies, and they could be allocated to the four species *D. longicolla*, *D. caulivora*, *D. eres*, and *D. novem*.

Morphological features used for species determination are highly variable within *Diaporthe* spp. and can overlap between different species. Accurate, specific, robust, and rapid species identification is essential to optimize control of the *Diaporthe* pathogens. Also, a large scale monitoring effort was planned that needs species identification. Hence, a quadruplex real-time (q)PCR using TaqMan probes was established to detect, distinguish, and quantify these four *Diaporthe* species simultaneously as a quick and specific method.

4.1. Isolation and identification of *Diaporthe* species from European soybeans

32 *Diaporthe* strains were isolated from 483 examined soybeans (21 seeds × 23 seed lots), which were plated on the surface of APDA plates (2.11.). The sampling scheme was designed to cover as large as possible an area and with plating only symptomatic seeds to achieve the highest possible diversity of *Diaporthe* isolates as possible with limited resources. Due to the broad distribution of sampling sites and the randomness of sampling inside the seed lots, the isolates were assumed to be representative for the *Diaporthe* population in central Europe.

Because of the overlapping morphological characteristics of *Diaporthe* species, these cannot be consistently distinguished morphologically. Therefore, molecular tools have been used to discriminate among *Diaporthe* species and for phylogenies of these fungi (Santos and Phillips, 2009; Udayanga et al. 2012; Gomes et al. 2013).

The isolated *Diaporthe* species were studied morphologically based on the shape and color of their cultures on APDA, production of sexual and asexual structures, and type and dimensions of spores. The identification of *Diaporthe* species based only on ITS sequences is not reliable. This is because the sequences are too similar, there are still sequences missing for many species and unfortunately quite frequently sequences have been entered into NCBI / GenBank with incorrect species annotations. The latter entries may either be old or come from surveys, where authors only sequenced ITS themselves and did not corroborate their results. Therefore, in addition to ITS the DNA sequences of the genes *TEF1* and *TUB* were used. By considering the results from morphological and molecular identification, the 32 *Diaporthe* isolates were assigned to the four *Diaporthe* species, *D. longicolla*, *D. caulivora*, *D. eres*, and *D. novem*.

D. longicolla is the main causal agent of soybean seed decay (Hobbs et al. 1985), and it was also most frequently isolated from soybean in this study. Regarding morphology, it is also consistent with earlier publications (Santos et al. 2011; Divilov, 2014) that my *D. longicolla* isolates did not produce β-conidia. Compared to the other *D. longicolla* isolates, DPC_HOH18 and DPC_HOH21 grew slower and had shorter necks on their pycnidia. Similarities could be observed between colony appearances of these two isolates and isolate IL12-Ds-2 described by Divilov (2014). According to his descriptions (Divilov, 2014), this isolate is more similar to *D. sojae* than to *D. longicolla*. However, from ITS, *TEF1*, and *TUB* sequences he classified it as *D. longicolla* and concluded that this molecular classification should be the correct one. My results appear quite similar and I am also quite convinced that all these isolates belong to the same species. It is possible that many isolates formerly

identified as *D. sojae* should be reassigned to *D. longicolla*. Apparently the colony appearance of *D. longicolla* can be very different between isolates.

D. caulivora did not produce any pycnidia in this study, neither cultures on APDA nor on soybean stems. This goes together with the first description that claims that *D. caulivora* is lacking an anamorph state (Athow and Caldwell, 1954) and also more recent reports from Croatia and Argentina (Santos et al. 2011; Grijalba and Ridao, 2012). Others have observed that *D. caulivora* can produce pycnidia rarely (Kmetz et al. 1978; Kulik, 1984). It has been reported that some *D. caulivora* isolates produced pycnidia with α-conidia (Frosheiser, 1957; Chao and Glawe, 1985), β-conidia (Kmetz et al. 1978), or both kinds of conidia (Fernández and Hanlin, 1996).

The presence of *D. eres* in Europe has already been shown since it was found on various hosts other than soybean in Austria, France, Italy, Latvia, and Netherlands (Gomes et al. 2013; Udayanga et al. 2014). Nevertheless, *D. eres* was reported as DSD causing agent from soybeans in Serbia first (Petrović et al. 2015). The *D. eres* isolates from this study probably represent the first report of the species on soybean in Austria.

D. novem has been previously known as *Phomopsis* sp. 9 from earlier investigations on sunflower, grapevine, and rooibos (Rekab et al. 2004; van Niekerk et al. 2005; van Rensburg et al. 2006). The name *D. novem* (novem = nine, Latin) was proposed by Santos et al. (2011). They established that *D. novem* is a heterothallic fungus and for this reason formation of perithecia occurs rarely and when they crossed isolates with opposite mating-types in culture perithecia could be observed.
In this study *D. novem* isolates only produced pycnidia. The α-conidia of my isolates were the same size as those of the *D. novem* isolates from Santos et al. (2011) and longer than *D. longicolla* and *D. eres* α-conidia. They were hyaline, unicellular, some had one but most two guttules, and had oval to cylindrical form as observed for the *D. novem* isolates in the study by Santos et al. (2011).

There were differences between the BLAST results for the different marker sequences. Most of these are probably because of inconsistencies in the annotations of sequences in the NCBI database. However, for isolate DPC_HOH11 a clear discrepancy was found. For this *D. novem* isolate, there is a completely separate clade in the ITS phylogeny and this must have natural reasons. There could have been a large mutation event, that changed many bases in the ITS sequence at the same time. Another likely alternative is that hybridization happened between a *D. novem* specimen and one from another *Diaporthe* species. Since the sequence

section that was changed is not similar to *D. longicolla, D. eres*, or *D. caulivora* it seems that this hybridization was with yet another species. The recent findings of Hilario et al. (2021) suggest recombination events among strains of *D. novem*, rather than hybridization between species. However, hybridization events between *Diaporthe* species could be a nice explanation for the overlapping morphologies within the species complex. Inter-species hybridizations and with that the emergence of new species might also contribute to the difficulties that have been encountered in resolving the DPC.

The *Diaporthe* species found on soybean in central Europe in this study were already identified as soybean pathogens in southern and southeastern Europe (Santos et al. 2011; Gomes et al. 2013). In Serbia *D. foeniculina*, *D. rudis* (Petrović et al. 2016), and *D. sojae* (Krsmanović et al. 2020) were also found. In the study by Krsmanović et al. (2020) *D. longicolla* emerged as most frequent *Diaporthe* species followed by *D. caulivora*. On the other hand, they found no *D. foeniculina* and *D. rudis*. From this it seems that *D. foeniculina* and *D. rudis* play a minor role. I did not find any of these three species in central Europe. This may not prove that they are not occurring here, but at least they seem to have a low incidence. In contrast to the opening sentences of this section it can be argued that 483 seeds or 32 isolates, respectively, cannot be enough to support the statement that these four *Diaporthe* species are the only ones relevant in central Europe and that *D. longicolla* is dominating. Testing a large number of seeds from more samples and other sites of infected soybean plants will be necessary to gain more depth of the data. Applying a combination of the quadruplex real-time PCR assay and seed plating, it will be decided what is the dominant species and it can be made sure that no other species are present or were introduced in the meantime. In this context also another (q)PCR based assay to detect *Diaporthe* spp. without species specificity (see below) can be useful: If *Diaporthe* spp. is detected in a sample but not *D. longicolla*, *D. caulivora*, *D. eres*, or *D. novem*, another *Diaporthe* species must be present and steps can be initiated to isolate and detect it.

4.2. Pathogenicity of the *Diaporthe* isolates

Several management strategies have been recommended for the control of DSD. Applying practical control methods like crop rotation and tillage can be effective for reduction of the level of infection, but not to avoid the diseases (Backman et al. 1985; Roth et al. 2020). Fungicides either for seed treatment or foliar sprays can also be useful for control of *Diaporthe* diseases. However, it is unresolved how they can deactivate the pathogenicity of the *Diaporthe* pathogens (Ghimire et al. 2019). Because of the destructive effects of

fungicides on the ecosystem and resistance of the pathogens, fungicide use should be minimized (Hartman and Sinclair, 1992). Sources of resistance to *Diaporthe* seed decay and stem canker diseases have been detected (Pioli et al. 2003; Li et al. 2015 b; Chang et al. 2016), but information about resistance genes in current soybean cultivars is scarce (Ghimire et al. 2019). Virulence studies of a pathogen or different strains against different cultivars of its host plant can determine differences in the pathogenicity of the strains and on the other hand cultivars with broad resistance against the pathogen can be found.

In this study a pathogenicity test was conducted by inoculation of healthy germinated soybeans in spore suspensions of the 32 *Diaporthe* isolates. All the 32 *Diaporthe* isolates could cause disease, so none of the isolates was found on soybean by random chance. For pod blight the disease score was similar for all isolates but there were differences in pycnidia formation on soybean stems.

Since the sole aim of this test was to corroborate pathogenicity, only cultivar Anushka was used. To gain additional information for choosing resistant cultivars for Germany, virulence tests of the *Diaporthe* isolates on several different cultivars would be useful. Differences in virulence between the species and the isolates may only occur in some cultivars. The findings for virulence of the different species on different cultivars should be combined with the finding about the incidence of the species to make decisions for cultivar choice.

4.3. Establishment of a quadruplex real-time PCR for detection of *Diaporthe* species

All studies testing the incidence and relevance of *Diaporthe* species in Europe so far as mentioned above, only tested a relatively small number of seeds. Consequently also only few isolates of the different species exist. Regarding epidemiological incidence and relevance, and for monitoring these studies have little true informative value. Therefore, a more comprehensive study with much wider sampling is necessary in European soybean producing areas. This should also help to restrict the distribution of *Diaporthe* pathogens. For this, a fast and accurate diagnostic assay is needed.

TaqMan real-time PCR was chosen for parallel detection of the four species. Especially with the large sample numbers expected for the epidemiological studies, multiplexing can save time and money. But specificity in multiplex real-time PCR is quite difficult to achieve. While normally the probe only gives additional specificity to the reaction that is already specific because of the primers, in a multiplex the probes have to be specific by themselves because otherwise they also detect the other species in the assay. Still the primers also have to

be specific, otherwise unspecific amplification could reduce sensitivity. So, to have specificity in a quadruplex assay, twelve specific oligonucleotides are needed.

Since PCR assays to detect *Diaporthe* species already existed, using primers that were already established was deemed more efficient than *de novo* design. So, first primer-probe sets were extracted from literature. These were the three sets, PL-5, PL-3, and DPC-3 developed by Zhang et al. (1999). PL-5 detects *D. longicolla, D. caulivora, D. sojae*, and *D. aspalathi* together but PL-3 is specific for *D. longicolla* and DPC-3 is specific for *D. caulivora*. By performing singleplex and duplex real-time PCR assays to test the specificity of the PL-3 and DPC-3 it became apparent that the sets are only specific when used on their own. This is mainly because the probes PL-3P and DPC-3P are identical. Since all three components of primer-probe sets need to be specific as mentioned above, it might have been a mistake to use the previously published primer-probe sets PL-3 and DPC-3 before checking *in silico* (using Primer-BLAST). Also, with regard to integration into a quadruplex real-time PCR, it would have been better to design just one primer-probe set *de novo* for *D. novem* with a different reporting dye instead of two primer-probe sets with FAM. It could be learned that assessment of the relevant sequence alignment should be done before testing any primer-probe set (published or *de novo*) in *in vitro* assays.

After facing these challenges finally the four species-specific TaqMan primer-probe sets DPCL, DPCC, DPCE, and DPCN could be designed based on *TEF1* sequences of *Diaporthe* isolates. In the first step the specificity of the sets was proven using Primer-BLAST and then their specificity and efficiency were checked in real-time PCR. These experiments clearly proved that the new primer-probe sets have the specificity needed to test for the *Diaporthe* species in central Europe.
D. longicolla could also be detected by the new quadruplex real-time PCR assay in stem samples that had been inoculated with this species (the pathogenicity test). This was the first experiment showing that the assay can work with infected plant material.

Standard curves for quantification were created by diluting the fungal DNA with soybean DNA. Though an LOD still needs to be determined for all species, it could be already estimated that they should be quite low, so the assay has high sensitivity.
Since seed screening was supposed to be the main application of the assay, this was tested. The fist tested seeds were infected with *D. eres* and *D. novem.* Both species could be detected in DNA prepared from different parts of the seeds. This showed that testing the seed coat is

sufficient for testing seeds, which is advantageous because in contrast to whole seeds seed coats can easily be broken down for DNA preparation using a common lab homogenizer.

The application of the assay to seed lots showed its full potential. It became clear that the different species can be found in seeds. Different amounts of the pathogens were found in different seeds and the pathogens were found in the seeds in different combination. These are data that could not have been achieved with any of the classical assays [for example (Petrović et al. 2016; Krsmanović et al. 2020)]. That individual seeds can have different infections shows the necessity to sample several seeds per lot. Concrete sampling schemes will have to be elaborated.

The seed soaking method seems an easy and interesting method to detect seed borne pathogens. In this method DNA extraction from the samples is not required. Seeds are soaked in water, and then the soaking water is directly added to the PCR reaction (Jaccoud-Filho et al. 2002). More recently this technique was applied to soybean seeds in Brazil to detect *S. sclerotiorum* (Grabicoski et al. 2015). Another study in Brazil was done by Ramiro et al. (2019) to detect *Diaporthe* spp. and *S. sclerotiorum* in parallel by soaking soybean seeds and applying the aliquots to real-time PCR assays using TaqMan primer-probe sets designed by Zhang et al. (1999) and Chen et al. (2010). My results from soaking 5 or 100 seeds revealed that use of the soaking water sometimes allowed for the real-time PCR detection of *Diaporthe* species but sometimes from the same sample nothing was detected. Thus, the results were assumed to be random (but not false) and it can be concluded that when the seeds are soaked, no DNA is released from the seeds (as assumed by Ramiro et al. (2019)), but fungal structures (spores and mycelium parts) are transferred directly and randomly into the real-time PCR reactions. The seed soaking liquids also seemed to contain a high amount of PCR inhibitors, which is in accordance with other reports (Williams et al. 2001; Freeman et al. 2002). To solve this problem, performing DNA extraction prior to PCR has been suggested by Grabicoski et al. (2015), although, in their own study DNA extraction was not required and they could detect the fungus in seed samples was possible even when only few seeds were infected. Soaking the target samples for a short time may be useful to test seeds (Carvalho-Vieira and Machado, 2002). This could avoid the release of inhibitors like lipids, polyphenols, and cellulose that are solubilized during long soaking (Rossen et al. 1992; Schrader et al. 2012). With larger amounts of fungal structures, inhibitors can cause a problem for real-time PCR assays as well. Another reason for negative results can be too little fungal DNA. On the other hand, the random results can be due to the low number of tested seeds. It is recommended that 400 seeds would be enough for seed sanitation tests of *S. sclerotiorum*

but with very little pathogen present still more seeds may be required for effective detection (Ramiro et al. 2019). Following from this it could be determined if this incidence is below of what can be tolerated anyway; in this case the detection would still be sensitive enough.
However, the reduction of labor presented by this approach constitutes a strong advantage. Hence, it should be pursued further by using more seeds, resolving the inhibitor problems, and developing absolute quantification methods.

Absolute quantification is another important aspect that should be considered in developing a seed soaking method. Since in seed soaking no DNA preparation is performed, the standard curves, which were obtained by using serial dilutions of genomic DNA of *Dipaorthe* isolates are not informative. Therefore, experiments were performed building on this study to get a different set of standard curves for each *Diaporthe* species to carry out absolute quantification.
Standard curves could be created by applying extracted DNAs from different amounts of mycelium of each *Diaporthe* isolate in real-time PCR assays. DNA extraction worked well in practice but some samples had unsuitable DNA concentrations. It can be assumed that the amounts of some mycelium samples were too small or too big. The small samples could be lost during DNA extraction and yielded less DNA than expected with a poor quality. For example, for *D. longicolla*, DNA concentration could not be measured for sample one with a mass of 3 mg. Presence of inhibitors in the extracted DNAs of samples with larger amounts of mycelium, led to high Cq values, which did not fit the standard curves and led to too high efficiency. The results revealed that DNA preparation and different efficiencies for different amounts of fungal material can have a strongly distorting effect on the correlations between fungal mass and Cq values. To avoid this problem, it was tested whether it is possible to directly add spores as fungal structures into the real-time PCR reactions, also directly representing what happens in seed soaking.
Serial dilutions of spore suspension of each *Diaporthe* species were prepared and added individually into the real-time qPCR assays. The resulting standard curve for *D. longicolla* had an efficiency of $E > 100\,\%$, which is theoretically impossible. The Cq values of the undiluted suspension and partially the 1:10 diluted suspension were too high, which could be due to contamination or inhibitors that interfere with the qPCR or the large amounts of spores in the undiluted suspension. Hence, the spore suspensions of *D. longicolla* were diluted further and the qPCR assay was performed again and acceptable efficiency could be observed. For *D. caulivora*, due to a small number of spores, few suspensions were prepared. The Cq values for the suspensions with more spores were high, maybe because of the inhibitors,

which could come from residual components of the mycelium, which was not completely retained by the filter. Thus, the high Cq values were deleted and a good efficiency could be achieved. The created standard curve using spore suspensions of *D. eres* had a low efficiency, probably because of an impurity in the undiluted suspension. The suspensions were diluted further and applied to the qPCR but the efficiency did not increase significantly. The standard curve of *D. novem* was the best one. The data points were not far outside of the linear, which was reflected in a good correlation.

In another experiment, DNA preparation was carried out on the spore suspensions and additional standard curves were created. Unfortunately, the standard curves, which were created from unprocessed spores, had low efficiencies and also the correlations of the standard curves for all four *Diaporthe* species were low. Therefore, DNA extraction seems to have a negative effect on linearity. Possible improvements could be counting the spores more precisely. Also, in order to exclude contamination and impurity, a better system for filtering the spore suspension should be used.

The standard curves for absolute quantification of *Diaporthe* pathogens still need improvement. In some cases, detection of the pathogen without quantification is enough to judge the batch of seeds. Actually, the current certification methods that are dependent on seed plating do not call for quantification but for certification a percentage of infected seeds is defined. For potentially destructive pathogens like *S. sclerotiorum* that can lead to epidemies, quarantine with zero tolerance is used in seed certification in Brazil (Botelho et al. 2015). Sampling schemes and the issue of the number of seeds to be tested will have to be discussed with seed companies and people involved in seed certification. Since the new assay offers more information about the pathogens in an individual seed than classical seed plating it may, for example, be possible to reduce the number of seeds that have to be tested for every seed lot. Together with the same people it should be clarified if the amount of pathogen in the seeds should be a criterion in judging a seed lot. It may well be that additional experiments will be necessary to establish if there is a connection between the amount of pathogen in a seed and the disease outcome in the field.

In conclusion, this established quadruplex real-time PCR assay is a time-effective and specific method for direct detection, quantification, and identification of four important *Diaporthe* species in plant tissues. In current seed testing the species is not routinely identified because that would involve producing pure cultures of the pathogens. Thus, this assay provides additional information and can improve laboratory diagnosis of *Diaporthe* spp., serve the breeders, seed producers, farmers and the processing industry.

5 Outlook

The quadruplex real-time PCR assay established in this research is a promising method to improve seed testing, distinguish and quantify the *Diaporthe* species and thus determine their incidence and their contribution to damages. However, implementation of the assay in regular seed testing and comprehensive surveys throughout soybean producing areas are still under way.

Soybean seeds are susceptible mainly to *D. longicolla* (Li et al. 2017 a; Petrovic et al. 2021). However, different *Diaporthe* species such as *D. sojae*, *D. caulivora*, *D. eres*, *D. novem*, *D. aspalathi*, *D. foeniculina*, and *D. rudis* were also reported as associated with *Diaporthe* seed decay (Li, 2011; Petrovic et al. 2015, 2016, 2021). On the other hand, the incidence of the *Diaporthe* species differs. *D. aspalathi*, for example, was first found on soybean in the southeastern USA (Fernández and Hanlin, 1996) but not in Croatia (Santos et al. 2011). This means that the spread of some species can still be restricted by seed screening. Thus, screening of soybeans on large scale is planned as well as sampling of soybean fields all over Germany. The qPCR based method for diagnosis should be established as a new standard for identification of *Diaporthe* spp. in Germany.

During the work the problems posed by *Diaporthe* spp. became more apparent. So additional aims that should be pursued in the future are: Additional basic research to characterize the lifestyle of the different species; developing a seed soaking method and improving standard curves for absolute quantification; developing detection and quantification of the *Diaporthe* spp. in soil, plant material, and seeds; designing one specific qPCR probe to detect the genus *Diaporthe*; identifying resistant cultivars; characterization of pathogen-induced defense reactions in soybean genotypes; screens for mycotoxin production; and biocontrol methods. In the following these goals are explained in more details.

5.1. Further characterization of the *Diaporthe* isolates based on mating-types *MAT1-1* and *MAT1-2*

In order to confirm PCR results to determine the mating types of *Diaporthe* isolates precisely (3.6.1.) and to get more reliable information to further refine the phylogenies, the sequences of the mating-type genes of the different *Diaporthe* isolates are checked. Specific primers are being designed and additional PCR to corroborate earlier results and further sequencing of the *MAT* genes is under way. The genome sequences of *D. longicolla* (Li et al. 2017 b) and the recently published genome of *D. caulivora* (Mena et al. 2022) are valuable resources here.

Also, the mating experiments will be performed *in vitro* once more using the method of Hilário et al. (2021). The heterothallic *Diaporthe* isolates will be mated on 2 % WA and 1/4 PDA plates with fennel sticks and pine needles. A number of different light conditions are planned for the incubation that should last at least three months.

5.2. Improving seed soaking and absolute quantification

The seed soaking method along with the quadruplex real-time PCR would be a further improvement in testing seed lots making the procedure easier and quicker. The randomness of results of our preliminary experiments showed that probably no DNA is released during soaking, but only later during PCR. PCR inhibitors may pose a problem with larger amounts of fungal structures.

Therefore, it is planned to improve this approach by testing different amounts of seeds from various samples and try to avoid PCR inhibitors.

Another important aspect of using seed soaking is the necessity of absolute quantification. Standard curves based on dilution series of spores proved to be the best approximation to absolute quantification. However, these still need to be improved, adding more dilutions and a limit of detection in number of spores / reaction needs to be established.

5.3. Detection and quantification of the *Diaporthe* species in plant material

In preliminary tests, *Diaporthe* detection in stems and pods of infected soybean plants using the quadruplex real-time PCR assay was successful. However, in pods it worked less well, since inhibitors for the PCR are present here. More plant parts (healthy and infected) will be tested in further experiments. Until now, DNA preparation from plant material was carried out using the DNeasy Plant Mini Kit. In order to solve the problem with the inhibitors, further methods of DNA preparation are being tested. An obvious possibility would be to use the DNeasy Plant Pro Kit (Qiagen), which, according to the description, promises a particularly efficient removal of inhibitors such as polyphenols and polysaccharides. Another possibility is to further purify the already prepared DNA by additional precipitation steps. It would be then possible to use the optimal method for DNA purification for the laboratory experiments.

Another aspect, which needs to be considered, is the course of the disease, which has so far hardly been investigated for *Diaporthe* species. It is still almost completely unclear how and when the pathogens spread in the plant. To close this knowledge gap, it is planned to take samples at different times and from different locations on the stems, leaves, or later also on

the pods from inoculated plants. These samples can then be tested for the presence of the pathogen using microscopy and real-time PCR. These results are then important for the choice of sample sites for the evaluation of virulence tests.

5.4. Detection and quantification of the *Diaporthe* species in soil

Another agricultural control measure is evaluation of the soil of fields to determine the inoculum of plant pathogens. It is likely that infested plant residues in the soil act as primary source of inoculum to infect young plants. Therefore, it makes sense to also check the soil of fields on which soybeans are to be cultivated before sowing, or before making a decision about sowing. In addition, sampling from soil represents a good additional possibility for investigating the distribution of the DPC species. Hence, an adaptation of the quadruplex real-time PCR method for the detection of DPC pathogens in soil is necessary. Here, DNA preparation from soil samples needs to be established. The primary tests can be carried out with artificially inoculated soil. Again, standard curves for absolute quantification and limits of detection need to be established, though the existing standard curves created with DNA from fungal cultures can be used in parallel to specify the DPC load in the soil in ng DPC DNA per g soil. The procedure will later be extended to samples from fields contaminated with DPC.

5.5. Analysis of the distribution of the *Diaporthe* species in Germany

Analyzing the species spectrum of the DPC in central Europe in this research was a big step towards a more comprehensive study of the distribution of the species in Europe, especially in Germany. It was established that *D. longicolla*, *D. caulivora*, *D. eres*, and *D. novem* occur in Germany, Austria, and France. For all four species and all isolates, the pathogenicity on soybean was also shown, therefore, all can be considered relevant *Diaporthe* species in Europe. In continuation of this work the frequency of occurrence of the species will be investigated. Even though most of the isolates in this study were *D. longicolla*, the conclusion that *D. longicolla* is dominant in Germany is based on very little data. Much more extensive studies are required, using the quadruplex qPCR assay. Since soybean cultivation is expanding in Germany and the climate is changing, it can be expected that further DPC species will appear in Germany. Therefore, there is a need for more isolation attempts on more samples from all over Germany to record new *Diaporthe* spp. or the species that would otherwise be overlooked.

5.6. Detection of *Diaporthe* with a genus-specific primer-probe set

Soybeans can be infected by other seed borne pathogens besides *Diaporthe* spp.. In this study in the seed plating assays (3.1.), pathogens like *Alternaria* spp. and *Fusarium* spp. could be identified. Also, according to results of the pathogenicity test (3.4.), it could be that there are no significant differences in virulence or the course of the disease between the different *Diaporthe* spp.. Thus, a genus-specific detection should also be established by designing just one genus-specific primer-probe set. Genus-specific detection of *Diaporthe* will be cheaper and simpler than quadruplex qPCR and can be integrated into multiplex detection of various soybean pathogens.

5.7. Virulence tests on different soybean varieties

The ability to cause a disease and the severity of disease are important factors to differentiate pathogenic species. Also, pathogenicity affects disease management (Mathew et al. 2015 b). Here, the 32 *Diaporthe* isolates were tested for their pathogenicity on cultivar Anushka by seed inoculation (3.4.). The throughput of this method is very limited because it takes very long. Pathogenicity of some of these isolates should be tested on other soybean varieties currently available in Germany (Sojaförderring, 2021) by different methods. Which inoculation method and which disease evaluation method should be used, is an important question. Different inoculation techniques for *Diaporthe* spp. exist (Ghimire et al. 2019). Most important are the toothpick method (Keeling, 1982; Lu et al. 2010; Campbell et al. 2017), the stem-wound method (Mathew et al. 2015 a, b; Mathew et al. 2018), the mycelium contact method (Thompson et al. 2011), and the spore injection method (Kmetz et al. 1979; Chen et al. 2009). All methods conform in the growth state and the organ that are inoculated: V2-V3 and stems ≈ 50 mm below the node of the first trifolium. For the toothpick method, autoclaved toothpicks overgrown with *Diaporthe* are inserted into the stems. As the term stem-wound method implies, the stem is wounded and an agar plug with mycelium is placed into the wound. Mycelium contact means that an agar plug with mycelium is fixed to the stem without any wounding. For the spore injection method, a spore suspension is prepared from colonized broad toothpicks, which is injected into stems using a syringe with needle.

Using one of these methods, the pathogen is introduced into the stem of a growing plant. Starting from there, the virulence can be quantified by measuring how fast the pathogen spreads through the plant or what biomass can be measured at a certain time point. This is much faster than evaluating the plant after months of growth.

An even higher throughput can be reached by using detached leaves. However, since growth of *Diaporthe* through the plant is little documented so far, optimal time points and sites for sampling (other than the point of inoculation) still need to be established.

Visual disease rating is common for identifying *Diaporthe* resistant soybean varieties but selection is difficult because the disease symptoms are expressed very inconsistently. The quadruplex real-time (q)PCR can complement the visual disease rating by quantification of the pathogen even without visible symptoms.

In addition, pathogenicity studies of these isolates not only as individual isolates but also as mixtures should be considered. Also, studies should compare greenhouse and field screening for *Diaporthe* resistance in soybean.

5.8. Characterization of pathogen-induced defense reactions in soybean genotypes

Plants are able to fight pathogens with several strategies. Improving knowledge of plant-pathogen interactions is important for resistance breeding.

Soybean interactions with *Diaporthe* pathogens have not been molecularly characterized very extensively. Induction of a protein inhibiting fungal endopolygalacturonase after *D. caulivora* infection indicates active plant defense against plant cell wall-degrading enzymes (PCWDEs) (Favaron et al. 2000). Li et al. (2017 b) identified several genes encoding PCWDEs in the *D. longicolla* genome and suggested them as putative virulence factors. Mena et al. (2020) observed plant cell wall degradation by *D. caulivora* and an increase of phenolic compounds incorporated into the cell walls as modification related to defense in infected tissues. By analyzing the promotor region of some defense genes it could be discovered that abscisic acid, jasmonic acid, ethylene, salicylic acid, and auxin are involved in signaling against *D. caulivora*.

Further analyses are required to gain insight into the mechanisms in combating DPC pathogens in soybean plants. Using the proper inoculation method cultivars which will be proven to be highly resistant in 5.7. and cultivars that are particularly susceptible will be compared for differential expression of defense related genes in different tissues. Since the whole plant is infected and defense responses might be expressed differently in different tissues this could yield interesting information and ensure that no responses are missed by chance because the wrong tissue was sampled.

Since the complete soybean genome is available and we expect to find soybean cultivars with resistance to *Diaporthe* spp. it should be possible to find genes involved in defense responses

against *Diaporthe* spp.. As part of a collaborative project concerned with the effects of fertilizing soybean with arginine phosphate-based product arGrow Granulate, which is performed at the Swedish University of Agricultural Sciences with our colleagues Dr. Regina Gratz and Dr. Justine Colou, we will use RNAseq analysis to find differentially regulated genes in *Diaporthe* infected soybean plants.

5.9. Biological control of *Diaporthe* species

Application of microbial biological control agents (BCAs) has increased, mainly for its potential to replace synthetic organic fungicides and pesticides, and consequently as an environmentally friendly control strategy (Thambugala et al. 2020; Lahlali et al. 2022). Using BCAs to control diseases has been tested in many economically important crops especially soybean (Begum et al. 2008; Wagner et al. 2018). *Trichoderma* spp. are widely known because of their antagonistic capability against many pathogenic fungi in several plants (Sánchez-Montesinos et al. 2021). The non-pathogenic plant-associated bacterial genera *Pseudomonas*, *Burkholderia*, *Bacillus*, *Streptomyces*, and *Serratia*, are antagonistic against many pathogens. They provide most BCAs for protection of the rhizosphere (Compant et al. 2005; Ciancio et al. 2019). Any of these still need to be tested against *Diaporthe* spp. (Roth et al. 2020). Just one study describes *T. harzianum* as a potential antagonist to suppress *D. sojae* in the field (Begum et al. 2008).

Potential antagonists are commonly screened *in vitro* before they are tested on plants or in the field (Merrimam and Russell, 1990). Preliminary *in vitro* screening of different BCAs was performed as part of this project. This pre-selection of potential antagonists is planned to be confirmed by further *in vitro* experiments. It would be of great interest to test the effectiveness of these antagonists especially *T. harzianum* and *T. asperellum* in *in vivo* greenhouse tests and subsequently in field trials.

5.10. Determination of mycotoxins formed by the *Diaporthe* species

Due to causing damages on their hosts, *Diaporthe* spp. have been studied for secondary metabolites (Chepkirui and Stadler, 2017). They produce several compounds with low molecular weight, chiefly polyketides particularly cytochalasins, which are considered mycotoxins (Horn et al. 1995; Pornpakakul et al. 2007). *Phomopsis leptostromiformis* (teleomorph: *Diaporthe toxica*) infects lupine by forming phomopsins. Phomopsins cause lupinosis in sheep through liver toxicity (van Warmelo et al. 1970). The physiological

function of the mycotoxins identified so far is often unclear, it is assumed that they act as either pathogenicity factors or contribute to host colonization as virulence factors.

Studies reporting on mycotoxin determination in DPC-infested soybean seeds are rather limited. This is surprising since DPC-damaged soybeans may be contaminated with mycotoxins and cause food safety concerns. To my knowledge, still nothing is known about mycotoxin production for the four species *D. longicolla*, *D. caulivora*, *D. eres*, and *D. novem*. Thus, it should be worthwhile to include identification of mycotoxin(s) produced by these DPC species in future studies and establish standards to test seed quality by determining mycotoxin content.

6 Literature

Adams, G. (2020). A beginner's guide to RT-PCR, qPCR and RT-qPCR. The Biochemist **42**: 48–53. DOI: 10.1042/bio20200034

Akintayo, S. O., Treinen, C., Vahidinasab, M., Pfannstiel, J., Bertsche, U., Fadahunsi, I., Oellig, C., Granvogl, M., Henkel, M., Lilge, L., and Hausmann, R. (2022). Exploration of surfactin production by newly isolated *Bacillus* and *Lysinibacillus* strains from food-related sources. Letters in Applied Microbiology **75**: 378–387. DOI: 10.1111/LAM.13731

Athow, K. L., and Caldwell, R. M. (1954). A comparative study of *Diaporthe* stem canker and pod and stem blight of soybean. Phytopathology **44**: 319–325

Babu, B. K., Mesapogu, S., Sharma, A., Somasani, S. R., and Arora, D. K. (2011). Quantitative real-time PCR assay for rapid detection of plant and human pathogenic *Macrophomina phaseolina* from field and environmental samples. Mycologia **103**: 466–473. DOI: 10.3852/10-181

Bachteler, K. (2018). *Diaporthe*/*Phomopsis* – most important fungal disease on soybeans. Taifun Soy Info, Taifun-Tofu GmbH.

Backman, P. A., Weaver, D. B., and Morgan-Jones, G. (1985). Soybean stem canker: an emerging disease problem. Plant Disease **69**: 641–647

Barnes, C. W., Szabo, L. J., and Bowersox, V. C. (2009). Identifying and quantifying *Phakopsora pachyrhizi* spores in rain. Phytopathology **99**: 328-338. DOI: 10.1094/PHYTO-99-4-0328

Begum, M. M., Sariah, M., Zainal Abidin, M. A., Puteh, A. B., and Rahman, M. A. (2008). Ultrastructural studies of soybean seed-borne infection by *Diaporthe phaseolorum* var. *sojae* and screening of antagonisitic potentiality by selected biocontrol agents *in vitro*. Pertanika Journal of Tropical Agricultural Science **31**: 247–256

Bienapfl, J. C., Malvick, D. K., and Percich, J. A. (2011). Specific molecular detection of *Phytophthora sojae* using conventional and real-time PCR. Fungal Biology **115**: 733–740. DOI: 10.1016/j.funbio.2011.05.007

Botelho, L. S., Barrocas, E. N., Machado, J. C., and Martins, R. S. (2015). Detection of *Sclerotinia sclerotiorum* in soybean seeds by conventional and quantitative PCR techniques. Journal of Seed Science **37**: 55–62. DOI: 10.1590/2317-1545v37n1141460

Brayford, D. (1990). Variation in *Phomopsis* isolates from *Ulmus* species in the British Isles and Italy. Mycological Research **94**: 691–697. DOI: 10.1016/S0953-7562(09)80670-9

Brill, L. M., McClary, R. D., and Sinclair, J. B. (1994). Analysis of two ELISA formats and antigen preparations using polyclonal antibodies against *Phomopsis longicolla*. Phytopathology **84**: 173–179

Brumer, B. B., Lopes-Caitar V. S., Chicowski, A. S., Beloti, J. D., Castanho, F. M., Gregório da Silva, D. C., de Carvalho, S., Lopes, I. O. N., Soares, R. M., Seixas, C. D. S.,

Abdelnoor, R. V., and Marcelino-Guimarães, F. C. (2018). Morphological and molecular characterization of *Diaporthe* (anamorph *Phomopsis*) complex and pathogenicity of *Diaporthe aspalathi* isolates causing stem canker in soybean. European Journal of Plant Pathology **151**: 1009–1025. DOI: 10.1007/s10658-018-1436-5

Cai, L., Giraud, T., Zhang, N., Begerow, D., Cai, G., and Shivas, R. G. (2011). The evolution of species concepts and species recognition criteria in plant pathogenic fungi. Fungal Diversity **50**: 121–133. DOI: 10.1007/s13225-011-0127-8

Campbell, M. A., Li, Z., and Buck, J. W. (2017). Development of southern stem canker disease on soybean seedlings in the greenhouse using a modified toothpick inoculation assay. Crop Protection **100**: 57–64. DOI: 10.1016/j.cropro.2017.05.026

Carbone, I., and Kohn, L. M. (1999). A method for designing primer sets for speciation studies in filamentous ascomycetes. Mycologia **91**: 553–556. DOI: 10.1080/00275514.1999.12061051

Carvalho-Vieira, M. G. G., and Machado, J. C. (2002). Applicability of molecular techniques for detection of seed-borne fungi under certification. In: Seed-borne fungi: a contribution to routine seed health analysis (Machado, J. C., Langerak, C. J., and Jaccoud-Filho, D. S. eds.). First edition, ISTA, Bassersdorf, Switzerland

Chaisiri, C., Liu, X., Lin, Y., Li, J., Xiong, B., and Luo, C. (2020). Phylogenetic analysis and development of molecular tool for detection of *Diaporthe citri* causing melanose disease of citrus. Plants **9**, 329. DOI: 10.3390/plants9030329

Chanda, A. K., Ward, N. A., Robertson, C. L., Chen, Z.-Y., and Schneider, R. W. (2014). Development of a quantitative polymerase chain reaction detection protocol for *Cercospora kikuchii* in soybean leaves and its use for documenting latent infection as affected by fungicide applications. Phytopathology **104**: 1118–1124. DOI: 10.1094/PHYTO-07-13-0200-R

Chang, H.-X., Lipka, A. E., Domier, L. L., and Hartman, G. L. (2016). Characterization of disease resistance loci in the USDA soybean germplasm collection using genome-wide association studies. Phytopathology **106**: 1139-1151. DOI: 10.1094/PHYTO-01-16-0042-FI

Chao, C. P., and Glawe, D. A. (1985). Studies on the taxonomy of *Diaporthe vaccinii*. Mycotaxon **23**: 371–381

Chen, C., Zhao, W., Zhou, M., and Wang, J. (2010). High-throughput detection of *Sclerotinia sclerotiorum* from oilseed rape by TaqMan quantitative real-time PCR. Phytopathology 100 (Supplement), S23

Chen, C. H., Wang, T. C., and Seo, M. J. (2009). First report of soybean pod and stem blight caused by *Diaporthe phaseolorum* var. *sojae* in Taiwan. Plant Disease **93**: 202. DOI: 10.1094/PDIS-93-2-0202A

Chen, X. H., Koumoutsi, A., Scholz, R., Eisenreich, A., Schneider, K., Heinemeyer, I., Morgenstern, B., Voss, B., Hess, W. R., Reva, O., Junge, H., Voigt, B., Jungblut, P. R., Vater, J., Süssmuth, R., Liesegang, H., Strittmatter, A., Gottschalk, G., and Borriss, R.

(2007). Comparative analysis of the complete genome sequence of the plant growth-promoting bacterium *Bacillus amyloliquefaciens* FZB42. Nature Biotechnology **25**: 1007–1014. DOI: 10.1038/nbt1325

Chepkirui, C., and Stadler, M. (2017). The genus *Diaporthe*: a rich source of diverse and bioactive metabolites. Mycological progress **16**: 477–494. DOI: 10.1007/s11557-017-1288-y

Choi, Y. W., Hyde, K. D., and Ho, W. H. (1999). Single spore isolation of fungi. Fungal Diversity **3**: 29–38

Ciancio, A., Pieterse, C. M. J., and Mercado-blanco, J. (2019). Editorial: harnessing useful rhizosphere microorganisms for pathogen and pest biocontrol – second edition. Frontiers in Microbiology **10**: 1935. DOI: 10.3389/fmicb.2019.01935

Coleman, K., Whitmore, A. P., Hassall, K. L., Shield, I., Semenov, M. A., Dobermann, A., Bourhis, Y., Eskandary, A., and Milne, A. E. (2021). The potential for soybean to diversify the production of plant-based protein in the UK. Science of the Total Environment **767**: 144903. DOI: 10.1016/j.scitotenv.2020.144903

Compant, S., Duffy, B., Nowak, J., Clement, C., and Barka, E. A. (2005). Use of plant growth-promoting bacteria for biocontrol of plant diseases: principles, mechanisms of action, and future prospects. Applied and Environmental Microbiology **71**: 4951–4959

Cure, J. D., and Acock, B. (1986). Crop responses to carbon dioxide doubling: a literature survey. Agricultural and Forest Meteorology **38**: 127–145. DOI: 10.1016/0168-1923(86)90054-7

Divilov, K. (2014). Taxonomy and biocontrol of *Diaporthe sojae* and screening for resistance to *Phomopsis* seed decay caused by an atypical *Diaporthe sojae* isolate using various assays. Dissertation, University of Illinois

Dong, Z., Manawasinghe, I. S., Huang, Y., Shu, Y., Phillips, A. J. L., Dissanayake, A. J., Hyde, K. D., Xiang, M., and Luo, M. (2021). Endophytic *Diaporthe* associated with *Citrus grandis* cv. Tomentosa in China. Frontiers in Microbiology **11**: 609387. DOI: 10.3389/fmicb.2020.609387

Eastburn, D. M., Degennaro, M. M., Delucia, E. H., Dermody, O., and Mcelrone, A. J. (2010). Elevated atmospheric carbon dioxide and ozone alter soybean diseases at SoyFACE. Global Change Biology **16**: 320–330. DOI: 10.1111/j.1365-2486.2009.01978.x

European Commission, (2019). EU-U.S. Joint Statement: The United States is Europe's main soya beans supplier with imports up by 121%. IP/19/2154, Brussels

Farr, D. F., Castlebury, L. A., and Rossman, A. Y. (2002). Morphological and molecular characterization of *Phomopsis vaccinii* and additional isolates of *Phomopsis* from blueberry and cranberry in the eastern United States. Mycologia **94**: 494–504. DOI: 10.1080/15572536.2003.11833214

Favaron, F., Destro, T., and D'Ovidio, R. (2000). Transcript accumulation of polygalacturonase inhibiting protein (PGIP) following pathogen infections in soybean. Journal of Plant Pathology **82**: 103–109. DOI: 10.4454/jpp.v82i2.1149

Fernández, F. A., and Hanlin, R. T. (1996). Morphological and RAPD analyses of *Diaporthe phaseolorum* from soybean. Mycologia **88**: 425–440

Frederick, R. D., Synder, C. L., Peterson, G. L., and Bonde, M. R. (2002). Polymerase chain reaction assays for the detection and discrimination of the soybean rust pathogens *Phakopsora pachyrhizi* and *P. meibomiae*. Phytopathology **92**: 217–227. DOI: 10.1094/PHYTO.2002.92.2.217

Freeman, J., Ward, E., Calderon, C., and McCartney, A. (2002). A polymerase chain reaction (PCR) assay for the detection of inoculum of *Sclerotinia sclerotiorum*. European Journal of Plant Pathology **108**: 877–886. DOI: 10.1023/A:1021216720024

Frosheiser, F. I. (1957). Studies on the etiology and epidemiology of *Diaporthe phaseolorum* var. *caulivora*, the cause of stem canker of soybeans. Phytopathology **47**: 87–94

Gao, X., Jackson, T. A., Lambert, K. N., Li, S., Hartman, G. L., and Niblack, T. L. (2004). Detection and quantification of *Fusarium solani* f. sp. *glycines* in soybean roots with real-time quantitative polymerase chain reaction. Plant Disease **88**: 1372–1380. DOI: 10.1094/PDIS.2004.88.12.1372

Gardes, M., and Bruns, T. D. (1993). ITS primers with enhanced specificity for basidiomycetes - application to the identification of mycorrhizae and rusts. Molecular Ecology **2**: 113–118. DOI: 10.1111/j.1365-294x.1993.tb00005.x

Ghimire, K., Petrovic, K., Kontz, B. J., Bradley, C. A., Chilvers, M. I., Mueller, D. S., Smith, D. L., Wise, K. A., and Mathew, F. M. (2019). Inoculation method impacts symptom development associated with *Diaporthe aspalathi*, *D. caulivora*, and *D. longicolla* on soybean (*Glycine max*). Plant Disease **103**: 677–684. DOI: 10.1094/PDIS-06-18-1078-RE

Giulietti, A., Overbergh, L., Valckx, D., Decallonne, B., Bouillon, R., and Mathieu, C. (2001). An overview of real-time quantitative PCR: applications to quantify cytokine gene expression. Methods **25**: 386–401. DOI: 10.1006/meth.2001.1261

Glass, N. L., and Donaldson, G. C. (1995). Development of primer sets designed for use with the PCR to amplify conserved genes from filamentous ascomycetes. Applied and Environmental Microbiology **61**: 1323–1330

Goldsmith, P. D. (2008). Economics of soybean production, marketing, and utilization. In: Soybeans: chemistry, production, processing, and utilization (Johnson, L. A., White, P. J., and Galloway, R. eds.). AOCS Press, Urbana, IL, Chapter 5: 117–150. DOI: 10.1016/B978-1-893997-64-6.50008-1

Gomes, R. R., Glienke, C., Videira, S. I. R., Lombard, L., Groenewald, J. Z., and Crous, P. W. (2013). *Diaporthe*: a genus of endophytic, saprobic and plant pathogenic fungi. Persoonia **31**: 1–41. DOI: 10.3767/003158513X666844

Grabicoski, E. M. G., Jaccoud-Filho, D. S., Pileggi, M., Henneberg, L., Pierre, M. L. C., Vrisman, C. M., and Dabul, A. N. G. (2015). Rapid PCR-based assay for

Sclerotinia sclerotiorum detection on soybean seeds. Scientia Agricola **72**: 69–74. DOI: 10.1590/0103-9016-2013-0395

Grijalba, P., and Ridao, A. C. (2012). Survival of *Diaporthe phaseolorum* var. *caulivora* (causal agent of soybean stem canker) artificially inoculated in different crop residues. Tropical Plant Pathology **37**: 271–274. DOI: 10.1590/S1982-56762012000400006

Hall, T. A. (1999). BioEdit: a user-friendly biological sequence alignment editor and analysis program for Windows 95/98/NT. Nucleic Acids Symposium Series **41**: 95–98

Hariharan, G., and Prasannath, K. (2021). Recent advances in molecular diagnostics of fungal plant pathogens: a mini review. Frontiers in Cellular and Infection Microbiology **10**: 600234. DOI: 10.3389/fcimb.2020.600234

Hartman, G. L., and Hill, C. B. (2010). Diseases of soybean and their management. In: The soybean: botany, production, and uses (Singh, G. ed.). CABI, Wallingford, UK, Chapter 13: 276–299

Hartman, G. L., Rupe, J. C., Sikora, E. J., Domier, L. L., Davis, J. A., and Steffey, K. L. (2015). Compendium of soybean diseases and pests. Fifth edition, APS Press, St. Paul, Minnesota, USA

Hartman, G. L., and Sinclair, I. B. (1992). Soybean disease management: chemical and biological control in tropical regions. In: Pest management in soybean (Copping, L. G., Green, M. B., and Rees R. T. eds.). Elsevier Applied Science, 164–173

Hartman, G. L., West, E. D., and Herman, T. K. (2011). Crops that feed the World 2. Soybean—worldwide production, use, and constraints caused by pathogens and pests. Food Security **3**: 5–17. DOI: 10.1007/s12571-010-0108-x

Hepperly, P. R., and Sinclair, J. B. (1978). Quality losses in *Phomopsis*-infected soybean seeds. Phytopathology **68**: 1684–1687

Hilário, S., Santos, L., Phillips, A. J. L., and Alves, A. (2021). Caveats of the internal transcribed spacer region as a barcode to resolve species boundaries in *Diaporthe*. Fungal Biology **126**: 54–74. DOI: 10.1016/j.funbio.2021.10.005

Hobbs, T. W., Schmitthenner, A. F., and Kuter, G. A. (1985). A new *Phomopsis* species from soybean. Mycologia **77**: 535–544. DOI: 10.1080/00275514.1985.12025139

Horn, W. S., Simmonds, M. S. J., Schwartz, R. E., and Blaney, W. M. (1995). Phomopsichalasin, a novel antimicrobial agent from an endophytic *Phomopsis* sp.. Tetrahedron **51**: 3969–3978. DOI: 10.1016/0040-4020(95)00139-Y

Hosseini, B., El-Hasan, A., Link, T., and Voegele, R. T. (2020). Analysis of the species spectrum of the *Diaporthe*/*Phomopsis* complex in European soybean seeds. Mycological Progress **19**: 455–469. DOI: 10.1007/s11557-020-01570-y

Hosseini, Voegele, R. T., and Link, T. I. (2021). Establishment of a quadruplex real-time PCR assay to distinguish the fungal pathogens *Diaporthe longicolla*, *D. caulivora*, *D. eres*, and *D. novem* on soybean. PLoS ONE **16**: e0257225. DOI: 10.1371/journal.pone.0257225

Hu, R., Fan, C., Li, H., Zhang, Q., and Fu, Y.-F. (2009). Evaluation of putative reference genes for gene expression normalization in soybean by quantitative real-time RT-PCR. BMC Molecular Biology **10**: 93. DOI: 10. 1186/1471-2199-10-93

Hufnagel, J., Reckling, M., and Ewert, F. (2020). Diverse approaches to crop diversification in agricultural research. A review. Agronomy for Sustainable Development **40**: 14. DOI: 10.1007/s13593-020-00617-4

IDH and IUCN NL, (2019). European Soy Monitor. Researched by B. Kuepper and M. Riemersma of Profundo. Coordinated by N. Sleurink of IDH, The Sustainable Trade Initiative and H. van den Hombergh of IUCN National Committee of the Netherlands

Jaccoud-Filho, D. S., Lee, D., Blakemore, E. J. A., and Reeves, J. C. (2002). Demonstration of the use of molecular techniques for detection of *Phomopsis* species in soya bean seeds. In: Seed-borne fungi: a contribution to routine seed health analysis (Machado, J. C., Langerak, C. J., and Jaccoud-Filho, D. S. eds.). ISTA, Bassersdorf, Switzerland, 92–110

Jackson, E. W., Feng, C., Fenn, P., and Chen, P. (2009). Genetic mapping of resistance to *Phomopsis* seed decay in the soybean breeding line MO/PSD-0259 (PI562694) and plant introduction 80837. Journal of Heredity **100**: 777–783. DOI: 10.1093/jhered/esp042

Jackson, E. W., Fenn, P., and Chen, P. (2005). Inheritance of resistance to *Phomopsis* seed decay in soybean PI 80837 and MO/PSD-0259 (PI562694). Crop Science **45**: 2400–2404. DOI: 10.2135/cropsci2004.0525

Kanematsu, S., Adachi, Y., and Ito, T. (2007). Mating-type loci of heterothallic *Diaporthe* spp.: homologous genes are present in opposite mating-types. Current Genetics **52**: 11–22. DOI: 10.1007/s00294-007-0132-3

Keeling, B. L. (1982). A seedling test for resistance to soybean stem canker caused by *Diaporthe phaseolorum* var. *caulivora*. Phytopathology **72**: 807–809. DOI: 10.1094/Phyto-72-807

Keeling, B. L. (1988). Measurement of soybean resistance to stem canker caused by *Diaporthe phaseolorum* var. *caulivora*. Plant Disease **72**: 217–220. DOI: 10.1094/PD-72-0217

Klittich, C. J. R., and Leslie, J. F. (1988). Nitrate reduction mutants of *Fusarium moniliforme* (*Gibberella fujikuroi*). Genetics **118**: 417–423. DOI: 10.1093/genetics/118.3.417

Kmetz, K. T., Ellett, C. W., and Schmitthenner, A. F. (1979). Soybean seed decay: sources of inoculum and nature of infection. Phytopathology **69**: 798–801. DOI: 10.1094/Phyto-69-798

Kmetz, K. T., Schmitthenner, A. F., and Ellett, C. W. (1978). Soybean seed decay: prevalence of infection and symptom expression caused by *Phomopsis* sp., *Diaporthe phaseolorum* var. *sojae*, and *D. phaseolorum* var. *caulivora*. Phytopathology **68**: 836–840

Koning, G., TeKrony, D. M., and Ghabrial, S. A. (2003). Soybean seedcoat mottling: association with soybean mosaic virus and *Phomopsis* spp. seed infection. Plant Disease **87**: 413–417. DOI: 10.1094/PDIS.2003.87.4.413

Koning, G., TeKrony, D. M., Pfeiffer, T. W., and Ghabrial, S. A. (2001). Infection of soybean with soybean mosaic virus increases susceptibility to *Phomopsis* spp. seed infection. Crop Science **41**:1850–1856. DOI: 10.2135/cropsci2001.1850

Kontz, B., Adhikari, S., Subramanian, S., and Mathew, F. M. (2016). Optimization and application of a quantitative polymerase chain reaction assay to detect *Diaporthe* species in soybean plant tissue. Plant Disease **100**: 1669–1676. DOI: 10.1094/PDIS-10-15-1204-RE

Krebs, B., Höding, B., Kübart, S., Workie, M. A., Junge, H., Schmiedeknecht, G., Grosch, R., Bochow, H., and Hevesi, M. (1998). Use of *Bacillus subtilis* as biocontrol agent. I. Activities and characterization of *Bacillus subtilis* strains. Journal of Plant Diseases and Protection **105**: 181–197

Krsmanović, S., Petrović, K., Ceran, M., Dordević, V., Ranđelović, P., Jaćimović, S., and Miladinov, Z. (2020). Diversity of phytopathogenic fungi on soybean seed in Serbia. Ratarstvo i Povrtarstvo **57**: 80–86. DOI: 10.5937/ratpov57-27516

Kulik, M. M. (1984). Symptomless infection, persistence, and production of pycnidia in host and non-host plants by *Phomopsis batatae*, *Phomopsis phaseoli*, and *Phomopsis sojae*, and the taxonomic implications. Mycologia **76**: 274–291. DOI: 10.1080/00275514.1984.12023837

Kumar, R., Gupta, A., Srivastava, S., Devi, G., Singh, V. K., Goswami, S. K., Gurjar, M. S., and Aggarwal, R. (2020). Diagnosis and detection of seed-borne fungal phytopathogens. In: Seed-borne diseases of agricultural crops: detection, diagnosis, and management (Kumar, R., and Gupta, A. eds.). Springer Nature Singapore Pte Ltd., Chapter 5: 107–142. DOI: 10.1007/978-981-32-9046-4_5

Kumar, S., Stecher, G., Li, M., Knyaz, C., and Tamura, K. (2018). MEGA X: molecular evolutionary genetics analysis across computing platforms. Molecular Biology and Evolution **35**: 1547–1549. DOI: 10.1093/molbev/msy096

Lahlali, R., Ezrari, S., Radouane, N., Kenfaoui, J., Esmaeel, Q., El Hamss, H., Belabess, Z., and Barka, E. A. (2022). Biological control of plant pathogens: a global perspective. Microorganisms **10**, 596. DOI: 10.3390/microorganisms10030596

Lalitha, B., Snow, J. P., and Berggren, G. T. (1989). Phytotoxin production by *Diaporthe phaseolorum* var. *caulivora*, the causal organism of stem canker of soybean. Phytopathology **79**: 499–504

Lau, H. Y., and Botella, J. R. (2017). Advanced DNA-based point-of-care diagnostic methods for plant diseases detection. Frontiers in Plant Science **8**: 2016. DOI: 10.3389/fpls.2017.02016

Li, S. (2011). *Phomopsis* seed decay of soybean. In: Soybean - molecular aspects of breeding (Sudaric, A. ed.). In Tech, Rijeka, Chapter 13: 277–292

Li, S., and Chen, P. (2013). Resistance to *Phomopsis* seed decay in soybean. ISRN Agronomy **2013**: 1–8. DOI: 10.1155/2013/738379

Li, S., Chen, P., and Hartman, G. L. (2015a). *Phomopsis* seed decay. In: Compendium of soybean diseases and pests (Hartman, G. L., Rupe, J. C., Sikora, E. J., Domier, L. L., Davis, J. A., and Steffey, K. L. eds.). Fifth edition, APS Press, St. Paul, Minnesota, USA, 47–48

Li, S., Darwish, O., Alkharouf, N. W., Musungu, B., and Matthews, B. F. (2017b). Analysis of the genome sequence of *Phomopsis longicolla*: a fungal pathogen causing *Phomopsis* seed decay in soybean. BMC Genomics **18**: 688. DOI: 10.1186/s12864-017-4075-x

Li, S., Hartman, G. L., and Boykin, D. L. (2010). Aggressiveness of *Phomopsis longicolla* and other *Phomopsis* spp. on soybean. Plant Disease **94**: 1035–1040. DOI: 10.1094/PDIS-94-8-1035

Li, S., Hartman, G. L., Domier, L. L., and Boykin, D. (2008). Quantification of *Fusarium solani* f. sp. *glycines* isolates in soybean roots by colony-forming unit assays and real-time quantitative PCR. Theoretical and Applied Genetics **117**: 343–352. DOI: 10.1007/s00122-008-0779-2

Li, S., Rupe, J., Chen, P., Shannon, G., Wrather, A., and Boykin, D. (2015b). Evaluation of diverse soybean germplasm for resistance to *Phomopsis* seed decay. Plant Disease **99**: 1517–1525. DOI: 10.1094/PDIS-04-14-0429-RE

Li, S., Sciumbato, G., Rupe, J., Shannon, G., Chen, P., and Boykin, D. (2017a). Evaluation of commercial soybean cultivars for reaction to *Phomopsis* seed decay. Plant Disease **101**: 1990–1997. DOI: 10.1094/PDIS-02-17-0204-RE

Liu, D., Coloe, S., Baird, R., and Pedersen, J. (2000). Rapid mini-preparation of fungal DNA for PCR. Journal of Clinical Microbiology **38**: 471. DOI: 10.1128/JCM.38.1.471-471.2000

Liu, K. (2008). Food use of whole soybeans. In: Soybeans: chemistry, production, processing, and utilization (Johnson, L. A., White, P. J., and Galloway, R. eds.). AOCS Press, Urbana, IL, Chapter 14: 441–482. DOI: 10.1016/B978-1-893997-64-6.50017-2

Livak, K. J., and Schmittgen, T. D. (2001). Analysis of relative gene expression data using real-time quantitative PCR and the $2^{-\Delta\Delta Cq}$ Method. Methods **25**: 402–408. DOI: 10.1006/meth.2001.1262

Lu, X., Robertson, A. E., Byamukama, E. Z., and Nutter, F. W., Jr. (2010). Evaluating the importance of stem canker of soybean in Iowa. Plant Disease **94**: 167–173. DOI: 10.1094/PDIS-94-2-0167

Malvick, D. K., and Impullitti, A. E. (2007). Detection and quantification of *Phialophora gregata* in soybean and soil samples with a quantitative, real-time PCR assay. Plant Disease **91**: 736–742. DOI: 10.1094/PDIS-91-6-0736

Mathew, F. M., Alananbeh, K. M., Jordahl, J. G., Meyer, S. M., Castlebury, L. A., Gulya, T. J., and Markell, S. G. (2015 b). *Phomopsis* Stem Canker: a reemerging threat to sunflower (*Helianthus annuus*) in the United States. Phytopathology **105**: 990–997. DOI: 10.1094/PHYTO-11-14-0336-FI

Mathew, F. M., Castlebury, L. A., Alananbeh, K., Jordahl, J. G., Taylor, C. A., Meyer, S. M., Lamppa, R. S., Pasche, J. A., and Markell, S. G. (2015 a). Identification of *Diaporthe longicolla* on dry edible pea, dry edible bean, and soybean in North Dakota. Plant Health Progress **16**: 71–72. DOI: 10.1094/PHP-RV-14-0045

Mathew, F. M., Jordahl, J. G., Gulya, T. J., and Markell, S. G. (2018). Comparison of greenhouse-based inoculation methods to study aggressiveness of *Diaporthe helianthi* isolates causing *Phomopsis* stem canker of sunflower (*Helianthus annuus*). Plant Health Progress **19**: 92–96. DOI: 10.1094/PHP-10-17-0059-RS

Mbofung, G. C. Y., Fessehaie, A., Bhattacharyya, M. K., and Leandro, L. F. S. (2011). A new TaqMan real-time polymerase chain reaction assay for quantification of *Fusarium virguliforme* in soil. Plant disease **95**: 1420–1426. DOI: 10.1094/PDIS-02-11-0120

Mena, E., Garaycochea, S., Stewart, S., Montesano, M., and Ponce de León, I. (2022). Comparative genomics of plant pathogenic *Diaporthe* species and transcriptomics of *Diaporthe caulivora* during host infection reveal insights into pathogenic strategies of the genus. BMC Genomics **23**: 175. DOI: 10.1186/s12864-022-08413-y

Mena, E., Stewart, S., Montesano, M., and Ponce de León, I. (2020). Soybean stem canker caused by *Diaporthe caulivora*; pathogen diversity, colonization process, and plant defense activation. Frontiers in Plant Science **10**: 1733. DOI: 10.3389/fpls.2019.01733

Mendelsohn, R., Nordhaus, W. D., and Shaw, D. (1994). The impact of global warming on agriculture: a ricardian analysis. The American Economic Review **84**: 753–771

Mengistu, A., Castlebury, L., Smith, R., Ray, J., and Bellaloui, N. (2009). Seasonal progress of *Phomopsis longicolla* infection on soybean plant parts and its relationship to seed quality. Plant Disease **93**: 1009–1018. DOI: 10.1094/PDIS-93-10-1009

Merriman, P., and Russell, K. (1990). Screening strategies for biological control. In: Biological control of soil-borne plant pathogens (Hornby, D. ed.). CABI, Wallingford, UK, 427–435

Miller, A. N., and Huhndorf, S. M. (2005). Multi-gene phylogenies indicate ascomal wall morphology is a better predictor of phylogenetic relationships than ascospore morphology in the Sordariales (Ascomycota, Fungi). Molecular Phylogenetics and Evolution **35**: 60–75. DOI: 10.1016/j.ympev.2005.01.007

Moleleki, N., Preisig, O., Wingfield, M. J., Crous, P. W., and Wingfield, B. D. (2002). PCR-RFLP and sequence data delineate three *Diaporthe* species associated with stone and pome fruit trees in South Africa. European Journal of Plant Pathology **108**: 909–912

Mueller, D., Bradley, C., Chilvers, M., Giesler, L., Mathew, F., Smith, D., and Wise, K. (2015). Pod and stem blight and *Phomopsis* seed decay. Soybean Disease Management CPN-1007

Nelson, G. C., Rosegrant, M. W., Koo, J., Robertson, R. D., Sulser, T., Zhu, T., Ringler, C., Msangi, S., Palazzo, A., Batka, M., Magalhaes, M., Valmonte-Santos, R., Ewing, M., and Lee, D. R. (2009). Climate change: impact on agriculture and costs of adaptation. International Food Policy Research Institute. DOI: 10.2499/0896295354

Nitschke, T. (1870). Pyrenomycetes germanici. Breslau, Eduard Trewendt **2**: 245

Okubara, P. A., Schroeder, K. L., and Paulitz, T. C. (2005). Real-time polymerase chain reaction: applications to studies on soilborne pathogens. Canadian Journal of Plant Pathology **27**: 300–313. DOI: 10.1080/07060660509507229

Omari, R. A., Yuan, K., Anh, K. T., Reckling, M., Halwani, M., Egamberdieva, D., Ohkama-Ohtsu, N., and Bellingrath-Kimura, S. D. (2022). Enhanced soybean productivity by inoculation with indigenous *Bradyrhizobium* strains in agroecological conditions of Northeast Germany. Frontiers in Plant Science **12**: 707080. DOI: 10.3389/fpls.2021.707080

O'Neal, M. E., and Johnson, K. D. (2010). Insect pests of soybean and their management. In: The soybean: botany, production, and uses (Singh, G. ed.). CABI, Wallingford, UK, Chapter 14: 300–324

Pariaud, B., Ravigne, V., Halkett, F., Goyeau, H., Carlier, J., and Lannou, C. (2009). Aggressiveness and its role in the adaptation of plant pathogens. Plant Pathology **58**: 409–424. DOI: 10.1111/j.1365-3059.2009.02039.x

Patil, G., Vuong, T. D., Kale, S., Valliyodan, B., Deshmukh, R., Zhu, C., Wu, X., Bai, Y., Yungbluth. D., Lu, F., Kumpatla, S., Shannon, J. G., Varshney, R. K., and Nguyen, H. T. (2018). Dissecting genomic hotspots underlying seed protein, oil, and sucrose content in an interspecific mapping population of soybean using high-density linkage mapping. Plant Biotechnology Journal **16**: 1939–1953. DOI: 10.1111/pbi.12929

Petrović, K., Riccioni, L., Dordević, V., Balešević-Tubić, S., Miladinović, J., Ceran, M., and Rajković, D. (2018). *Diaporthe pseudolongicolla* – the new pathogen on soybean seed in Serbia. Ratarstvo i Povrtarstvo **55**: 103–109. DOI: 10.5937/ratpov55-18582

Petrović, K., Riccioni, L., Vidić, M., Dordević, V., Balešević-Tubić, S., Đukić, V., and Miladinov, Z. (2016). First report of *Diaporthe novem*, *D. foeniculina*, and *D. rudis* associated with soybean seed decay in Serbia. Plant Disease **100**: 2324. DOI: 10.1094/PDIS-03-16-0353-PDN

Petrović, K., Skaltsas, D., Castlebury, L. A., Konzt, B., Allen, T. W., Chilvers, M. I., Gregory, N., Kelly, H. M., Koehler, A. M., Kleczewski, N. M., Mueller, D. S., Price, P. P., Smith, D. L., and Mathew, F. M. (2021). *Diaporthe* seed decay of soybean [*Glycine max* (L.) Merr.] is endemic in the United States, but new fungi are involved. Plant Disease **105**: 1621–1629. DOI: 10.1094/PDIS-03-20-0604-RE

Petrović, K., Vidić, M., Riccioni, L., Dordević, V., and Rajković, D. (2015). First report of *Diaporthe eres* species complex causing seed decay of soybean in Serbia. Plant Disease **99**: 1186. DOI: 10.1094/PDIS-01-15-0056-PDN

Pioli, R. N., Morandi, E. N., Martinez, M. C., Lucca, F., Tozzini, A., Bisaro, V., and Hopp, H. E. (2003). Morphologic, molecular, and pathogenic characterization of *Diaporthe phaseolorum* variability in the core soybean-producing area of Argentina. Phytopathology **93**: 136–146

Pornpakakul, S., Roengsumran, S., Deechangvipart, S., Petsom, A., Muangsin, N., Ngamrojnavanich, N., Sriubolmas, N., Chaichit, N., and Ohta, T. (2007). Diaporthichalasin, a novel CYP3A4 inhibitor from an endophytic *Diaporthe* sp.. Tetrahedron Letters **48**: 651–655. DOI: 10.1016/j.tetlet.2006.11.102

Ramiro, J., Ciampi-Guillardi, M., Caldas, D. G. G., de Moraes, M. H. D., Barbieri, M. C. G., Pereira, W. V., and Massola Jr., N. S. (2019). Quick and accurate detection of *Sclerotinia sclerotiorum* and *Phomopsis* spp. in soybean seeds using qPCR and seed-soaking method. Journal of Phytopathology **167**: 273–282. DOI: 10.1111/jph.12796

Rehner, S. A., and Uecker, F. A. (1994). Nuclear ribosomal internal transcribed spacer phylogeny and host diversity in the coelomycete *Phomopsis*. Canadian Journal of Botany **72**: 1666–1674. DOI: 10.1139/b94-204

Reicks, S. (2017). *Diaporthe*/*Phomopsis* fungi complex in soybeans. DuPont Pioneer Agronomy Sciences

Rekab, D., Del Sorbo, G., Reggio, C., Zoina, A., and Firrao, G. (2004). Polymorphisms in nuclear rDNA and mtDNA reveal the polyphyletic nature of isolates of *Phomopsis* pathogenic to sunflower and a tight monophyletic clade of defined geographic origin. Mycological Research **108**: 393–402

Rodeva, R., Stoyanova, Z., and Pandeva, R. (2009). A new fruit disease of pepper in Bulgaria caused by *Phomopsis capsica*. Acta Horticulturae **830**: 551–556. DOI: 10.17660/ActaHortic.2009.830.79

Rossen, L., Norskov, P., Holmstrom, K., and Rasmussen, O. F. (1992). Inhibition of PCR by components of food samples, microbial diagnosis assays and DNA-extraction solutions. International Journal of Food Microbiology **17**: 37–45

Rosskopf, E. N., Charudattan, R., Shabana, Y. M., and Benny, G. L. (2000). *Phomopsis amaranthicola*, a new species from *Amaranthus* sp.. Mycologia **92**: 114–122. DOI: 10.1080/00275514.2000.12061135

Rossman, A. Y., Adams, G. C., Cannon, P. F., Castlebury, L. A., Crous, P. W., Gryzenhout, M., Jaklitsch, W. M., Mejia, L. C., Stoykov, D., Udayanga, D., Voglmayr, H., and Walker, D. M. (2015). Recommendations of generic names in *Diaporthales* competing for protection or use. IMA Fungus **6**: 145–154. DOI: 10.5598/imafungus.2015.06.01.09

Roth, M. G., Webster, R. W., Mueller, D. S., Chilvers, M. I., Faske, T. R., Mathew, F. M., Bradley, C. A., Damicone, J. P., Kabbage, M., and Smith, D. L. (2020). Integrated management of important soybean pathogens of the United States in changing climate. Journal of Integrated Pest Management **11**: 17; 1–28. DOI: 10.1093/jipm/pmaa013

Sánchez-Montesinos, B., Santos, M., Moreno-Gavíra, A., Marín-Rodulfo, T., Gea, F. J., and Diánez, F. (2021). Biological control of fungal diseases by *Trichoderma aggressivum* f. *europaeum* and its compatibility with fungicides. Journal of Fungi 7, 598. DOI: 10.3390/jof7080598

Santos, J. M., Correia, V. G., and Phillips, A. J. L. (2010). Primers for mating-type diagnosis in *Diaporthe* and *Phomopsis*: their use in teleomorph induction *in vitro* and biological species definition. Fungal Biology **114**: 255–270. DOI: 10.1016/j.funbio.2010.01.007

Santos, J. M., and Phillips, A. J. L. (2009). Resolving the complex of *Diaporthe* (*Phomopsis*) species occurring on *Foeniculum vulgare* in Portugal. Fungal Diversity **34**: 111–125

Santos, J. M., Vrandečić, K., Ćosić, J., Duvnjak, T., and Phillips, A. J. L. (2011). Resolving the *Diaporthe* species occurring on soybean in Croatia. Persoonia **27**: 9–19. DOI: 10.3767/003158511X603719

Santos, L., Alves, A., and Alves, R. (2017). Evaluating multi-locus phylogenies for species boundaries determination in the genus *Diaporthe*. PeerJ **5**: e3120. DOI: 10.7717/peerj.3120

Savary, S., Willocquet, L., Pethybridge, S. J., Esker, P., McRoberts, N., and Nelson, A. (2019). The global burden of pathogens and pests on major food crops. Nature Ecology and Evolution **3**: 430–439. DOI: 10.1038/s41559-018-0793-y

Schoch, C. L., Seifert, K. A., Huhndorf, S., Robert, V., Spouge, J. L., Levesque, C. A., Chen, W., and Fungal Barcoding Consortium. (2012). Nuclear ribosomal internal transcribed spacer (ITS) region as a universal DNA barcode marker for fungi. Proceedings of the National Academy of Sciences **109**: 6241–6246. DOI: 10.1073/pnas.1117018109

Schrader, C., Schielke, A., Ellerbroek, L., and Johne, R. (2012). PCR inhibitors - occurrence, properties and removal. Journal of Applied Microbiology **113**: 1014–1026. DOI: 10.1111/j.1365-2672.2012.05384.x

Shenoy, B. D., Jeewon, R., and Hyde, K. D. (2007). Impact of DNA sequence-data on the taxonomy of anamorphic fungi. Fungal Diversity **26**: 1–54

Sinclair, J. B. (1993). *Phomopsis* seed decay of soybeans – a prototype for studying seed disease. Plant Disease **77**: 329–334

Sinclair, J. B., and Shurtleff, M. C. (1975). Compendium of soybean diseases. First edition, APS Press, St. Paul, Minnesota, USA

Sojaförderring, D. (2021). "Übersicht der lieferbaren Sojasorten und Bezugsquellen 2021." from https://www.sojafoerderring.de/wp-content/uploads/2021/01/SortenBezug21.pdf.

Sutton, B. C. (1980). The coelomycetes. Fungi imperfecti with pycnidia, acervuli and stromata. Commonwealth Mycological Institute, Kew, Surrey, England

Svec, D., Tichopad, A., Novosadova, V., Pfaffl, M. W., and Kubista, M. (2015). How good is a PCR efficiency estimate: Recommendations for precise and robust qPCR efficiency assessments. Biomolecular Detection and Quantification **3**: 9–16. DOI: 10.1016/j.bdq.2015.01.005

Tamura, K., and Nei, M. (1993). Estimation of the number of nucleotide substitutions in the control region of mitochondrial DNA in humans and chimpanzees. Molecular Biology and Evolution **10**: 512–526. DOI: 10.1093/oxfordjournals.molbev.a040023

Tamura, K., Nei, M., and Kumar, S. (2004). Prospects for inferring very large phylogenies by using the neighbor-joining method. Proceedings of the National Academy of Sciences of the United States of America **101**: 11030–11035. DOI: 10.1073/pnas.0404206101

Thambugala, K. M., Daranagama, D. A., Phillips, A. J. L., Kannangara, S. D., and Promputtha, I. (2020). Fungi vs. fungi in biocontrol: an overview of fungal antagonists applied against fungal plant pathogens. Frontiers in Cellular and Infection Microbiology **10**: 604923. DOI: 10.3389/fcimb.2020.604923

Thompson, S. M., Tan, Y. P., Shivas, R. G., Neate, S. M., Morin, L., Bissett, A., and Aitken, E. A. B. (2015). Green and brown bridges between weeds and crops reveal novel *Diaporthe* species in Australia. Persoonia **35**: 39–49. DOI: 10.3767/003158515X687506

Thompson, S. M., Tan, Y. P., Young, A. J., Neate, S. M., Aitken, E. A. B., and Shivas, R. G. (2011). Stem cankers on sunflower (*Helianthus annuus*) in Australia reveal a complex of pathogenic *Diaporthe* (*Phomopsis*) species. Persoonia **27**: 80–89. DOI: 10.3767/003158511X617110

Tyler, D. D., Overton, J. R., and Chambers, A. Y. (1983). Tillage effects on soil properties, diseases, cyst nematodes, and soybean yields. Journal of Soil and Water Conservation **38**: 374–376

Udayanga, D., Castlebury, L. A., Rossman, A. Y., Chukeatirote, E., and Hyde, K. D. (2014). Insights into the genus *Diaporthe*: phylogenetic species delimitation in the *D. eres* species complex. Fungal Diversity **67**: 203–229. DOI: 10.1007/s13225-014-0297-2

Udayanga, D., Castlebury, L. A., Rossman, A. Y., Chukeatirote, E., and Hyde, K. D. (2015). The *Diaporthe sojae* species complex: Phylogenetic re-assessment of pathogens associated with soybean, cucurbits and other field crops. Fungal Biology **119**: 383–407. DOI: 10.1016/j.funbio.2014.10.009

Udayanga, D., Liu, X., Crous, P. W., McKenzie, E. H. C., Chukeatirote, E., and Hyde, K. D. (2012). A multi-locus phylogenetic evaluation of *Diaporthe* (*Phomopsis*). Fungal Diversity **56**: 157–171. DOI: 10.1007/ s13225-012-0190-9

Udayanga, D., Liu, X., McKenzie, E. H. C., Chukeatirote, E., Bahkali, A. H. A., and Hyde, K. D. (2011). The genus *Phomopsis*: biology, applications, species concepts and names of common pathogens. Fungal Diversity **50**: 189–225. DOI: 10.1007/s13225-011-0126-9

Upchurch, R. G., and Ramirez, M. E. (2010). Defense-related gene expression in soybean leaves and seeds inoculated with *Cercospora kikuchii* and *Diaporthe phaseolorum* var. *merdionalis*. Physiological and Molecular Plant Pathology **75**: 64–70. DOI: 10.1016/j.pmpp.2010.08.007

USDA-FAS, (2022). Oilseeds: World markets and trade. https://www.fas.usda.gov/data/oilseeds-world-markets-and-trade

van der Aa, H. A., Noordeloos, M. E., and de Gruyter, J. (1990). Species concepts in some larger genera of the Coelomycetes. Studies in Mycology **32**: 3–19

van Niekerk, J. M., Groenewald, J. Z., Farr, D. F., Fourie, P. H., Halleer, F., and Crous, P. W. (2005). Reassessment of *Phomopsis* species on grapevine. Australasian Plant Pathology **34**: 27–39. DOI: 10.1071/AP04072

van Rensburg, J. C. J., Lamprecht, S. C., Groenewald, J. Z., Castlebury, L. A., and Crous, P. W. (2006). Characterisation of *Phomopsis* spp. associated with die-back of rooibos (*Aspalathus linearis*) in South Africa. Studies in Mycology **55**: 65–74. DOI: 10.3114/sim.55.1.65

van Warmelo, K. T., Marasas, W. F. O., Adelaar, T. F., Kellerman, T. S., van Rensburg, I. B. J., and Minne, J. A. (1970). Experimental evidence that lupinosis of sheep is a mycotoxicosis caused by the fungus *Phomopsis leptostromiformis* (Kühn) Bubak. Journal of South African Veterinary Association **41**: 235–247

Vechiato, M. H., Maringoni, A. C., and Martins, E. M. F. (2006). Development of primers and method for identification and detection of *Diaporthe phaseolorum* var. *meridionalis* in soybean seeds. Summa Phytopathologica **32**: 161–169. DOI: 10.1590/S0100-54052006000200011

Vidić, M., Đorđević, V., Petrović, K., and Miladinović, J. (2013). Review of soybean resistance to pathogens. Ratarstvo i Povrtarstvo **50**: 52–61

Vrandečić, K., Cosic, J., Riccioni, L., Duvnjak, T., and Jurkovic, D. (2005). Isolation of *Diaporthe phaseolorum* var. *caulivora* from *Abutilon theophrasti* in Croatia. Plant pathology **54**: 576. DOI: 10.1111/j.1365-3059.2005.01196.x

Vrandečić, K., Jurković, D., Riccioni, L., Cosic, J., and Duvnjak, T. (2010). *Xanthium italicum*, *Xanthium strumarium* and *Arctium lappa* as new hosts for *Diaporthe helianthi*. Mycopathologia **170**: 51–60. DOI: 10.1007/s11046-010-9289-2

Wagner, A., Norris, S., Chatterjee, P., Morris, P. F., and Wildschutte, H. (2018). Aquatic *Pseudomonads* inhibit oomycete plant pathogens of *Glycine max*. Frontiers in Microbiology **9**: 1007. DOI: 10.3389/fmicb.2018.01007

Walcott, R. R. (2003). Acidified PDA method for the detection of *Phomopsis* complex on *Glycine max*. In: International rules for seed testing, Annexe to Chapter 7: Seed health methods. International Seed Testing Association (ISTA), Bassersdorf, Switzerland, 7–016

Wehmeyer, L. E. (1933). The genus *Diaporthe* Nitschke and its segregates. University of Michigan Studies, Scientific Series **9**: 1–349

Westergaard, M., and Mitchell, H. K. (1947). Neurospora V. A synthetic medium favoring sexual reproduction. American Journal of Botany **34**: 573–577. DOI: 10.1002/j.1537-2197.1947.tb13032.x

Westphal, A., Li, C., Xing, L., Mckay, A., and Malvick, D. (2014). Contributions of *Fusarium virguliforme* and *Heterodera glycines* to the disease complex of sudden death syndrome of soybean. PLoS ONE **9**: e99529. DOI: 10.1371/journal.pone.0099529

White, T. J., Bruns, T., Lee, J., and Taylor, J. (1990). Amplification and direct sequencing of fungal ribosomal RNA genes for phylogenetics. In: PCR protocols: a guide to methods and applications (Innis, M. A., Gelfand, D. H., Sninsky, J. J., and White, T. J. eds.). Academic Press, New York, Chapter 38: 315–322

Williams, R. H., Ward, E., and McCartney, H. A. (2001). Methods for integrated air sampling and DNA analysis for detection of airborne fungal spores. Applied and Environmental Microbiology **67**: 2453–2459. DOI: 10.1128/AEM.67.6.2453-2459.2001

Wirtz, L., Massola Júnior, N. S., Linhares de Castr, R. R., Ruge-Wehling, B., Schaffrath, U., and Loehrer, M. (2021). *Colletotrichum* spp. from soybean cause disease on lupin and can induce plant growth-promoting effects. Microorganisms **9**, 1130. DOI: 10.3390/microorganisms9061130

Wrather, J. A., Sleper, D. A., Stevens, W. E., Shannon, J. G., and Wilson R. F. (2003). Planting date and cultivar effects on soybean yield, seed quality, and *Phomopsis* spp. seed infection. Plant Disease **87**: 529–532

Xue, A. G., Morrison, M. J., Cober, E., Anderson, T. R., Rioux, S., Ablett, G. R., Rajcan, I., Hall, R., and Zhang, J. X. (2007). Frequency of isolation of species of *Diaporthe* and *Phomopsis* from soybean plants in Ontario and benefits of seed treatments. Canadian Journal of Plant Pathology **29**: 354–364. DOI: 10.1080/07060660709507481

Yang, H.-C., Haudenshield, J. S., and Hartman, G. L. (2015). Multiplex real-time PCR detection and differentiation of *Colletotrichum* species infecting soybean. Plant Disease **99**:1559–1568. DOI: 10.1094/PDIS-11-14-1189-RE

Zhang, A. W., Hartman, G. L., Curio-Penny, B., Pedersen, W. L., and Becker, K. B. (1999). Molecular detection of *Diaporthe phaseolorum* and *Phomopsis longicolla* from soybean seeds. Phytopathology **89**: 796–804. DOI: 10.1094/PHYTO.1999.89.9.796

Zhang, A. W., Hartman, G. L., Riccioni, L., Chen, W. D., Ma, R. Z., and Pedersen, W. L. (1997). Using PCR to distinguish *Diaporthe phaseolorum* and *Phomopsis longicolla* from other soybean fungal pathogens and to detect them in soybean tissues. Plant Disease **81**: 1143–1149. DOI: 10.1094/PDIS.1997.81.10.1143

Zhang, A. W., Riccioni, L., Pedersen, W. L., Kollipara, K. P., and Hartman, G. L. (1998). Molecular identification and phylogenetic grouping of *Diaporthe phaseolorum* and *Phomopsis longicolla* isolates from soybean. Phytopathology **88**: 1306–1314. DOI: 10.1094/PHYTO.1998.88.12.1306

7 Appendix

7.1. Quadruplex real-time PCR assays by using the mixture of primer-probe sets DPCL, DPCC, DPCE(1), and DPCN

The mixture of the four primer-probe sets DPCL, DPCC, DPCE(1), and DPCN was tested in the quadruplex real-time PCR assays the same way as described (see 3.5.4.2.2.) for DPCL, DPCC, DPCE, and DPCN. This combination can also detect *D. longicolla*, *D. caulivora*, *D. eres*, and *D. novem* in parallel in one PCR reaction (Figure 7.1).

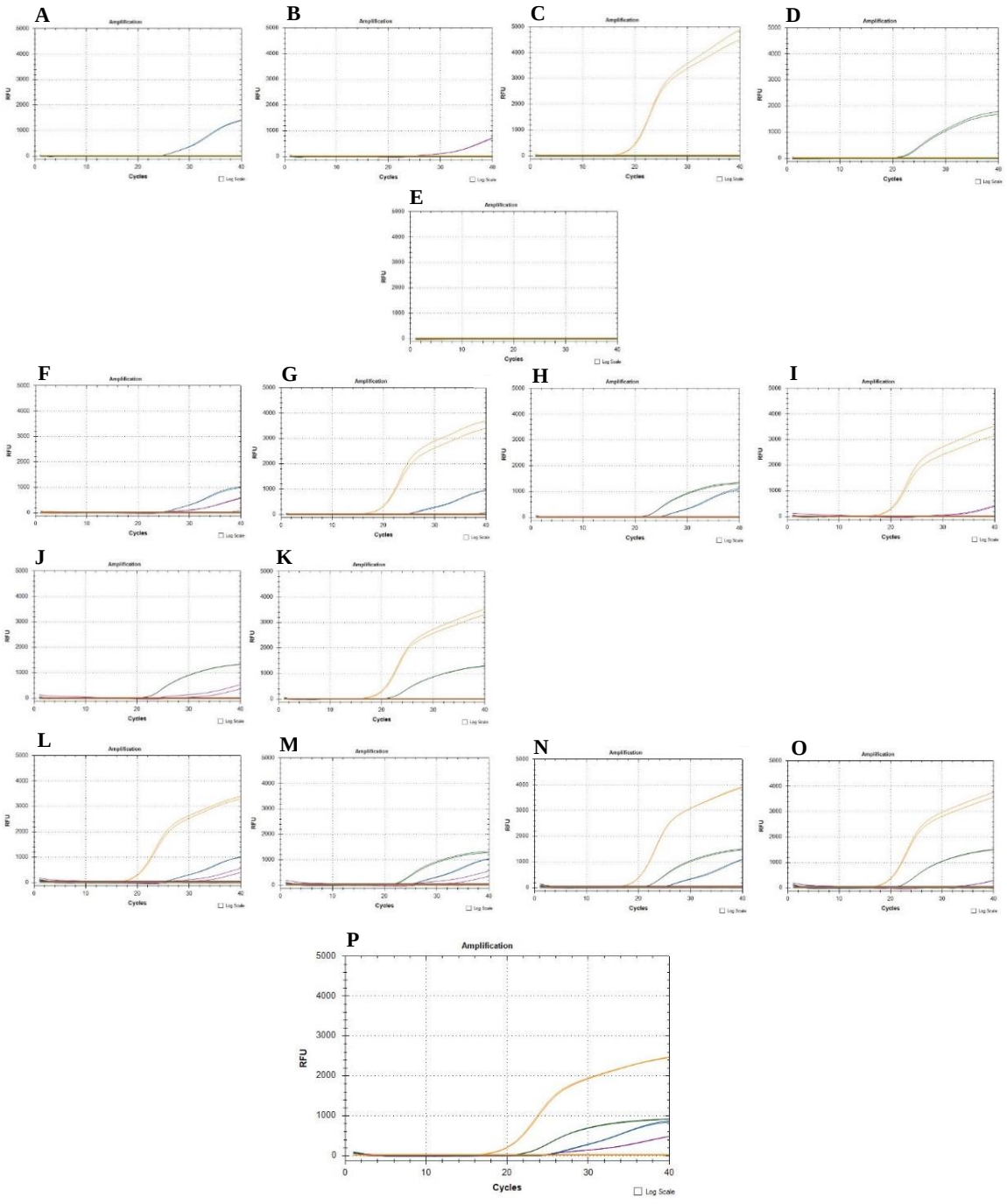

Figure 7.1 (previous page): Specificity of the quadruplex real-time PCR assay using primer-probe sets DPCL, DPCC, DPCE(1), and DPCN.
Since the graphs for different isolates of the target species and also of all the non-target species are highly similar, only one representative graph is shown each. 0.4 ng DNA from **A**) *D. longicolla* DPC_HOH28, **B**) *D. caulivora* DPC_HOH2, **C**) *D. eres* DPC_HOH3, and **D**) *D. novem* DPC_HOH15 was added individually to the mix that contained all four primer-probe sets. **E**) Shows the result for the non-target species *D. aspalathi*, *D. foeniculina*, *C. kikuchii*, *F. solani*, *Alternaria* sp., *S. sclerotiorum* DSMZ, or *S. sclerotiorum* IZS, *C. truncatum*, *F. tricinctum*, *P. pachyrhizi*, *U. fabae*, *U. appendiculatus*, healthy soybean leaf, and healthy soybean stem. For these species and also *D. longicolla* isolate PL-157a and *D. eres* isolate PS-74 DNA amounts varied between 350 ng and 2.5 µg. Parallel detection of two (**F-K**), three (**L-O**), or all four (**P**) different *Diaporthe* species in the quadruplex real-time PCR assay using primer-probe sets DPCL, DPCC, DPCE(1), and DPCN. 0.4 ng DNA from **F**) *D. longicolla* (blue) and *D. caulivora* (purple), **G**) *D. longicolla* and *D. eres* (orange), **H**) *D. longicolla* and *D. novem* (green), **I**) *D. caulivora* and *D. eres*, **J**) *D. caulivora* and *D. novem*, **K**) *D. eres* and *D. novem*, **L**) *D. longicolla*, *D. caulivora*, and *D. eres*, **M**) *D. longicolla*, *D. caulivora*, and *D. novem*, **N**) *D. longicolla*, *D. eres*, and *D. novem*, **O**) *D. caulivora*, *D. novem*, and *D. eres*, and **P**) *D. longicolla*, *D. caulivora*, *D. eres*, and *D. novem* were added to the mix that contained all four primer-probe sets.

7.2. Quantification of the amount of *Diaporthe* DNA in soybean seeds

In addition to Figure 3.21 A, B (in 3.5.6.1.2.), which shows the results from sampling two different seed lots, the results from sampling the other four seed lots are provided below (Figure 7.2).

Figure 7.2 (following page): Sampling soybean seed lots via the quadruplex real-time PCR assay.
A) Seed lot from a field in Rheinau, Germany; half of the seed samples was infected with mainly *D. longicolla* and a few with *D. novem*. **B**) Seed lot from a field in Dt. Jarndorf, Austria; in this seed samples just two of the seeds were infected with *D. caulivora* in a low amount. **C**) Seed lot from a field in Voiron, France; from 30 seed samples, three seeds were infected with *D. novem* and two seeds were infected with *D. eres*. **D**) Seed lot from a field in Südliches Anhalt, Germany; 25 of the seeds were infected with *D. eres* or with *D. eres* and *D. novem* simultaneously. Bars represent ng *Diaporthe* DNA/ng soybean DNA; because of the strong variation a logarithmic scale was chosen. The numbers on the x-axis represent the 30 seeds that were individually tested.

A

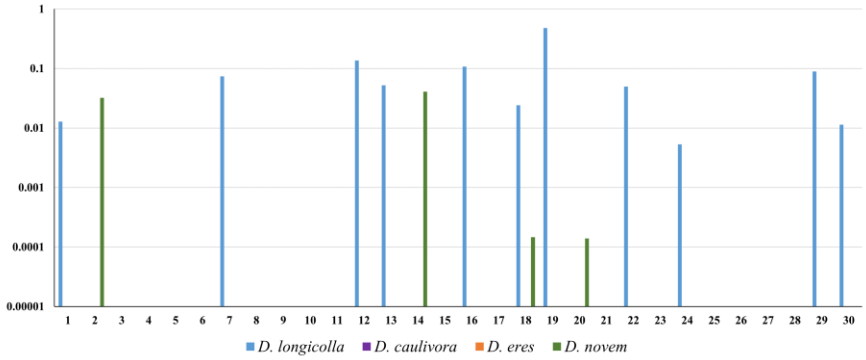
1
0.1
0.01
0.001
0.0001
0.00001
1 2 3 4 5 6 7 8 9 10 11 12 13 14 15 16 17 18 19 20 21 22 23 24 25 26 27 28 29 30
D. longicolla
D. caulivora
D. eres
D. novem

B

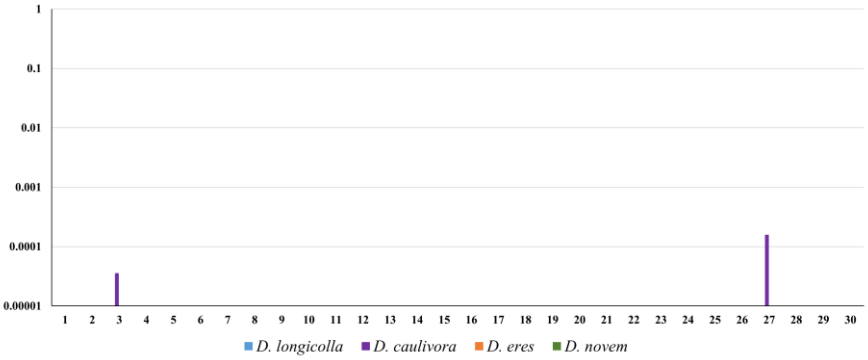
1
0.1
0.01
0.001
0.0001
0.00001
1 2 3 4 5 6 7 8 9 10 11 12 13 14 15 16 17 18 19 20 21 22 23 24 25 26 27 28 29 30
D. longicolla
D. caulivora
D. eres
D. novem

C

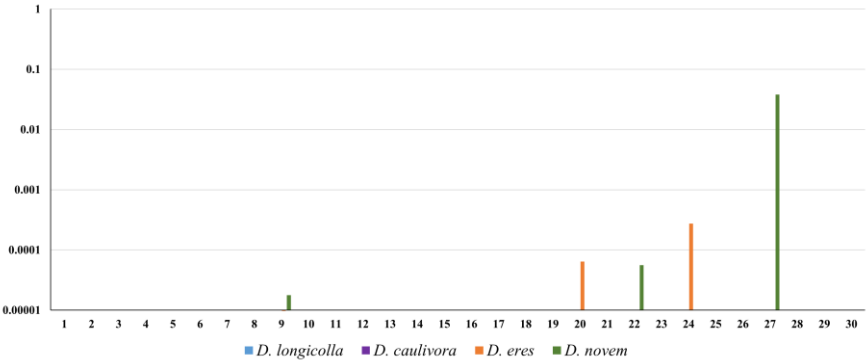
1
0.1
0.01
0.001
0.0001
0.00001
1 2 3 4 5 6 7 8 9 10 11 12 13 14 15 16 17 18 19 20 21 22 23 24 25 26 27 28 29 30
D. longicolla
D. caulivora
D. eres
D. novem

D

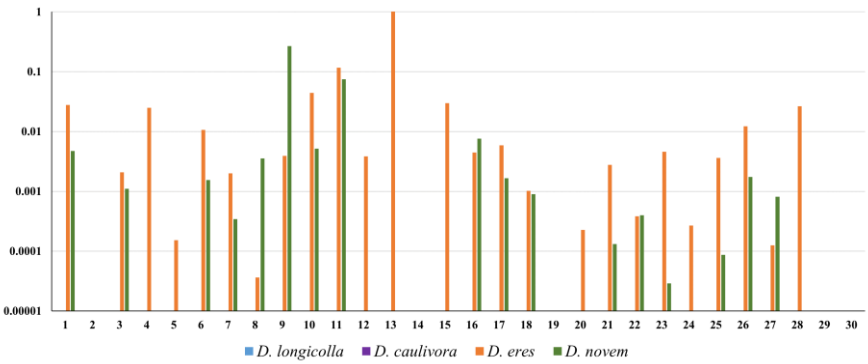
1
0.1
0.01
0.001
0.0001
0.00001
1 2 3 4 5 6 7 8 9 10 11 12 13 14 15 16 17 18 19 20 21 22 23 24 25 26 27 28 29 30
D. longicolla
D. caulivora
D. eres
D. novem

7.3. Standard curves for *Diaporthe* species spores

Standard curves resulting from performing qPCR assays for spore suspensions (serial dilutions 10^{-1} to 10^{-7}) of *Diaporthe* spp. are shown below (Figure 7.3 A-D).

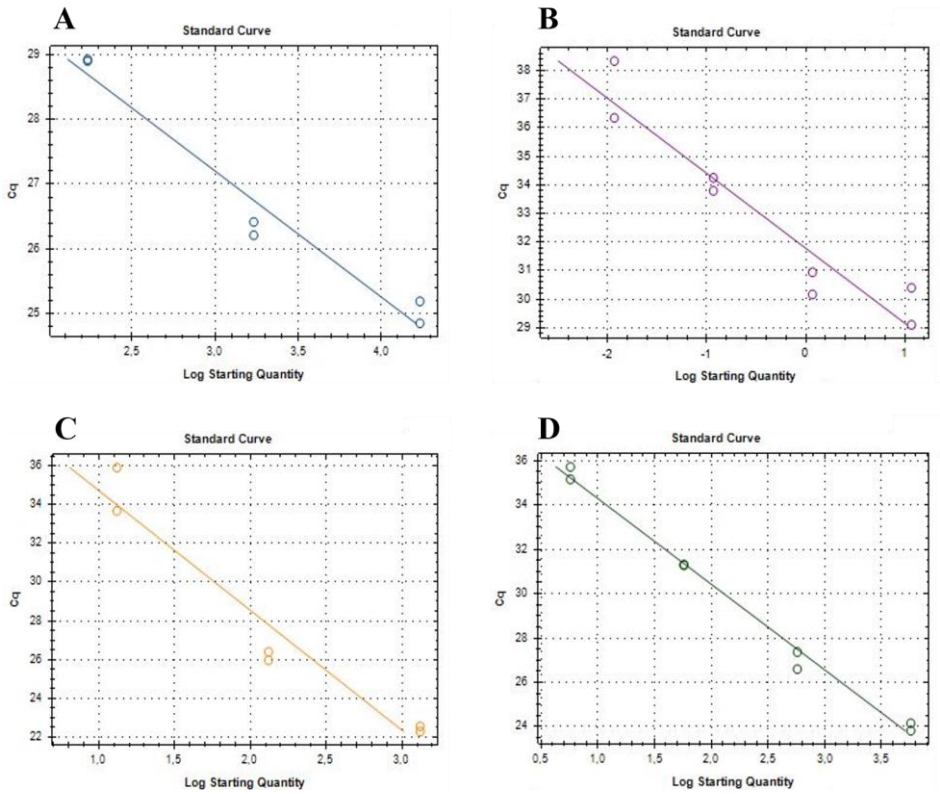

Figure 7.3: Standard curves for *Diaporthe* species spores.
A) *D. longicolla* isolate DPC_HOH20, standard curve for undiluted (17,100 spores in 2 µL) to 1:100 diluted (171 spores in 2 µL) samples. **B**) *D. caulivora* isolate DPC_HOH2, standard curve for undiluted (197 spores in 2 µL) to 1:1,000 diluted (less than one spore in 2 µL) samples. **C**) *D. eres* isolate DPC_HOH7, standard curve for 1:10 (1,317 spores in 2 µL) to 1:1,000 diluted (13 spores in 2 µL) samples. **D**) *D. novem* isolate DPC_HOH15, standard curve for undiluted (5,730 spores in 2 µL) to 1:1,000 diluted (6 spores in 2 µL) samples. Log Starting Quantity corresponds to the number of spores.

7.4. Standard curves from extracted DNAs of *Diaporthe* species spores

Concentration of the extracted DNAs was measured using spectrometry and recorded (Table 7.1). To create the standard curves the DNA samples were added in quadruplex real-time PCR assays. The resulting standard curves are shown below (Figures 7.4 and 7.5).

Table 7.1: DNA concentration of serial dilutions of spore suspensions from *Diaporthe* species

Serial dilution	*D. longicolla*		*D. caulivora*	
	Spores (in 1 mL)	DNA concentration	Spores (in 1 mL)	DNA concentration
Undiluted	8,550,000	71	98,500	508
10^{-1}	855,000	7	9,850	247
10^{-2}	85,500	12	985	5
10^{-3}	8,550	8	99	0
10^{-4}	550	9	10	12

Serial dilution	*D. eres*		*D. novem*	
	Spores (in 1 mL)	DNA concentration	Spores (in 1 mL)	DNA concentration
Undiluted	6,587,000	6	2,865,000	9
10^{-1}	658,700	19	286,500	8
10^{-2}	65,870	7	28,650	5
10^{-3}	6,587	6	2,865	10
10^{-4}	659	9	287	0

The standard curve of the spore DNA of *D. longicolla* was determined just from two samples (undiluted and diluted 1:10) (Figure 7.4 A, B), since only these curves intersect the threshold at RFU = 30. For the further dilutions no DNA could be detected. However, the Cq values of the second sample are still quite low. The resulting efficiency with E = 78.4 % and the correlation with $R^2 = 0.997$ are not bad, but samples with low DNA concentrations were not used (Figure 7.4 A). Where ng DNA was put instead of number of spores in the x-axis, the resulting standard curve from the real-time qPCR assay has E = 79.0 % and $R^2 = 0.997$ (Figure 7.4 B).

Four samples were used for the standard curve of the spore DNA of *D. caulivora* in Figure 7.4 C, D; since the $1:10^4$ dilution probably contained too little DNA for detection. The software determined E = 47 % and $R^2 = 0.964$ (RFU = 30), which does not correspond to an optimal regression. The $1:10^3$ dilution of the DNA preparation worked worse because of small amounts of the spores, as was previously the case with small amounts of mycelium. Where ng DNA was put instead of number of spores in the x-axis, the resulting standard curve from the real-time qPCR assay has E = 52.3 % and $R^2 = 0.979$ (Figure 7.4 D).

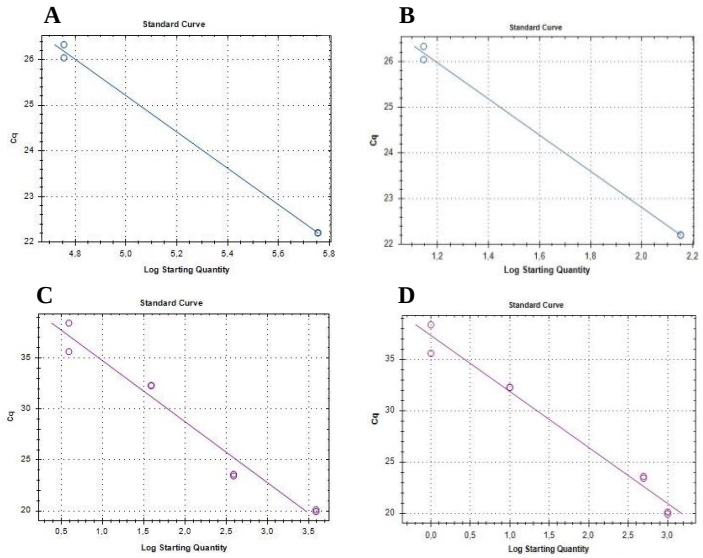

Figure 7.4: Standard curves from extracted DNAs of *Diaporthe* species spores. A, B) *D. longicolla* isolate DPC_HOH20. C, D) *D. caulivora* isolate DPC_HOH2.
Log Starting Quantity in **A** and **C** corresponds to the number of spores.
Log Starting Quantity in **B** and **D** corresponds to the amount of fungal DNA from spores in ng.

The efficiency and correlation of the standard curve of the conidial DNA of *D. eres* E = 37.6 % and $R^2 = 0.961$ were obtained (RFU = 31) (Figure 7.5 A). According to the resulting standard curve (Figure 7.5 A), the DNA concentration for the 1:10 diluted sample was not correct (Table 7.1). Where ng DNA put instead of number of spores in the x-axis, the resulting standard curve from the real-time qPCR assay has E = 344.9 % and $R^2 = 0.003$ (Figure 7.5 B). The values are very low, which again suggests poor DNA preparations from samples with little biomass.

The efficiency of the standard curve of the spore DNA of *D. novem* was E = 66.8 % and the correlation was $R^2 = 0.993$ (RFU = 30) (Figure 7.5 C). Compared to the standard straight curve, which was created from unprocessed spores (E = 82.1 %), this was somewhat worse and speaks against a DNA preparation. Where ng DNA was put instead of number of spores in the x-axis, the resulting standard curve from the real-time qPCR assay has E = 2.7 % and $R^2 = 0.993$ (Figure 7.5 D).

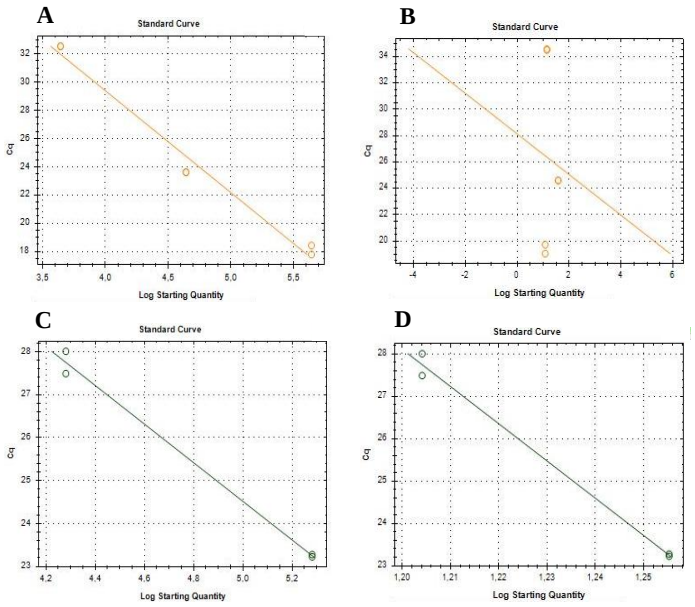

Figure 7.5: Standard curves from extracted DNAs of *Diaporthe* species spores. A, B) *D. eres* isolate DPC_HOH7. C, D) *D. novem* isolate DPC_HOH15.
Log Starting Quantity in **A** and **C** corresponds to the number of spores.
Log Starting Quantity in **B** and **D** corresponds to the amount of fungal DNA from spores in ng.